FPL

ORIGINAL

March 20, 2000

Blanca S. Bayo, Director
Records and Reporting
Florida Public Service Commission
4075 Esplanade Way, Room 110
Tallahassee, Florida 32399-0850

000000 FPJ

Re: Florida Power and Light Company's Commercial/Industrial Solar Desiccant Research Project
Docket No. 970391-EG Order No. PSC-97-1336-FOF-EG

Enclosed for filing on behalf of Florida Power & Light Company (FPL) are the original and fifteen (15) copies of FPL's Commercial/Industrial Solar Desiccant Research Project findings.

This research was performed by the University of Florida Solar Energy and Energy Conversion Laboratory.

This study shows that the concepts of desiccant-enhanced air conditioning (DEAC), and solar-enhanced desiccant-enhanced air conditioning (SDEAC), are technically feasible and can be accomplished. Further, the study shows that, in a humid climate, significant energy savings can be accomplished by using SDEAC systems instead of conventional vapor-compression air conditioning systems.

Unfortunately, the research found that SDEAC systems are not something we can offer to our customers as an energy conservation measure at this time because:

- The systems are not commercially available. Significant efforts would be required by HVAC equipment manufacturers to ready this equipment for the market. Since the economics are not compelling, it is not likely that they would be interested in the required product development.
- The projected capital cost of the equipment required is high, and the research study estimated paybacks in the 9 year range. This does not compete with other more proven HVAC alternatives currently available.

AFA
APP
CAF
CMU
CTR
(3) EAG
LEG
MAS
OPC
RRR
SEC
WAW
OTH

RECEIVED & FILED
FPSC-BUREAU OF RECORDS

The FPSC approved budget for this project was $106,000. Actual expenditures were $72,518.

FPL will continue to monitor the development of this technology.

Dennis Brandt
Director
Product Support & Services

EVALUATION OF A HYBRID DESICCANT AIR CONDITIONING SYSTEM

FINAL REPORT

December 1999

Submitted to:

Greg Whiting

Florida Power and Light Co.

BY

Principal Investigator:

D.Y. Goswami, Ph.D., P.E.

Graduate Assistants:

Pedro Mago

Nelson Fumo

Solar Energy and Energy Conversion Laboratory
Department of Mechanical Engineering
P.O. Box 116300
University of Florida
Gainesville, FL 32611-6300

TABLE OF CONTENTS

TABLES

FIGURES

EXECUTIVE SUMMARY

Conditioning of ventilation air in the hot and humid climate of Florida is a very energy intensive process. Since ventilation air must be adequately dried for humidity control, the ratio of latent to total cooling load is large. Previous studies have shown that in order to meet the increased ventilation requirements of the ASHRAE Standard 62-1989, conventional vapor compression cooling systems may be inadequate to meet the load for humidity control. In such cases, a desiccant system may be used in conjunction with solar energy to provide adequate dehumidification. If a solar desiccant system is combined with a conventional vapor compression system in a hybrid mode, it can provide complete dehumidification and temperature control.

In a hybrid solar desiccant air conditioning system, the air is dehumidified by bringing it in contact with a desiccant, followed by sensible cooling of the air by a conventional vapor compression cooling system. A large part of the total cooling load is latent cooling, which can be satisfied by the desiccant system. Therefore the size of the vapor compression cooling system is much smaller than what would otherwise be needed.

This results in savings of electrical energy needed to run the system. In a hybrid solar desiccant system, solar energy is used to regenerate the desiccant. Electric resistance heat may be used as a back-up for solar heat. Two types of desiccant materials may be used, solids such as silica gel or liquids such as triethylene glycol (TEG) and aqueous lithium chloride (LICl) solution. Since liquid desiccants may be pumped for convenient regeneration by solar energy they offer an advantage for solar desiccant systems. This project was carried out to study the feasibility of hybrid solar liquid desiccant systems for air conditioning in Florida, by simulation, laboratory tests and a field test.

The initial feasibility study showed that by using a hybrid solar liquid desiccant system in Miami, Florida, as much as 80% of electrical energy can be saved compared to a conventional vapor compression cooling system. In addition the hybrid solar desiccant system provides a better humidity control. The feasibility study also showed that if electrical resistance heating is

used as the auxiliary heat for desiccant regeneration, a large solar fraction (>0.86) is needed in order to save electrical energy compared to the conventional system.

Extensive laboratory tests were conducted to study the performance of packed bed liquid desiccant dehumidifiers and regenerators. The objective of the laboratory investigation was to provide experimental data to aid in the design of desiccant systems. The dehumidifier and regenerator performance was studied experimentally and modeled theoretically by studying the impact of varying air and desiccant flow rates, air temperature and humidity, desiccant temperature and concentration, and tower height.

Initially, triethylene glycol (TEG) was chosen as a desiccant because of its low vapor pressure, low surface tension and non-corrosive properties. However, it was later replaced by LiCl because trace amounts of TEG vapors in the air caused a sweet smell that could not be eliminated. The laboratory tests were then repeated for LiCl as the desiccant.

Field tests of a hybrid solar liquid desiccant cooling system were conducted at the Solar House at the University of Florida's Energy Research and Education Park. These tests consisted of operating the air conditioning system in two configurations: the conventional vapor compression, and the hybrid desiccant system, with data collected to compare the performance of both arrangements. In each of the modes, the system was operated with: (a) recirculation air; and (b) 100% ventilation air. Based on the field test results it is concluded that the hybrid desiccant system improves the air conditioning performance in the field test house by decreasing the outlet humidity and temperature of the air.

An analysis of electricity use for both the conventional vapor compression system and the hybrid solar liquid desiccant system was done for the case of 100% fresh air ventilation, because it showed the most advantage for a hybrid liquid desiccant system. The analysis was based on the test data for the two systems at the field test house. The analysis showed that a hybrid system consisting of a liquid desiccant system with a tower height of 2.5m and a vapor compression system of a nominal capacity of 2.5 tons, is equivalent to that of a nominal 6-ton vapor compression system. The savings in electricity costs using the equivalent hybrid liquid

system instead of the 6 ton conventional vapor compression system, were calculated to be $649/year or 60%. Based on the cost estimates of the conventional system, the hybrid liquid desiccant system and the associated solar system, the simple payback period was calculated to be 9.2 years. The actual payback period will be slightly higher than 9.2 years because of additional maintenance costs.

A big advantage of the solar hybrid desiccant system is that it can provide better humidity control, and can meet the load, while a conventional system may not be able to meet the humidity load.

The costs and payback shown above were calculated using reasonable assumptions about the cost of building desiccant systems similar to those used in this study. The liquid desiccant system analyzed in this study is simple to construct; however, it is not available commercially at this time.

INTRODUCTION

Hot and humid regions such as Florida, experience significant latent cooling demands. In such regions, solar energy may be used for dehumidification using liquid or solid desiccants. Rangarajan et al [17] compared a number of strategies for ventilation air-conditioning for Miami, FL and found that a conventional vapor compression system, without a solar desiccant system attached could not even meet the increased ventilation requirements of ASHRAE Standard 62-1989. By pretreating the ventilation air with a desiccant system, proper indoor humidity conditions could be maintained and significant electrical energy could be saved. A number of researchers have shown that a combination of a solar desiccant and a vapor compression system can save from 15 to 80 percent of the electrical energy consumption and demand in commercial applications, such as supermarkets [10, 15, 18, 19].

In a desiccant air-conditioning system, moisture is removed from the air by bringing it in contact with the desiccant and followed that with sensible cooling of the air by a vapor compression cooling system, vapor absorption cooling systems, or evaporative cooling system. The driving force for the process is the water vapor pressure. When the water vapor pressure in air is higher than on the desiccant surface, moisture is transferred from the air to the desiccant until an equilibrium is reached (see Fig. 1). In order to regenerate the desiccant for reuse, the desiccant is heated, which increases the water vapor pressure on its surface. If air with lower vapor pressure is brought in contact with this desiccant, the moisture passes from the desiccant to the air (Fig. 1), thus the desiccant is recharged. Two types of desiccants can be: solids, such as silica gel and lithium chloride; or liquids, such as salt solutions and glycols.

BACKGROUND

Solid Desiccant Cooling System

The two desiccant materials that have been used in solar systems are silica gel and molecular sieve, a selective absorber. Figure 2 shows the equilibrium absorption capacity of several substances. Note that the molecular sieve has the highest capacity up to 30 percent humidity, and silica gel is optimal between 30 and 75 percent -- the typical humidity range for buildings.

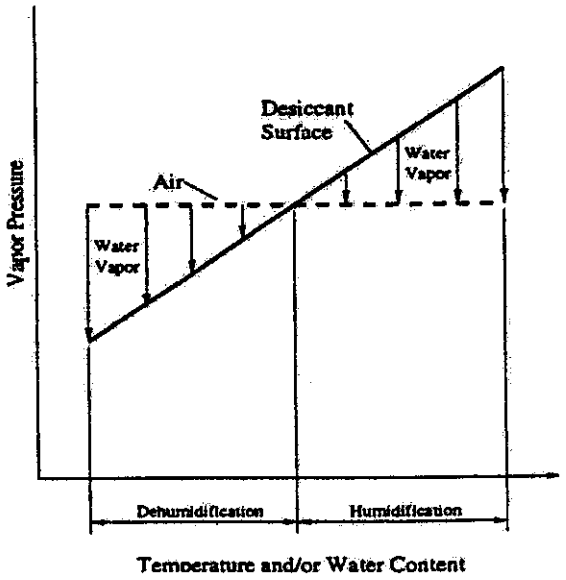

Figure 1. Vapor pressure versus temperature and water content for desiccant air interface.

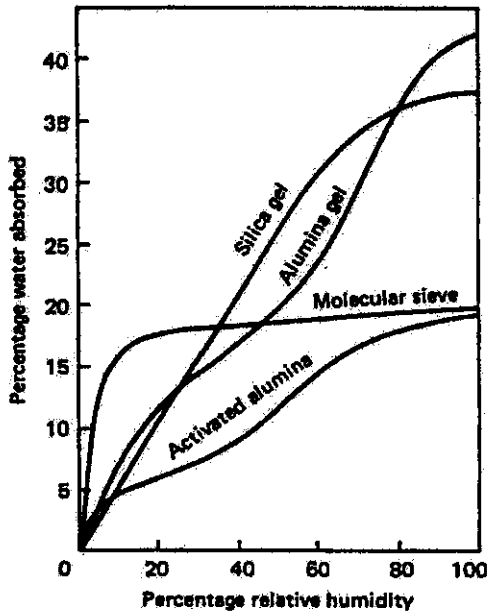

Figure 2. Equilibrium capacities of common water absorbents.

Figure 3 is a schematic diagram of a desiccant cooling ventilation cycle (also known as a Pennington cycle), which achieves both dehumidification and cooling. The desiccant bed is normally a rotary wheel of a honeycomb type substrate impregnated with the desiccant. As the air passes through the rotating wheel, it is dehumidified while its temperature increases (processes 1 and 2) due to the latent heat of condensation. Simultaneously, a hot air stream passes through the opposite side of the rotating wheel which removes moisture from the wheel. The hot and dry air at state 2 is cooled in a heat exchanger wheel to condition 3 and further

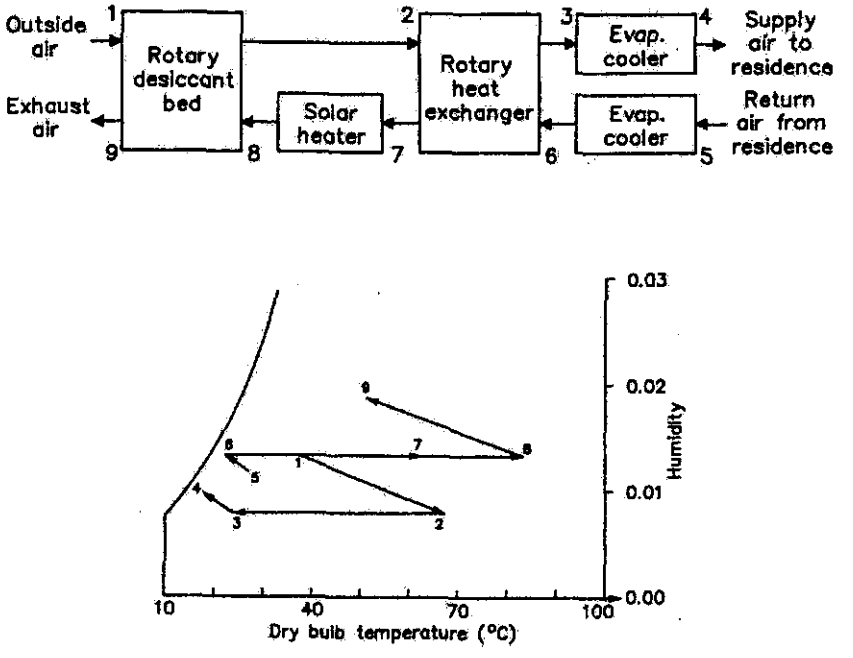

Figure 3. Schematic of a desiccant cooling ventilation cycle: a) schematic air flow; b) process on a psychromatic chart.

cooled by evaporative cooling to condition 4. Air at condition 3 may be further cooled by vapor compression or vapor absorption systems instead of evaporative cooling. The return air from the conditioned space is cooled by evaporative cooling (processes 5 and 6), which in turn cools the heat exchanger wheel. This air is then heated to condition 7. Using solar heat, it is further heated to condition 8 before going through the desiccant wheel to regenerate the desiccant. A number of researchers have studied this cycle, or an innovative variation of it, and have found thermal *COPs* in the range of 0.5 to 2.58 [16] for different systems.

Liquid Desiccant Cooling System

Liquid desiccants offer a number of advantages over solid desiccants. The ability to pump a liquid desiccant makes it possible to use solar energy for regeneration more efficiently. It also allows several small dehumidifiers to be connected to a single regeneration unit. Since a liquid desiccant does not require simultaneous regeneration, the liquid may be stored for later regeneration when solar heat is available. A major disadvantage is that the vapor pressure of the desiccant itself may be enough to cause some desiccant vapors to mix with the air. This disadvantage, however, may be overcome by proper choice of the desiccant material.

A schematic of a liquid desiccant system is shown in Fig. 4. Air is brought in contact with concentrated desiccant in a countercurrent flow in a dehumidifier. The dehumidifier may be a spray column or packed bed. The packings provide a very large area for heat and mass transfer between the air and the desiccant. After dehumidification, the air is sensibly cooled before entering the conditioned space. The dilute desiccant exiting the dehumidifier is regenerated by heating and exposing it to a countercurrent flow of a moisture scavenging air stream.

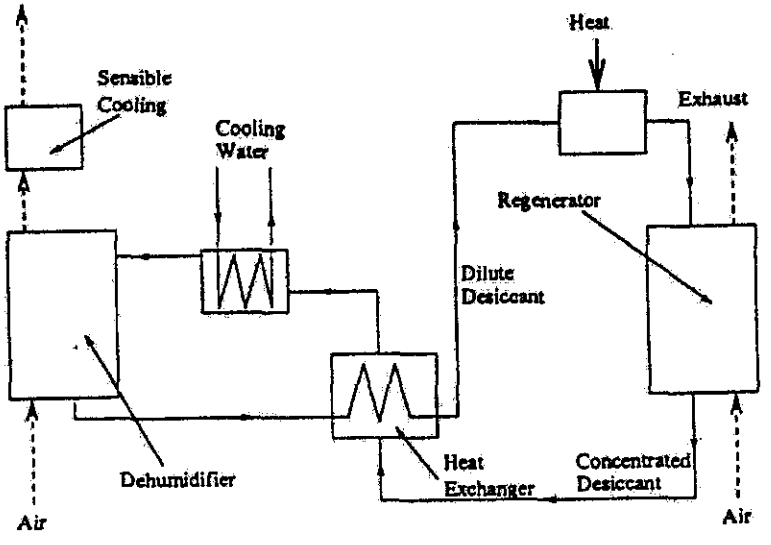

Figure 4. A conceptual liquid desiccant cooling system.

Liquid desiccants commonly used are aqueous solutions of salts such as lithium bromide, lithium chloride, calcium chloride, mixtures of these solutions and triethylene glycol (TEG). (See Oberg and Goswami [15]). Vapor pressures of these common desiccants are shown in Fig. 5 as a

function of concentration and temperature, based on a number of references [8-10, 12, 41]. Although salt solutions and TEG have similar vapor pressures, the salt solutions such as lithium chloride are corrosive and have higher surface tension. The disadvantage of TEG is that it requires higher pumping power because of higher viscosity. In this project both TEG and Lithium Chloride were initially considered for experimental evaluation. Eventually 35% Lithium Chloride solution was chosen as the liquid desiccant despite its disadvantage of being corrosive. The main reason was that TEG introduced a faint sweet smell in the air which is likely to be unacceptable to consumers. Based on the preliminary studies, a hybrid liquid desiccant system consisting of a packed bed tower lithium chloride desiccant system followed by the existing vapor compression system was installed on a field test house at the UF Solar Energy and Energy Conversion Laboratory. The system was evaluated for performance with and without the desiccant system.

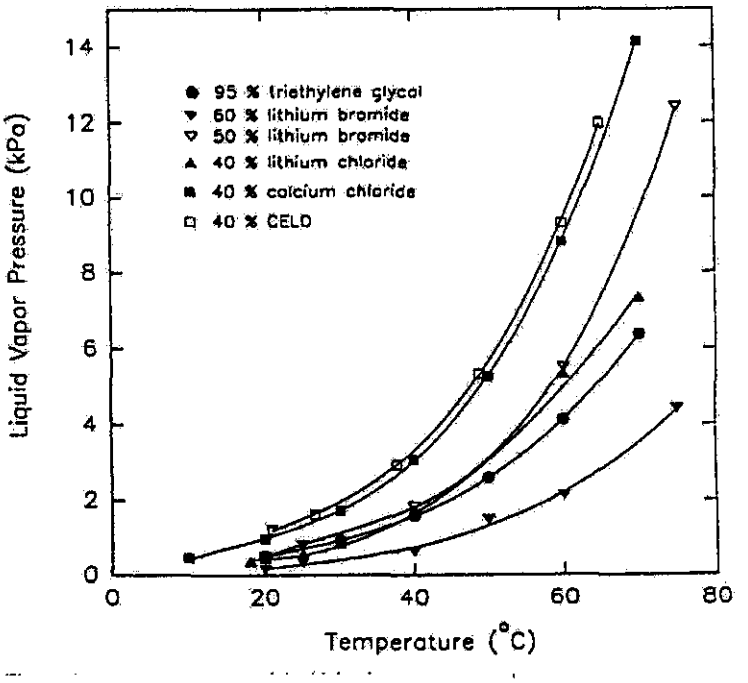

Figure 5. Vapor pressures of liquid desiccants.

OBJECTIVES

The objective of this project was to determine the feasibility, design, build and measure the performance of a hybrid liquid desiccant air conditioning system utilizing solar energy for the regeneration of the desiccant. To accomplish this objective, three steps were established:

1. **Feasibility study,** where a performance simulation of a hybrid liquid air conditioning system was conducted, to assess the performance and economics of such a system for applications having a large latent cooling demand (e.g. , supermarkets or restaurants).
2. **Laboratory test,** where the performance of a packed bed desiccant dehumidifier and desiccant regeneration was studied experimentally.
3. **Field test** of solar hybrid desiccant air conditioning system.

FEASIBILITY STUDY

A feasibility study was conducted by simulating the performance of solar liquid desiccant cooling for ventilation air preconditioning for the month of August in Miami, Florida. The study is described in detail in Appendix A. A summary of the study and the results are described in this section. The feasibility study was conducted with TEG as the desiccant. However, later in the experimental part of this project the desiccant was changed to an aqueous salt solution of Lithium Chloride because TEG introduced a faint sweet smell in the air. The desiccant system simulated in this study used packed bed towers for dehumidification and regeneration. Solar heat is provided through a solar collector/storage system for regeneration. Air coming out of the desiccant system is further conditioned by a conventional vapor compression air conditioning system, if needed, to obtain the final conditions. The system is therefore called a **hybrid solar desiccant cooling system**. Figure 6 shows the hybrid solar liquid desiccant system which was simulated for preconditioning of 0.5 m^3/s (1000 cfm) of ventilation air. The electrical energy requirements of the hybrid system are compared to those for a conventional system. The feasibility study did not account for the advantage of the hybrid desiccant system which provides better control of humidity. This advantage becomes more important in conditioning the ventilation air. In this simulation the ventilation air is cooled and dehumidified from the ambient conditions to 24°C

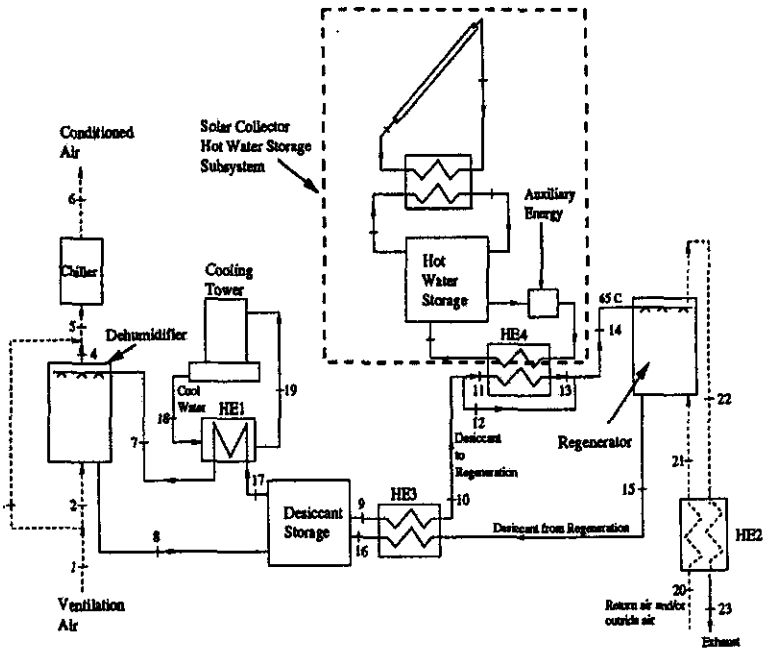

Figure 6. Solar hybrid liquid desiccant cooling system for ventilation air preconditioning.

(75°F) and 50% relative humidity. In the hybrid desiccant system the ventilation air is first dried in the packed bed desiccant dehumidifier and then cooled sensibly in the vapor compression system. The desiccant used is 95% by weight triethylene glycol. For regeneration, the desiccant is heated and brought into contact with a moisture scavanging air stream in a packed bed tower. The temperature of the desiccant entering the regenerator is set at 65°C (149°F). The regeneration heat is provided by flat plate solar collectors and hot water storage. Electricity is used (as resistance heat) to supplement the solar heat, if needed, for regeneration.

The performance simulation was carried out in three steps. First, the loads were generated using the weather data for the month of August for Miami, Florida. Next, the performance of the cooling and dehumidification system, excluding the solar subsystems, was modeled by a computer model developed earlier by Öberg and Goswami [6]. Finally, the solar hot water system for regeneration was modeled by using TRNSYS (Klein et al., 1990 [10]). The model was used to compare both the solar and non-solar systems for the same temperature and humidity conditions.

Results of the Feasibility Study

The daily cooling loads necessary to bring 0.5 m^3/s (1000 cfm) of ventilation air from the ambient air conditions to 24 °C (75 °F) and 50% relative humidity in August in Miami are shown in Figure 7. It can be seen that the latent cooling load makes up a large part of the total cooling load.

Based on the detailed study described in Appendix A, it is seen that by using solar hybrid liquid desiccant cooling for ventilation air preconditioning in a hot and humid climate, as much as 80% electrical energy can be saved compared to a conventional vapor compression cooling system. Another advantage of the hybrid solar desiccant system over the conventional vapor compression cooling is better humidity control. If electrical resistance heating is used as the auxiliary energy for desiccant regeneration, a large solar fraction for regeneration (>0.86) is needed in order to save electrical energy compared to conventional system (Fig. 8). To account for continuous cloudy days when no useful energy is provided by the solar system, very large collector area and hot water storage volume would be required in order to obtain such high monthly solar fractions. Since the simulation was conducted on a per air flow rate basis the results are independent of the size of the system.

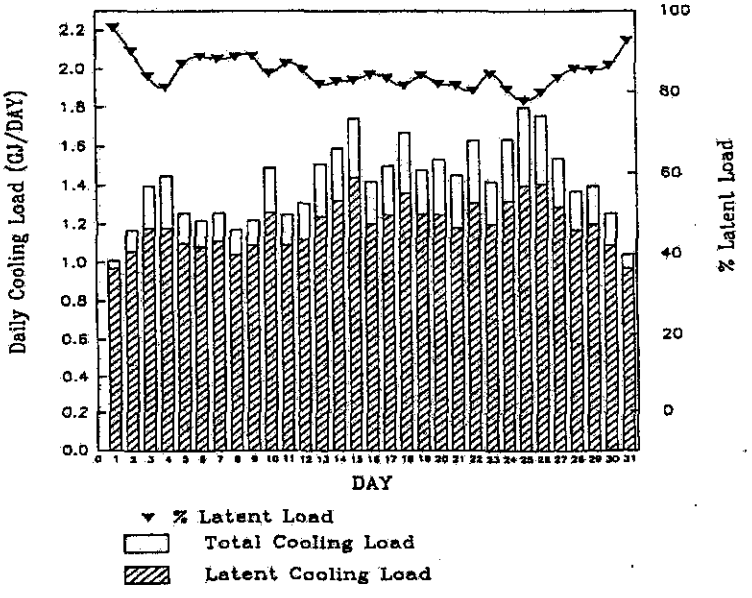

Figure 7. Daily total and latent cooling loads for pre-conditioning of 0.5 m^3/s ventilation air for the month of August in Miami, Florida.

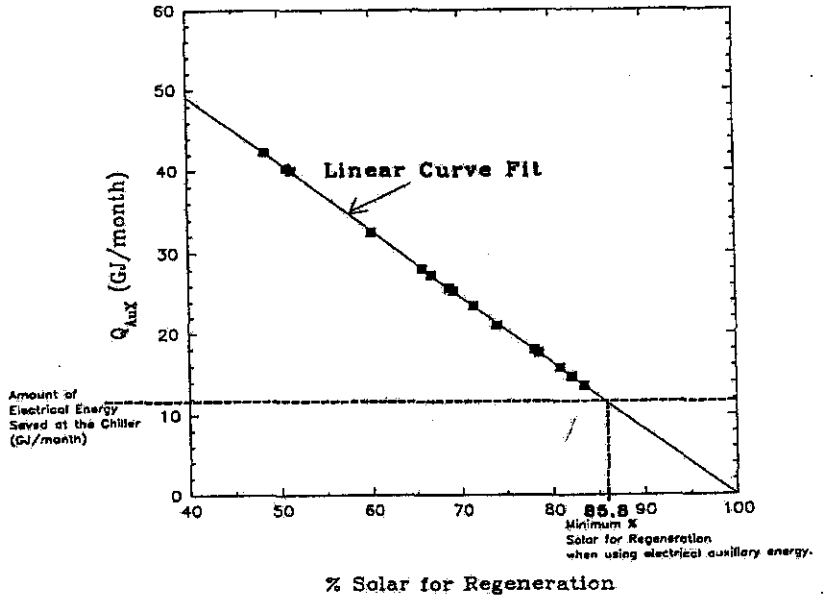

Figure 8. Auxiliary energy requirement versus percent solar for regeneration.

LABORATORY TESTS

Extensive laboratory tests were conducted to study the performance of packed bed liquid desiccant dehumidifiers and regenerators. The objective of the laboratory investigation was to provide experimental data to aid in the design of desiccant systems. Impact of variables such as air and desiccant flow rates, air temperature and humidity, desiccant temperature and concentration, and tower height on the performance of the dehumidifiers and regenerators was studied experimentally and modeled theoretically. Initially triethylene glycol (TEG) was chosen as a desiccant because of its low vapor pressure, low surface tension and non-corrosive properties. However, it was later replaced by LiCl because trace amounts of TEG vapors in the air caused a sweet smell that could not be eliminated. The laboratory tests were then repeated for LiCl as the desiccant.

Laboratory Tests For Triethylene Glycol

A detailed description of the experimental study for TEG as the desiccant is given in Appendix B. For the laboratory test, 95 % by weight triethylene glycol (TEG) was used as the

desiccant. The experimental facility consists of a packed bed absorption tower constructed from a 25.4-cm (24 cm ID) diameter acrylic with variable height. The packing used was 2.45 cm (1 in) polypropylene Rauschert Hiflow rings with specific surface area of 210 m^2/m^3. Figure 9 shows a complete schematic of the experimental facility. Measurements were taken using a PC-based data acquisition system. These measurements included inlet and outlet temperatures of the desiccant, as well as inlet and outlet air relative humidity. The rate of moisture removal from the air (water condensation rate) was studied experimentally as a function of the following variables: air and desiccant flow rates; air temperature and humidity ratio; desiccant temperature and concentration and packed bed (tower) height. For the same variables an analysis of the tower efficiency was done through the humidity effectiveness.

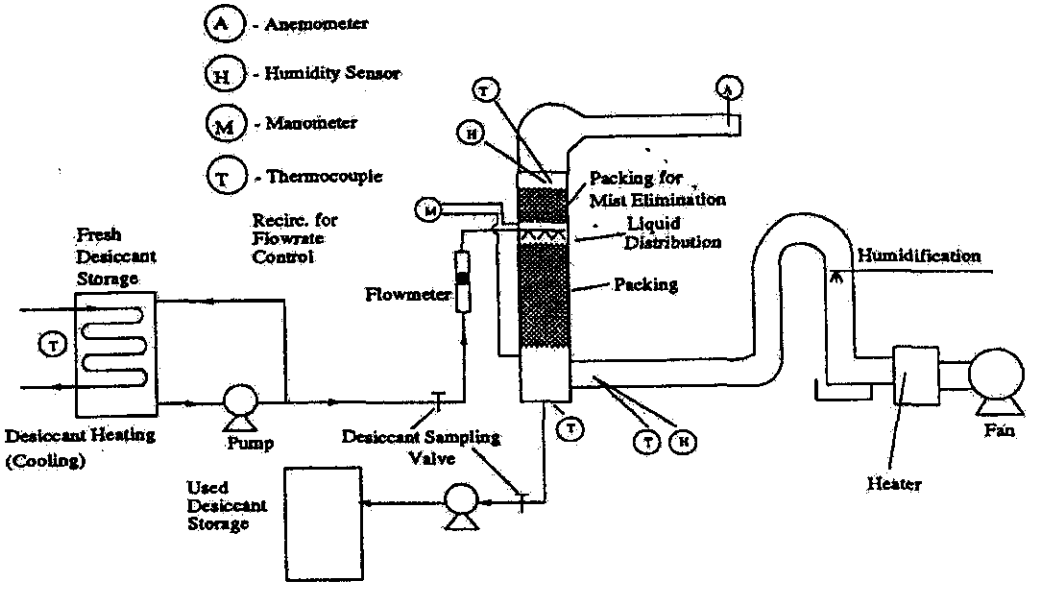

Figure 9. Experimental facility.

Results for Triethylene Glycol Laboratory Tests

Design variables found to have the largest impact on the performance of the packed bed dehumidifier and regenerator are: the air flow rate and the humidity; the desiccant temperature and concentration; and the packed bed height. The fluid flow rate and the air temperature did not

have a significant effect; however, the liquid flow rate must be high enough to ensure adequate wetting of the packing. A humidity effectiveness and an enthalpy effectiveness were defined as effective measures of the performance of the dehumidifiers and regenerators. These were defined as the ratio of the actual change to the maximum possible. Correlations were also developed to model these parameters. As seen from the results in Figures 10 and 11 the humidity effectiveness for TEG was found in the range of 85% to 90% and the enthalpy effectiveness was around 80%. Results show that TEG works well as a desiccant. Its good characteristics are: low vapor pressure so that it readily absorbs moisture from the air, it is noncorrosive which simplifies the equipment materials selection; and it has low surface tension which makes it relatively easy to wet the packing material. However pure TEG does not have a zero vapor pressure and this causes some TEG to evaporate into the air. Despite all the efforts, the use of TEG added a sweet smell to the air. Although triethylene glycol is nontoxic, any evaporation into the supply air stream makes it unacceptable for the use in air conditioning of an occupied building.

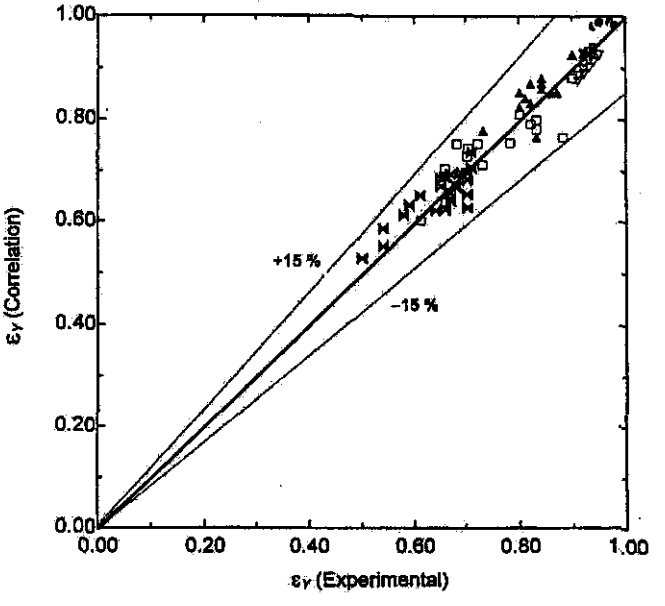

● Chung et al. (1995)–dehumidification, TEG, 13 mm Ceramic Intalox Saddles
▽ Chung et al. (1995)–dehumidification, TEG, 16 mm Polypropylene Flexi Rings
▲ Oberg and Goswami (1998b)–dehumidification, TEG, 25 mm Polypropylene Rauschert Hiflow Rings
□ Oberg and Goswami (1998c)–regeneration, TEG, 25 mm Polypropylene Rauschert Hiflow Rings
⋈ Chung et al. (1993)–dehumidification, LiCl, 16 mm Polypropylene Flexi Rings

Figure 10. Correlation for humidity effectiveness ε_Y for packed bed absorber/regenerator.

For this reason salts solutions such as lithium chloride appear to be better desiccant candidates, even though the salts are corrosive and have higher surface tension as compared to TEG. An analysis of the salts solutions available in the market led to the selection of aqueous solution of lithium chloride as the best candidate to replace the TEG. Therefore, the laboratory tests were repeated for lithium chloride as the desiccant.

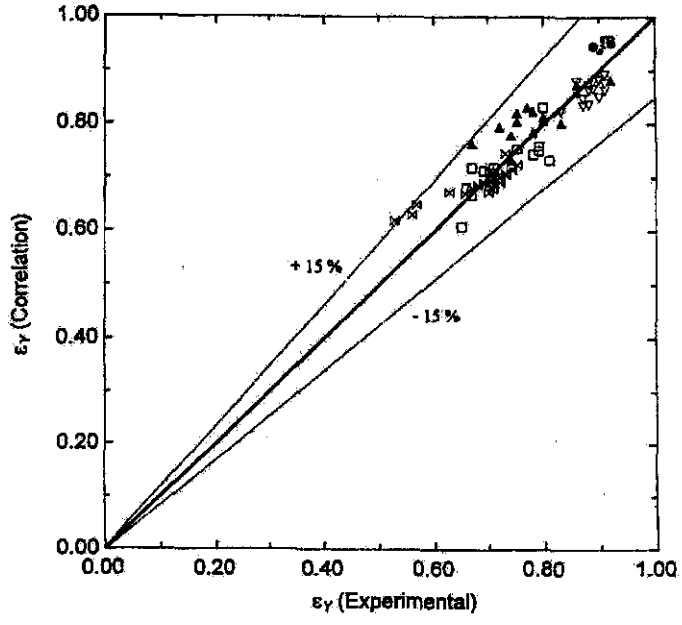

Figure 11. Correlation for enthalpy effectiveness ϵ_H for packed bed absorber/regenerator.

Laboratory Tests for Lithium Chloride

For the laboratory test, 35 % by weight aqueous solution of lithium chloride (LiCI) was used. The experimental facility is the same as described for TEG, with some materials changes to prevent corrosion. For a constant tower height of 60 cm(~2 ft.), the rate of moisture removal from the air (water condensation rate) was studied experimentally as a function of the following variables: air and desiccant flow rates; air temperature and humidity ratio; and desiccant temperature and concentration. For the same variables an analysis of the tower efficiency was done through the humidity effectiveness. Experiments were conducted for each of the six

variables at three levels (low, intermediate, and high value) while keeping the other variables constant. Three experiments were conducted at each level and an average was used in the results. Therefore, a total of 54 experiments were conducted . Appendix C describes the results in detail.

Results for Lithium Chloride Laboratory Tests

The laboratory results show that LiCl has good thermal characteristics as a desiccant, and therefore a good candidate for hybrid solar desiccant air conditioning.

The variables found to have the most significant effect on the dehumidifier performance are: air flow rate, humidity ratio, desiccant temperature, and desiccant concentration. The water condensation rate increases with the air flow rate inlet air humidity ratio, and desiccant concentration. The desiccant flow rate does not cause significant variation in the water condensation rate, however, it must be high enough to ensure wetting of the packing.

For the range of the variables studied, humidity effectiveness for the dehumidifier remains mostly stable, no variation higher than 6% were found. The only clear trends observed were: slight decrease in the humidity effectiveness with air flow rate and air temperature; and slight increase in the humidity effectiveness with desiccant flow rate. The lower value of humidity effectiveness was 75% and the higher 84%.

The regeneration performance is affected significantly by all the variables studied except air temperature. Efficiency of the regenerator is more sensitive than the dehumidifier. For the range of the variables studied, humidity effectiveness for the regenerator varies between 71 and 87%. Two tendencies were noticed from the results. One tendency is the apparent lineal decrease of the humidity effectiveness for an increase in the air flow rate (Fig. 12). The second tendency is the apparent lineal increase of humidity effectiveness with the increase of desiccant flow rate (Fig. 13).

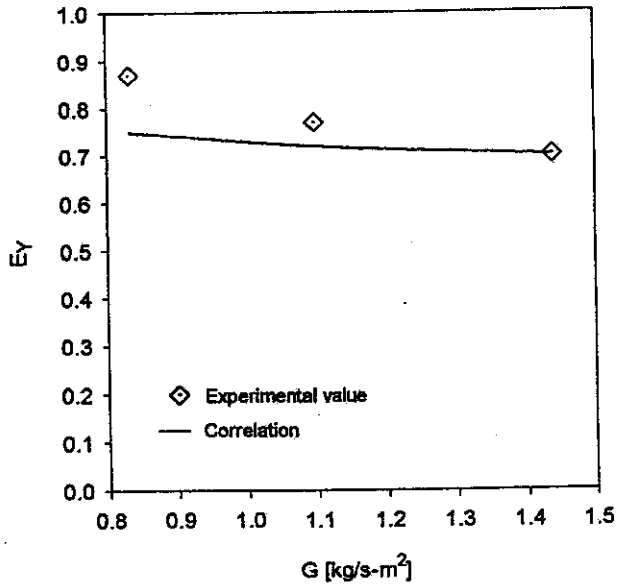

Figure 12. Influence of increased airflow rate on humidity effectiveness.

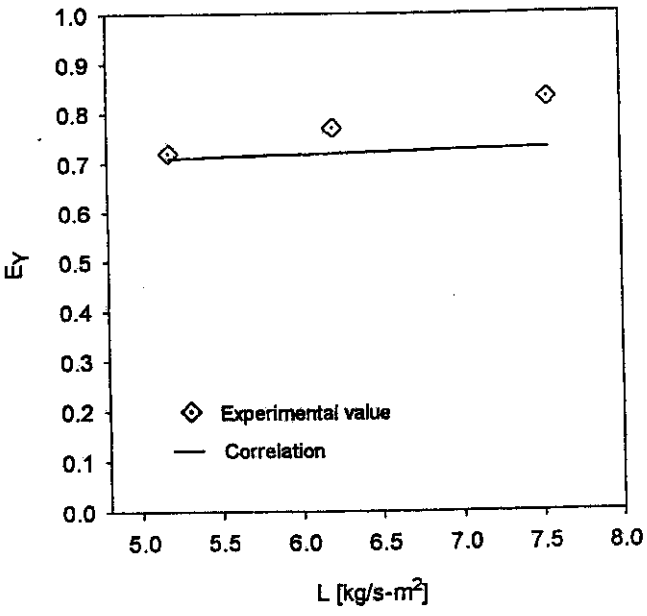

Figure 13. Influence of decreased airflow rate on humidity effectiveness.

FIELD TEST

Field tests of a hybrid solar liquid desiccant cooling system were conducted at the Solar House at the University of Florida's Energy Research and Education Park. These tests consisted of operating the air conditioning system in two configurations – the conventional vapor compression system, and the hybrid desiccant system. Figures 14a and 14b show the air conditioning configuration with a vapor compression system only and Figures 15a and 15b show the configuration with a hybrid desiccant air conditioning system. The system was operated in the two modes (vapor compression system with and without the liquid desiccant system) and the data was collected to compare the performance of both arrangements. In each of the modes, the system was operated with: (a) recirculation air; and (b) 100% ventilation air. Figures 14a and 15a show the arrangement for recirculation air for the two systems, and Figures 14b and 15b show the arrangement for 100% ventilation air for the two systems.

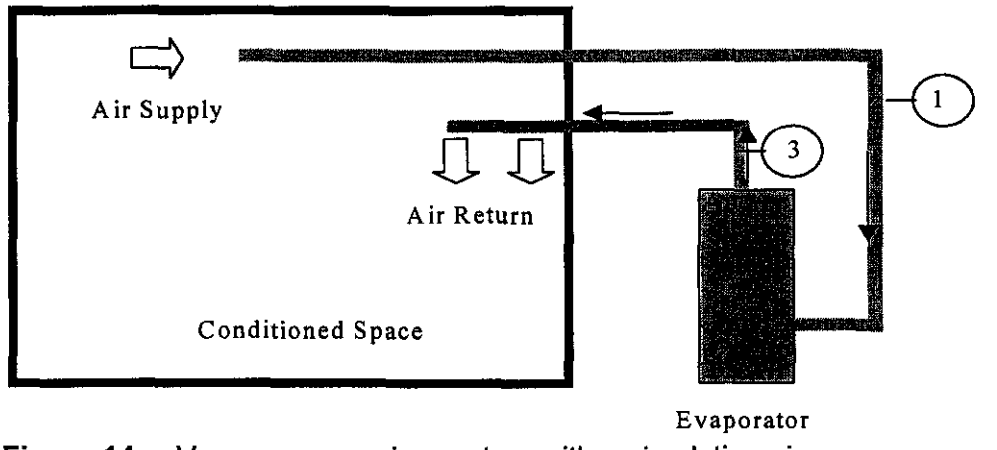

Figure 14a. Vapor compression system with recirculating air.

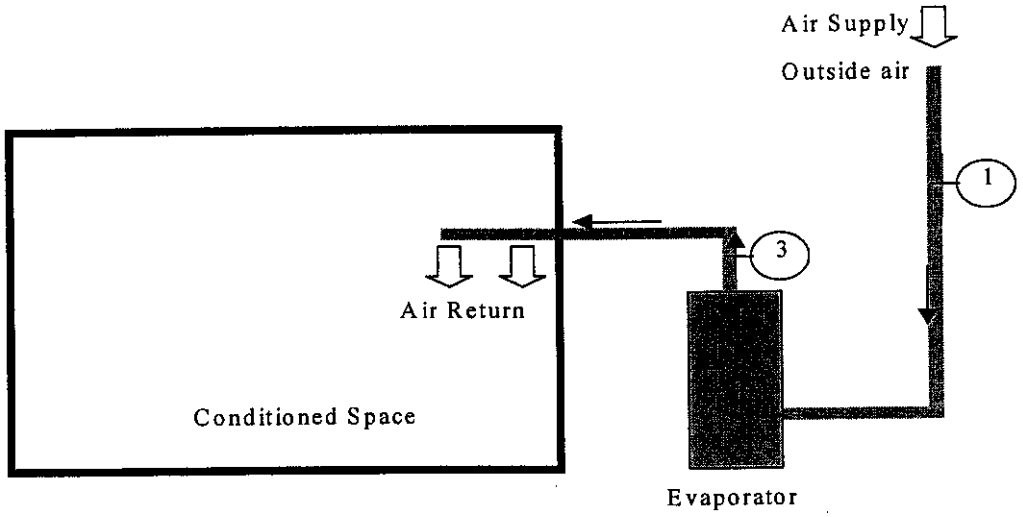

Figure 14b: Vapor compression system with 100% fresh air.

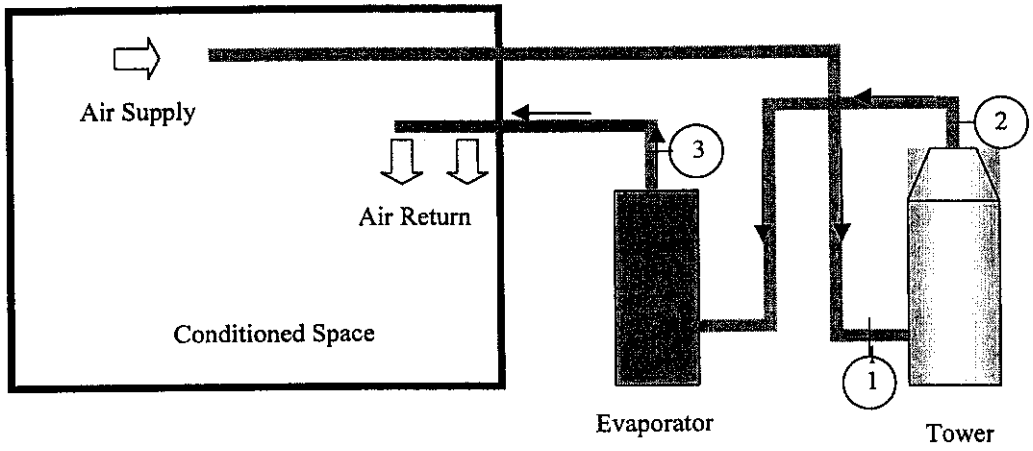

Figure 15a: Liquid desiccant system with recirculating air.

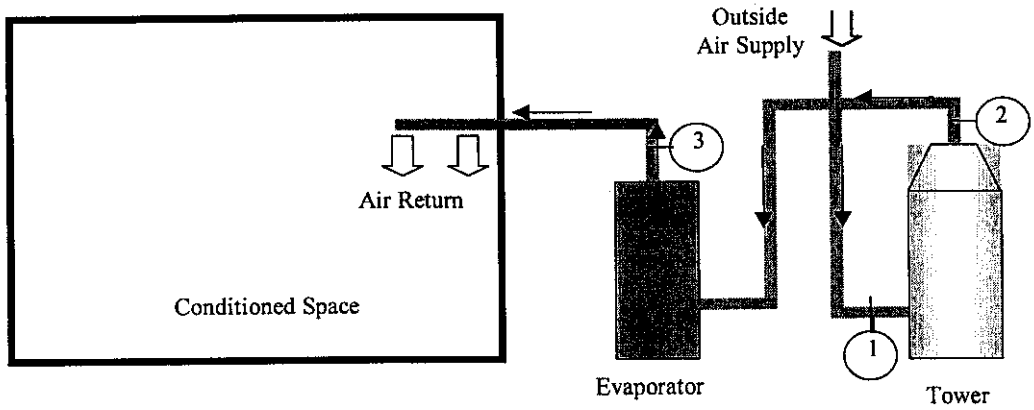

Figure 15b. Liquid desiccant system with 100% fresh air.

FIELD TEST RESULTS

The air conditioning system in the field test house was run in both configurations – the hybrid desiccant system and the conventional vapor compression system, in order to compare their performances. The systems were also run for various air flow rates, inlet air temperatures and desiccant temperatures. The details of these experiments and an analysis of the results is described in Appendix D. Some typical results are described in this section. Tables 1 and 2 show the typical performance results for the vapor compression system and the hybrid liquid desiccant system respectively. The performance was measured for both the systems in the recirculation (Experiment A), and the 100% fresh air (Experiment B) modes.

Table 1. Performance for the Vapor Compression System

System Mode	Conditions of Air Entrance				Conditions of Air Exit				Change of Enthalpy of Air
	Temp. °C (°F)	RH %	Hum. Ratio	Enthalpy KJ/Kg	Temp. °C (°F)	RH %	Hum. Ratio	Enthalpy KJ/Kg	KJ/Kg
A Recirculation	26 (78.8)	53	0.011	54.4	17 (62.6)	80	0.0097	41.5	12.8
B 100% Fresh Air	33 (91.5)	51	0.016	74.4	27 (80.6)	63	0.014	62.5	11.7

Table 2. Liquid Desiccant Cooling System

	Conditions of Air at Entrance of Desiccant Tower				Conditions of Air at Exit of the tower			
System Mode	Tem °C	RH %	Hum. Ratio	Enthalpy KJ/Kg	Tem °C	RH %	Hum. Ratio	Enthalpy KJ/Kg
A	26	53	0.011	54.4	27	40	0.009	49.7
B	33	51	0.016	74.4	34	40	0.013	68.5

Table 2. Liquid Desiccant Cooling System, continued

	Conditions of Air at Exit of Vapor Compression System				Change in Enthalpy of Air		
System Mode	Tem °C	RH %	Hum. Ratio	Enthalpy KJ/Kg	Desiccant Tower KJ/Kg	Vapor Compression System KJ/Kg	System Total KJ/Kg
A	16	78	0.0088	38.6	4.7	11.1	15.8
B	26	54	0.0114	54.9	5.9	13.6	19.5

Experiment A was done with recirculation of the air in the house, and Experiment B was done using 100% fresh air. Comparing Experiment A for both cases, we can see that using the hybrid liquid desiccant cooling system the total change of enthalpy in the system was 16 KJ/Kg, while for the vapor compression system, it was 12.8 KJ/Kg. Therefore, the hybrid liquid desiccant system was able to remove 3.2 KJ/Kg more enthalpy from the air than the conventional vapor compression system. It shows that the capacity of the equipment to extract heat from the air is higher using the liquid desiccant cooling system. Also the change of humidity ratio using liquid desiccant cooling system was almost twice that of the change using the vapor compression system only and the temperature dropped by one degree Celsius (1.8 °F).

Comparing Experiment B (100% fresh air) for both cases we can see that using the hybrid liquid desiccant cooling system the total change of enthalpy in the system was 19.5 KJ/Kg as compared to 11.7 kJ/kg for the vapor compression system only. The change in enthalpy increased by 6.6 KJ/Kg for the hybrid liquid desiccant system. This result shows that the hybrid liquid desiccant cooling system offers more advantage when 100% fresh air is required. It is because the fresh air is much more humid than the recirculation air, and the main function of using the liquid desiccant is to reduce the humidity before the air enters the evaporator. Also, the change in humidity ratio is more than twice with the liquid desiccant system than without it.

Based on these results it is concluded that the hybrid desiccant system improves the air conditioning performance in the field house by decreasing the outlet humidity and temperature of the air. However, the size of the field tests' desiccant system is too small since the vapor

compression system has to condense some moisture in addition to sensible cooling of the air. Ideally, in a hybrid desiccant cooling system, the desiccant system should do all of the dehumidification and the vapor compression system should provide only the sensible cooling. The present desiccant tower height is 0.6m. The system could be optimized by increasing the height of the desiccant tower and decreasing the size of the vapor compression system. The optimized system would not only reduce the electrical consumption but also decrease the peak load significantly by using a smaller size vapor compression system. The following analysis of the electricity consumption is done for the present desiccant tower height of 0.6m and for a height of 2.5m.

ANALYSIS OF ELECTRICITY USE

An analysis of electricity use for both the conventional vapor compression system and the hybrid liquid desiccant system was done for the case of 100% fresh air ventilation since that case

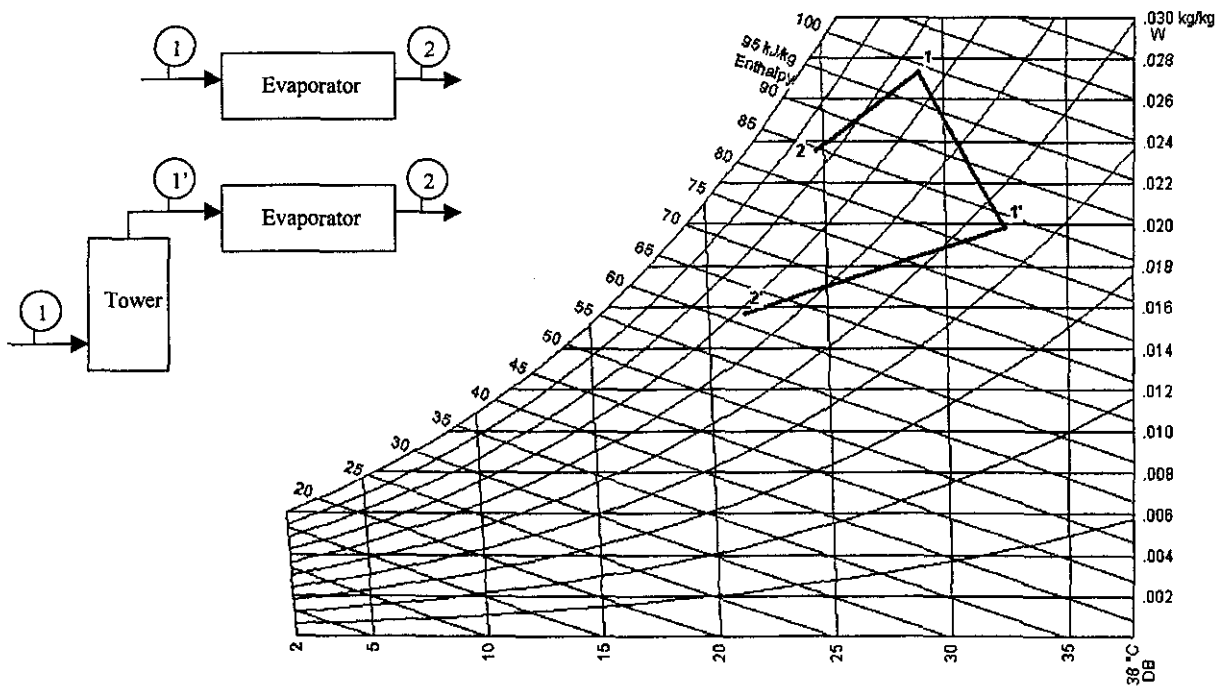

Figure 16. Representation of the air conditioning processes on the psychrometric chart.

shows the most advantage for a hybrid liquid desiccant system. This analysis is based on the actual field test data for the two systems at the Solar test house. The test data is presented in Tables 3a and 3b, and on the psychrometric chart in Figure 16. The air conditioning process using only the vapor compression system is designated as "Process 1-2", and for the hybrid liquid desiccant system it is designated as "Process 1-1'-2". As seen from the data, the vapor compression system provides a total cooling of 6.65 kW or 1.9 tons (approximately 2 tons) which is also the rated capacity of the system. However, it is unable to cool the ventilation air to comfort conditions. By adding the desiccant cooling system to it, the system capacity is increased to 16.86 kW or 4.8 tons (approximately 5 tons), which is able to cool the ventilation air to comfort conditions. Ideally, a hybrid solar desiccant system should be designed such that the desiccant system provides all the dehumidification and the vapor compression system provides only the sensible cooling. Therefore, an optimized system for the test house would have

Table 3a. Experimental results for the Process 1.2, Vapor Compression System

Inlet		Outlet		Change of Enthalpy evaporator (kW)	Rate of condensation evaporator (g/s)
T (°C)	RH (%)	T (°C)	RH (%)		
29	75	24.7	83.7	6.65	1.56

Table 3b. Experimental Results for the Process 1-1'-2, Hybrid Liquid Desiccant System (Air Flow rate = 0.6 kg/s)

Inlet Tower		Outlet Tower		Outlet Evap.		Change of Enthalpy (kW)			Rate of condensation (g/s)		
T (°C)	RH (%)	T (°C)	RH (%)	T (°C)	RH (%)	Tower	Evap	Syst.	Tower	Evap.	Syst.
29	75	32.5	45.1	21.6	68.1	5.77	11.09	16.86	3.10	1.72	4.82

a larger than present desiccant system (tower height 0.6m) and a smaller than present vapor compression system (2 ton). For analysis purposes we increased the desiccant system size while keeping the vapor compression system the same. By increasing the desiccant tower height to 2.5m, the desiccant system provides all of the dehumidification and the vapor compression system provides all of the sensible cooling. The results are shown in Tables 4a and 4b, and on the psychrometric chart in Figure 17. It is seen from these results that a 5.6 ton (nominal 6 tons) vapor compression system is equivalent to a hybrid desiccant system consisting of a desiccant system with a tower height of 2.5m and a vapor compression system of 2.2 tons (nominal 2.5 tons). It means that a hybrid solar desiccant system consisting of a 2.5 ton tower and 2.5 ton (nominal) vapor compression system is equivalent to a 6 ton (nominal) conventional vapor compression system and the two systems will give the same duty cycling characteristics when matched to the same loads. A simple cost analysis is therefore done using the commercially available prices of vapor compression systems for the nominal sizes as noted above. Unfortunately, liquid desiccant systems are not available commercially. Therefore, the cost of a liquid desiccant system is estimated based on the costs of the commercially available components and estimated labor charges.

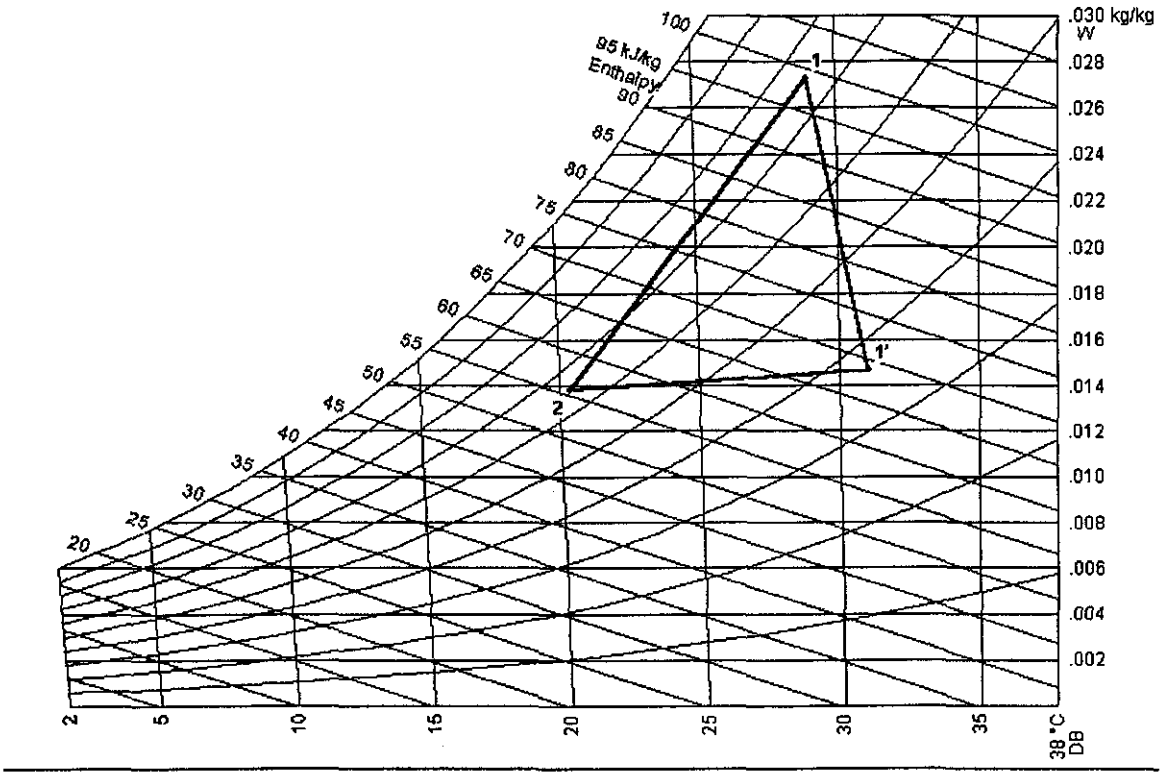

Figure 17. Representation of the air conditioning processes on the psychrometric chart.

Table 4a. Expected Results for Process 1-2, A 5.6 ton (6 ton nominal) Vapor Compression System (Air flow rate = 0.6 kg/S).

Inlet		Outlet		Change of Enthalpy evaporator (kW)	Rate of condensation evaporator (g/s)
T (°C)	RH (%)	T (°C)	RH (%)		
29	75	20.4	65	19.52	5.58

Table 4b. Expected Results for Process 1-1'-2, Hybrid Liquid Desiccant System.
(Tower height 2.5 m, Vapor Compression System Capacity = 7.79 kW=2.21 ton or 2.5 ton nominal).

Inlet Tower		Outlet Tower		Outlet Evap.		Change of Enthalpy (kW)			Rate of condensation (g/s)		
T (°C)	RH (%)	T (°C)	RH (%)	T (°C)	RH (%)	Tower	Evap	Syst.	Tower	Evap.	Syst.
29	75	31.03	37.64	20.4	65	11.69	7.83	19.52	5.06	0.52	5.58

To calculate the electricity consumption for these processes it is assumed that the vapor compression system has a SEER (seasonal energy efficiency ration) equal to 9 Btuh/W. The electricity cost is calculated based on the small commercial rate schedule of FP&L, which is: 3.548¢ / kWh, $6.25/kW demand charge.

Process 1-2. (Vapor Compression System Only)

The cooling capacity of the evaporator is 19.52 kW = 66,602.24 Btuh cooling)

$$\text{Electricity consumption} = 66{,}602.24\,Btuh \times \frac{1W}{9\,Btuh} \times \frac{1kW}{1000W} \times 2000\frac{h}{yr} = 14{,}800.5\frac{kWh}{yr}$$

$$\text{Consumption Cost} = 14{,}800.5\frac{kWh}{yr} \times \frac{\$0.03548}{kwh} = \frac{\$525}{yr}$$

$$\text{Demand Cost} = 7.4kW \times \frac{\$6.26}{kW-month} \times \frac{12months}{yr} = \frac{\$555}{yr}$$

$$\text{Total Cost} = \frac{\$1080}{yr}$$

Process 1-1′-2. (Hybrid Desiccant System)

Since the latent load is satisfied by the desiccant system, a much smaller vapor compression system is needed. The cooling capacity of the evaporator is 7.8 kW = 26,613.6 Btuh cooling)

$$\text{Electricity consumption} = 26{,}613.6\,Btuh \times \frac{1W}{9\,Btuh} \times \frac{1kW}{1{,}000W} \times 2000\frac{h}{yr} = 5{,}914.13\frac{kWh}{yr}$$

$$\text{Consumption Cost} = 5{,}914.13\frac{kWh}{yr} \times \frac{\$0.03548}{kwh} = \frac{\$210}{yr}$$

$$\text{Demand Cost} = 2.95kW \times \frac{\$6.25}{kW-month} \times \frac{12months}{yr} = \frac{\$221}{yr}$$

$$\text{Total Cost} = \frac{\$431}{yr}$$

The savings in electricity costs using a hybrid liquid-desiccant system instead of the vapor compression system alone are $649/yr or 60%.

If we use the residential rate schedule (7.086¢/kWh, no demand charge) the operating costs of the above two systems will be as below:

Conventional system = $1,049/year

Hybrid Solar Desiccant System = $419/year

Savings = $630 or 60%

SOLAR SYSTEM FOR THE REGENERATION PROCESS

A closed loop solar water heating system was chosen for the desiccant regeneration process as shown in Figure 18. As shown by the detailed calculations in Appendix D, for the hybrid desiccant system analyzed, a solar system with four high-efficiency 4-foot x 8-foot solar collectors, a 120-gallon storage tank and the associated hardware such as a pump, piping, etc. would be sufficient to provide the heat needed to regenerate the desiccant. The commercial cost of such a solar system was found to be about $6,530.

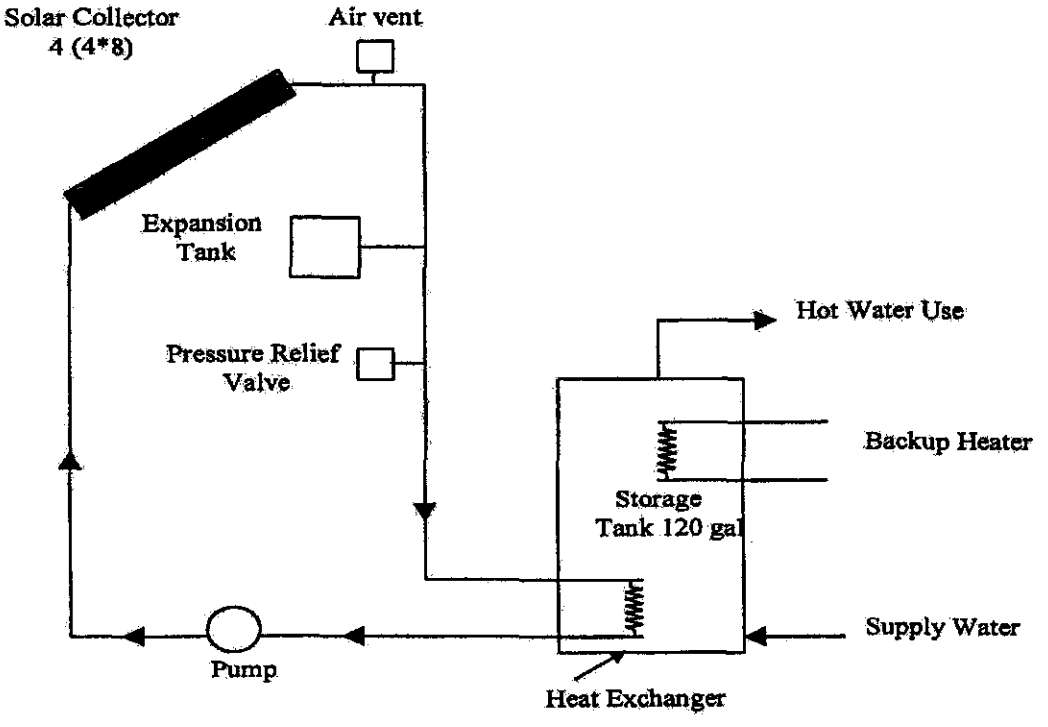

Figure 18. Closed loop system for the regeneration process.

The cooling load for the system analyzed requires a conventional vapor compression unit of 6 tons, which would cost about $2,800. An equivalent hybrid liquid desiccant system would require a desiccant tower of 2.5m height and a vapor compression system of 2.5 tons, with a total cost of $2,250. A solar system for regeneration of the desiccant would cost about $6,530 making the total costs of a solar hybrid liquid desiccant system to be $8,780. Therefore, the additional capital costs due to a solar hybrid liquid desiccant system over the vapor compression system are $5,980. It is estimated that the electrical savings from using the hybrid solar desiccant system would be $649/year, which gives a simple payback of 9.2 years. The actual payback period will be slightly higher than 9.2 years because of additional maintenance costs.

A big advantage of the solar hybrid desiccant system is that it can provide better humidity control, and can meet the load, while a conventional system may not be able to meet the humidity load.

The costs and payback shown above were calculated using reasonable assumptions about the cost of building desiccant systems similar to those used in this study. The liquid desiccant system analyzed in this study is simple to construct; however, it is not available commercially at this time.

REFERENCES

1. ASHRAE. 1997. *Handbook of Fundumentals.* Atlanta, GA: American Society of Heating, Refrigerating and Air-Conditioning Engineers.
2.. Chung, T.-W. 1989. Predictions of the moisture removal efficiencies for packed-bed dehumidification systems. *Solar Engineering -- 1989, Proc. of* the *llth Annual ASME Solar Energy Conf,* San Diego, California, 371-377.
3. Cyprus Foote Mineral Company. *Technical data on lithium bromide and lithium chloride, Bulletins 145 and 151,* Kings Mountain, NC: Cyprus Foote Mineral Company.
4. Dow Chemical Company. 1996. *Calcium Chloride Handbook,* Midland, Michigan: Dow Chemical Company.
5. Dow Chemical Company. 1992. *A guide to glycols.* Midland, Michigan: Dow Chemical Company.
6. Ertas, A., E.E. Anderson, and I. Kiris. 1992. Properties of a new liquid desiccant solution: lithium chloride and calcium chloride mixture. *Sol. Energy* 49: 205-212.
7. Goswami, D.Y., F. Kreith and J.F. Kreider, "Principles of Solar Engineering," Taylor and Francis, N.Y., N.Y., 1999.
8. Kettleborough, C.F., and D.G. Waugaman. 1995. An alternative desiccant cooling cycle. *J. of Sol. EnergyEng.* 117:251-255.
9. Khan, A.Y. 1994. Sensitivity analysis and component modeling of a packed-type liquid desiccant system at partial load operating conditions. *Int. Journal Res.* 18: 643-655.
10. Klein, S., et al., 1990. "TRNSYS—A Transient System Simulation Program, Verson 13.1, Solar Energy Laboratory, University of Wisconsin, Madison, WI.
11. Meckler, H. 1994. Desiccant-assisted air conditioner improves IAQ and comfort. *Heating. Piping & Air Conditioning* 66(10): 75-84.
12. Meckler, M. 1995. Desiccant outdoor air preconditioners maximize heat recovery ventilation potentials. *ASHRAE Transactions,* 101, Pt. 2,992-1000.
13. Meckler, M. 1988. "Off-peak desiccant cooling and cogeneration combine to maximize gas utilization." *ASHRAE Transactions,* 94, Pt. 1: 575-596.

14. Meckler, M., Y.O. Parent, and A.A. Pesaran. 1993. Evaluation of dehumidifiers with polymeric desiccants. *Gas Institute Report,* Contract No.5091-246-2247. Chicago, Illinois: Gas Research Institute.

15. Öberg, V., and D.Y. Goswami. 1998. Experimental study of heat and mass transfer in a packed-bed liquid desiccant air dehumidifier. In J.H. Morehouse and R.E. Hogan, (Eds.) *Solar Engineering,* 155-166.

16. Öberg, V., and D.Y. Goswami. 1998. A review of liquid desiccant cooling. *Advances in Solar Energy,* ASES 12: 431-470.

17. Pesaran, A.A., T.R. Penney, and A.W. Czanderna. 1992. Desiccant cooling: State-of-the-art assessment. *National Renewable Laboratory,* Golden Colorado, NREL, Report No. NREL/TP-254-4147, October.

18. Rangarajan, K., D.B. Shirley, 1111, and R.A. Raustad. 1989. Cost-effective HVAC technologies to meet ASHRAE Standard 62-1989 in hot and human climates." *ASHRAE Trans.,* Pt. I: 166-182.

19. Spears, J.W., and 3. Judge. 1997. Gas-fired desiccant system for retail super center. *ASHRAE Journal* 39: 65-69.

20. Thornbloom, M., and B. Nimmo. 1995. An economic analysis of a solar open cycle desiccant dehumidification system. *Solar Engineering -- 1995, Proc. of the 13th Annual ASME Conference,* Hawaii 1:705-709.

21. Thornbloom, M., and B. Nimmo. 1996. Impact of design parameters on solar open cycle liquid desiccant regenerator performance. *SOLAR '96, Proc. of 1996 Annual Conf. of the American Solar Energy Society,* Asheville, NC, 107-1ll.

22. Ullah, M.R., C.F. Kettleborough, and P. Gandhidasan. 1988. Effectiveness of moisture removal for an adiabatic counter-flow packed tower absorber operating with $CaCl_2$-air contact system. *Jour. of Solar Energy Eng.* 110:98-101.

23. Zaytsev, 1.0., and G.G. Aseyev. 1992. *Properties of aqueous solutions of electrolytes.* Boca Raton, Florida: CRC Press.

APPENDIX A

Performance Simulation of Solar Hybrid Liquid Desiccant Cooling for Ventilation Air Pre-Conditioning

Performance Simulation of Solar Hybrid Liquid Desiccant Cooling for Ventilation Air Pre-Conditioning

ABSTRACT

The performance of solar hybrid liquid desiccant cooling for ventilation air pre-conditioning has been simulated for the month of August in Miami, Florida. In the system analyzed, triethylene glycol was used as the desiccant. The air dehumidifier and the desiccant regenerator consisted of packed bed absorption towers, with the heat required for desiccant regeneration provided by a solar collector/storage subsystem. Performance of the desiccant system was analyzed as a function of system design parameters such as the desiccant storage volume, the regenerator size, the hot water storage volume, and the solar collector area. The chiller electrical energy requirement, the regeneration auxiliary energy demand, and the solar fraction for regeneration were evaluated as functions of the variables listed above. The simulation revealed that by using solar hybrid liquid desiccant cooling for ventilation air pre-conditioning in a hot and humid climate, as much as 80 % electrical energy can be saved compared to a conventional vapor compression system. However, if electrical energy is to be used as auxiliary energy for the desiccant regeneration, a large solar fraction for regeneration (> 0.86) is needed in order to save electrical energy compared to a conventional system.

1. INTRODUCTION

Conditioning of ventilation air in a hot and humid climate is an energy intensive process. Since ventilation air must be adequately dried for building humidity control, the ratio of latent to total cooling load is large. A number of strategies are possible for ventilation air conditioning, as examplified by Rengarajan et al. (1996). In this study, the increased ventilation requirement due to ASHRAE Standard 62-1989 was found to increase the annual energy requirement and operating cost by 10-15 % for a large office building in Miami, Florida. Through mathematical modeling, the authors found that the conventional vapor compression system was unable to meet the increased latent cooling load, with the result that the indoor relative humidity frequently exceeded 60 %. Pre-treating the outside air with a 100 % outside air DX (direct expansion) unit or a gas fired desiccant unit maintained the indoor relative humidity below 60 % for a larger part of the time (95 %), as compared to pre-treatment using a heat pipe assisted water coil (90 % of the time) and an enthalpy recovery wheel (93 to 95 % of the time). Also, the desiccant system was found to reduce the annual electric energy use significantly. Other researchers have demonstrated the viability of desiccant systems for ventilation air conditioning. For example, Meckler (1995) showed that the installed chiller capacity could be reduced by 30 % by using the desiccant pre-conditioning unit. Thornbloom and Nimmo (1995) compared a solar liquid desiccant dehumidification system to a conventional vapor compression system for treating the ventilation air required for a supermarket in Miami, Florida. In their system, calcium chloride was used as the desiccant and it was regenerated in a trickle solar collector regenerator. A packed bed dehumidifier handled the latent cooling and a vapor compression unit handled the sensible cooling. A cost analysis showed that the annual operating cost of the desiccant system was significantly lower than for a conventional system. In

another recent study, Spears and Judge (1997) presented results from a one year evaluation of a gas-fired desiccant ventilation air conditioner for a Wal-Mart super center. The control of the indoor humidity was significantly better in the store that used the desiccant system as compared to a store using standard air conditioning. Besides the benefit of improved comfort, the store using the desiccant system saved 13 % energy compared to the control store.

With such promising results, desiccant cooling is of great interest for the application of ventilation air pre-conditioning. Of the two basic types of desiccants, liquid desiccants offer some advantages over solid desiccant systems: the pressure drop through a liquid desiccant system is smaller than the pressure drop through a solid desiccant wheel (Howell, 1987); the ability to pump the liquid makes it possible to connect several small dehumidifiers to one large regeneration unit (Harriman, 1992), which may be advantageous in large buildings; and concentrated desiccant may be stored for use during the times when no suitable source of regeneration heat is available. This paper gives the results from a system performance simulation of solar hybrid liquid desiccant ventilation air conditioning for the month of August in Miami, Florida. A desiccant dehumidification system handles the latent cooling load, while a conventional chiller is used to sensibly cool the air. The system examined in this study uses triethylene glycol as a desiccant and packed bed absorbers as the dehumidifier and the desiccant regenerator. Solar heat is provided indirectly through a solar collector/storage system. Findings from a previously conducted experimental and theoretical study of the performance of the packed bed dehumidifier/regenerator (Goswami and Öberg, 1997) were used as the basis for the design of these components. The present investigation focuses on the influence of system design parameters such as the desiccant storage volume, the regenerator size, the hot water storage volume, and the solar collector area. Insight into

the design of solar hybrid desiccant systems is provided through an evaluation of the chiller electrical energy requirement, the regeneration auxiliary energy demand, and the solar fraction for regeneration, as functions of the parameters listed above.

2. SIMULATION MODEL DESCRIPTION

This study simulates the pre-conditioning of 0.5 m^3/s (1000 cfm) ventilation air using a solar hybrid liquid desiccant system (Figure 1), and compares the electrical energy requirement for this process to that of a conventional system. The air is assumed to be cooled and dehumidified from the ambient conditions to 24 ° C and 50 % relative humidity, corresponding to a humidity ratio Y=9.5 g/kg. In the desiccant system, the air is dried in a packed bed dehumidifier before it is sensibly cooled by the chiller. Before the desiccant (95 % by weight triethylene glycol) enters the dehumidifier, it is cooled by exchanging heat with water from a cooling tower. Desiccant storage provides a buffer so that the desiccant can be regenerated during the hours of the day when solar energy is available. In this study, it was assumed that the regenerator operates at a constant desiccant flow rate between 10 AM and 7 PM solar time, and that no regeneration takes place during the rest of the day. For regeneration, the desiccant is heated and brought into contact with a moisture scavenging air stream in a packed bed tower. The temperature of the desiccant entering the regenerator is set at 65 °C, with regeneration heat provided by a flat plate solar collector and hot water storage subsystem, and by an auxiliary source if needed.

The performance simulation was carried out in three steps. Initially, hourly weather data for the month of August in Miami, Florida, was obtained using a weather generating subroutine available in the simulation program TRNSYS (Klein et al., 1990). Next, the performance of the

system, excluding the solar subsystem, was modeled by carrying out mass and energy balances on each component. This analysis was conducted using a Fortran computer program. Hourly chiller loads and regeneration energy requirement for the desiccant system were calculated as a function of the desiccant storage volume and the desiccant flow rate to the regenerator during daytime hours. This flow rate influences the size of the regenerator part of the system, including the size of the solar subsystem. The electrical energy requirements to meet the chiller loads were found by dividing the cooling loads by the coefficient of performance (COP). In the desiccant system, the chiller mostly handles the sensible cooling load. Thus, it should be noted that since the air does not have to be cooled below its dew point to condense moisture, the chiller may be able to operate at a higher evaporator temperature compared to that in a conventional system. Therefore, the COP for the chiller in the desiccant system may be higher than the COP for a conventional chiller. Nevertheless, a constant COP of 2.9 (corresponding to an EER=10) was assumed for both chillers in this study. Finally, using the hourly regeneration heat requirement obtained from the simulation described above, the solar hot water storage subsystem was modeled separately using TRNSYS (Klein et al., 1990). Results from this part of the simulation included the monthly solar fraction for regeneration (i.e., the part of the regeneration heat provided by solar energy), and auxiliary energy requirement as a function of the hot water storage volume and the solar collector area. For this simulation, the solar collectors were at a tilt angle of 20 °, facing south.

Components in the desiccant system were described using algebraic equations representing energy and mass balances, with certain simplifying assumptions described below. The cooling tower was modeled by using a linear relationship between the temperature of the water leaving the cooling tower and the ambient wet bulb temperature. This relationship was obtained from a curve

fit of cooling tower performance data given by ASHRAE (1992). The performance of the packed bed dehumidifier and regenerator was modeled using the following realtionships: a dehumidification effectiveness, ϵ_Y (equation 1), defined as the actual change in humidity ratio across the packed bed divided by the maximum possible change; and an enthalpy effectiveness, ϵ_H (equation 2), defined as the actual change in air enthalpy across the packed bed divided by the maximum possible change.

$$\epsilon_Y = \frac{Y_{IN} - Y_{OUT}}{Y_{IN} - Y_{equ}} \tag{1}$$

$$\epsilon_H = \frac{H_{a,IN} - H_{a,OUT}}{H_{a,IN} - H_{equ}} \tag{2}$$

Here, subscript equ refers to the value of the humidity ratio and enthalpy of air in equilibrium with the desiccant at the local desiccant temperature and concentration. Both the dehumidification effectiveness and the enthalpy effectiveness were assumed to be constant at 0.8. Findings from experimental and theoretical modeling of the packed bed absorber/regenerator have shown that this is a conservative assumption, as the values may be as high as 0.9 (Goswami and Öberg, 1997). In keeping with the operating ranges specified by Goswami and Öberg (1997), the liquid to air mass flow ratios in the dehumidifier and the regenerator were set at 4.5 and 3.75, respectively. It should also be noted that only the amount of air necessary to meet the load is passed through the dehumidifier. That is, if the conditions of the air and the desiccant entering are such that the humidity ratio of the air leaving the dehumidifier will be lower than 9.5 g/kg, some of the air is

bypassed so that the humidity ratio at the mixing point following the dehumidifier is 9.5 g/kg. The desiccant flow rate through the dehumidifier is then adjusted to maintain the same liquid to air mass flow ratio. Furthermore, if the dehumidifier cannot meet 100 % of the latent load, the remaining latent cooling requirement is imposed on the chiller. The effectiveness of the liquid-to-liquid heat exchangers was assumed to be 0.8, and the effectiveness of the air-to-air heat exchanger in the regenerator section was assumed to be 0.6.

In the system simulation, desiccant storage volumes between 2.5 m^3 and 10 m^3 were considered, and the desiccant flow rate to the regenerator was varied between 7650 kg/hr and 12000 kg/hr. The performance of the solar system was modeled using the output from the system simulation for the case with 5 m^3 desiccant storage and the desiccant flow rate to the regenerator equal to 7650 kg/hr. With this flow rate, and assuming that the amount of air to be exhausted from the building equals the amount of ventilation air, dry return air can be used in the regenerator , which gives the desired desiccant to air flow ratio 3.75. In the solar subsystem simulation, the solar collector area was varied between 200 m^2 and 600 m^2, and the hot water storage volume was varied between 5 m^3 and 15 m^3. Due to additional system components in the desiccant system compared to the conventional system some parasitic electrical energy will be required, e.g., pumping power for desiccant and water, and additional fan power due to increased system air pressure drop. For the present study, these parasitic energy requirements have been assumed negligible compared to the fan and chiller power requirement of a conventional system.

3. RESULTS AND DISCUSSION

Figure 2 shows the daily solar radiation incident on the solar collectors for the month of August in Miami, Florida. The daily cooling loads necessary to bring 0.5 m^3/s from the ambient conditions to 24 °C and 50 % relative humidity are plotted in Figure 3. It can be seen that the latent cooling load makes up a large part of the total cooling load. The system performance is presented below as a function of design parameters such as storage size and collector area.

3.1. Effect of desiccant storage volume and desiccant regenerator size.

The driving force for the mass transfer process in the dehumidifier is the difference in the vapor pressures in the air and the desiccant. When the desiccant vapor pressure is lower than the vapor pressure in the air, water is absorbed from the air into the desiccant. A higher desiccant concentration and/or a lower desiccant temperature decreases its vapor pressure. In order to meet the dehumidification requirement of the ventilation air conditioning, the desiccant concentration and temperature entering the dehumidifier must be such that the equilibrium air humidity ratio at the top of the dehumidifier (Y_{equ}) is low enough so that the outlet air humidity ratio (Y_{OUT}) can meet the load. During the hours when the regenerator is not operating, the desiccant concentration in the storage will steadily decrease. At some point, it may be too low to satisfy the latent cooling requirement. The average concentration in the desiccant storage tank during a 24 hour period can be maintained at higher levels by increasing the storage volume, by regenerating for longer hours, and/or by increasing the desiccant flow rate to the regenerator during the hours when the regenerator is operating. For a given packed bed height, if the inlet conditions of the air and desiccant to the regenerator, and the liquid to air mass flow ratio are constant, the change in the desiccant

concentration through the regenerator is constant regardless of the desiccant flow rate. Thus, by increasing the desiccant flow rate to the regenerator, more water is removed from the desiccant storage per unit time. However, increasing the desiccant flow rate requires a larger regenerator, making a larger solar subsystem necessary.

Figure 4 shows the monthly percent latent load met by the dehumidifier, as a function of the desiccant storage volume and the desiccant flow rate to the regenerator. Over 90 % of the latent load is met by the desiccant system for the entire range of operating conditions. The percent of the latent load met by the dehumidifier slightly increases with increasing desiccant flow rate and/or increasing desiccant storage volume. Figure 4 also shows the percent electrical energy saved at the chiller, which is only marginally influenced by the two parameters. In summary, Figure 4 illustrates that in order to handle 100 % of the latent load in the dehumidifier, the desiccant storage volume and the desiccant flow rate to the regenerator must be very large. However, the resulting additional electrical energy savings at the chiller may be insignificant, so it is more advisable to size the system at lower percentages.

3.2. Effect of hot water storage volume and solar collector area.

The amount of auxiliary energy is a function of the amount of solar heat provided by the solar subsystem. Therefore, the monthly auxiliary energy requirement was determined as a function of the hot water storage size as well as the solar collector area, as shown in Figure 5 (a). For a given hot water storage volume, the auxiliary energy requirement decreases rapidly with increasing solar collector area until a collector area is reached where the slope of the curve flattens out. Figure 5 (b) shows the daily auxiliary energy requirement for three days with varying cloudiness. For a very

clear day (August 16) the auxiliary energy requirement is eliminated by using a collector area of 300 m^2, while for a very cloudy day (August 11) increasing the collector area has no effect on the auxiliary energy requirementl. Figure 5 (a) displays that a combination of large collector area and large hot water storage volume gives the largest reduction in auxiliary energy requirement. However, not even 600 m^2 collector area in combination with a 15 m^3 hot water storage eliminates the need for auxiliary energy to pre-condition 0.5 m^3/s (1000 cfm) ventilation air.

It is also of interest to know the fraction of the regeneration energy that can be provided by solar energy. Figure 6 (a) shows the monthly percent solar energy for regeneration as a function of the hot water storage volume and the solar collector area. For a fixed solar collector area, increasing the hot water storage volume from 5 m^3 to 10 m^3 significantly increases the percent of the regeneration energy that is provided by solar energy. An additional increase of the storage volume from 10 m^3 to 15 m^3 does not have as large an effect. Also, for a given hot water storage volume, as the solar collector area increases the percent solar energy for regeneration increases. However, as the solar collector area becomes large the slope of this curve levels off. Figure 6 (b) shows that for a very clear day, a 300 m^2 collector area makes it possible for the solar subsystem to provide all of the regeneration heat. However, on a very cloudy day the solar system does not provide any heat for regeneration regardless of collector area.

Figures 5 and 6 indicate that to design a system using 100 % solar energy for regeneration would require a very large solar collector area in combination with a very large hot water storage volume. Thus, it seems more likely that a system would use some auxiliary energy. Figure 7 shows that a linear relationship exists between the auxiliary energy requirement and the percent solar energy used for regeneration as obtained from all the simulations performed on the solar subsystem.

The monthly electrical energy saving at the chiller as compared to a conventional system is also indicated in Figure 7. The auxiliary energy requirement cannot be larger than the electrical savings at the chiller if electrical heaters are to be used for supplementary regeneration energy. Thus, the minimum percent solar for using electrical auxiliary energy is found from the curve fit by setting the auxiliary energy requirement equal to the savings at the chiller. In this study, this minimum value was found to be about 86 %. Similarly high values (about 88 %) were obtained by Hernández et al. (1996) in their performance analysis of a solar-assisted hybrid liquid desiccant system combining a solar absorption chiller with a desiccant dehumidifier.

3.3. Low temperature and low concentration desiccant system.

Operating the desiccant system at a temperature below 20 °C has been suggested as an alternative mode of operation. Sick et al. (1988) studied a liquid desiccant system in which the desiccant was cooled in a chiller before entering the dehumidifier. Thus, both latent and sensible cooling of ventilation air was obtained in the packed bed desiccant conditioner. Because of its simplicity, such a configuration appears attractive. Furthermore, when using triethylene glycol as the desiccant, lower temperatures will minimize the evaporation of glycol in the dehumidifier. Chung et al. (1995 and 1993) carried out experimental studies of the dehumidification of air in packed bed absorption towers using desiccant temperatures between 15 °C and 21 °C. In a humid climate, such low desiccant temperatures are not always possible to obtain by using cooling water from a cooling tower, so cooling using a chiller may be required.

To examine the use of a cool and more dilute desiccant in the solar hybrid desiccant system, a simulation was carried out for an average day in Miami Florida, using triethylene glycol at 20 °C.

Because the desiccant is now cooler, a more dilute desiccant can be used while still maintaining the vapor pressure low enough to achieve dehumidification. The system layout was modified as shown in Figure 8. By using the cool desiccant, both the dehumidification and sensible cooling of the air took place in the dehumidifier. The chiller was placed between the desiccant storage tank and the dehumidifier. Overall, this layout decreases the number of system components, which could help in reducing the first cost of the system. Another benefit of operating at low desiccant temperature and concentration is that the desiccant temperature at the regenerator entrance is now 45 °C compared to 65 °C when using a higher desiccant concentration. A lower regeneration temperature results in a higher efficiency of the solar collectors.

Results from the simulation of the low desiccant temperature desiccant are shown in Figure 9. The hourly chiller load of this system is compared to that of a conventional vapor compression system. As shown, the desiccant system has a much higher chiller load compared to a conventional system. This is due to the parasitic heat added to the desiccant storage, especially during the hours of regeneration (10 AM to 7 PM). Configurations where a cooling tower was added between the desiccant storage and the chiller and between the regenerator side and the desiccant storage were also examined. No significant improvement of the desiccant system was obtained by these additions, which can be attributed to the high wet bulb temperatures in Miami. Therefore, despite the apparent benefits of using a cool dilute desiccant, it is not desirable from an energy point of view. These findings differ from the results presented by Sick et al. (1988), who showed the chiller load and the operating cost to be reduced for the solar desiccant system as compared to a conventional system. This may be explained by the lower ratio of desiccant flow rate to air flow rate in the dehumidifier as compared to the ratio in the present study. For a lower desiccant to air flow

ratio, the amount of desiccant to be cooled per unit mass of air to be conditioned is lower. As previously mentioned, the higher desiccant flow rates employed in the present study were selected based on experiments conducted on a packed bed absorption tower (Goswami and Öberg, 1997). With a low flow rate, adequate wetting of the packing was not possible, and resulted in low effectiveness of the dehumidification and regeneration processes. Thus, in actual desiccant cooling systems, the need for relatively high desiccant to air flow ratios may severely penalize this particular configuration.

4. CONCLUDING REMARKS

By using solar hybrid liquid desiccant cooling for ventilation air pre-conditioning in a hot and humid climate, as much as 80 % electrical energy can be saved compared to a conventional vapor compression system. If electrical energy is to be used as auxiliary energy for the desiccant regeneration, a large solar fraction for regeneration (> 0.86) is needed in order to save electrical energy compared to a conventional system. Because of cloudy days where no useful energy is provided by the solar system, very large collector area and hot water storage volume are required in order to obtain such high monthly solar fractions.

Since the simulation was conducted on a per air flow rate basis, the results presented in this paper can be scaled up or down depending on the flow rate needed. Some cases where ventilation air pre-conditioning may result in large annual electrical energy savings and improved indoor humidity control are laboratories, supermarkets, and health care facilities. Therefore, future studies of desiccant cooling for these applications are warranted.

NOMENCLATURE

COP	coefficient of performance
EER	energy efficiency ratio (ratio of cooling in Btu/h to the electrical power input in W)
H	enthalpy (kJ/kg)
I_T	solar radiation incident on a tilted surface (MJ/m^2-DAY)
Q	energy requirement (GJ/DAY, MJ/DAY, or GJ/month)
Y	air humidity ratio (kg water/kg dry air or g water/kg dry air)
ϵ_H	enthalpy effectiveness
ϵ_Y	dehumidification effectiveness

Subscripts

a	air
equ	equilibrium
IN	inlet
OUT	outlet

REFERENCES

ASHRAE, 1992, ASHRAE Systems and Equipment Handbook, American Society of Heating, Refrigerating and Air-Conditioning Engineers, Inc., Atlanta, Georgia.

Chung, T.-W., Ghosh, T. K., Hines, A. L., and Novosel, D., 1995 , "Dehumidification of Moist Air with Simultaneous Removal of Selected Pollutants by Triethylene Glycol Solutions in a Packed-Bed Absorber", Separation Science and Technology, 30(7-9), pp. 1807-1832.

Chung, T.-W., Ghosh, T. K., and Hines, A. L., 1993, "Dehumidification of Air by Aqueous Lithium Chloride in a Packed Column", Separation Science and Technology, 28(1-3), pp. 533-550.

Goswami, D. Y., and Öberg, V., 1997, Solar Hybrid Liquid Desiccant Air Conditioning Demonstration, Report No. UFME/SEECL-9705, Solar Energy and Energy Conversion Laboratory, University of Florida, 1997.

Harriman, L. G., 1992, The Dehumidification Handbook, 2nd edition, Munters Cargocaire, Amesbury, MA.

Hernández, H. R., González, J. E., and Khan, A. Y., 1996, "Modeling of a Solar-Assisted Absorption/Desiccant System for Applications in Puerto Rico and the Caribbean", Proceedings of 1996 Annual Conference of the American Solar Energy Society, Asheville, NC, Technical Papers, pp. 124-132.

Howell, J. R., 1987, "A Survey of Active Solar Cooling Methods", Progress in Solar Engineering, Goswami, D. Y., editor, pp. 171- 182.

Klein et al., 1990, TRNSYS - A Transient System Simulation Program, Version 13.1, Solar Energy Laboratory, University of Wisconsin - Madison, Madison, Wisconsin.

Meckler, M., 1995,"Desiccant Outdoor Air Preconditioners Maximize Heat Recovery

Ventilation Potentials", ASHRAE Transactions, pt. 2, pp. 992-1000.

Rengarajan, K., Shirey, D. B. III, and Raustad, R. A., 1996, "Cost-Effective HVAC Technologies to meet ASHRAE Standard 62-1989" in Hot and Humid Climates", ASHRAE Transactions, pt. 1, pp. 166-182.

Sick, F., Buschulte, T. K., Klein, P., Northey, P., and Duffie, J. A., 1988, "Analysis of the Seasonal Performance of Hybrid Liquid Desiccant Cooling Systems", Solar Energy, 40, pp. 211-217.

Spears, J. W., and Judge, J., 1997, "Gas-Fired Desiccant System for Retail Super Center", ASHRAE Journal, 39, pp. 65-69.

Thornbloom, M., and Nimmo, B., 1995, "An Economic Analysis of a Solar Open Cycle Desiccant Dehumidification System", Proceedings of the 13th Annual ASME Conference, Solar Engineering - 1995, Hawaii, 1, pp. 705-709.

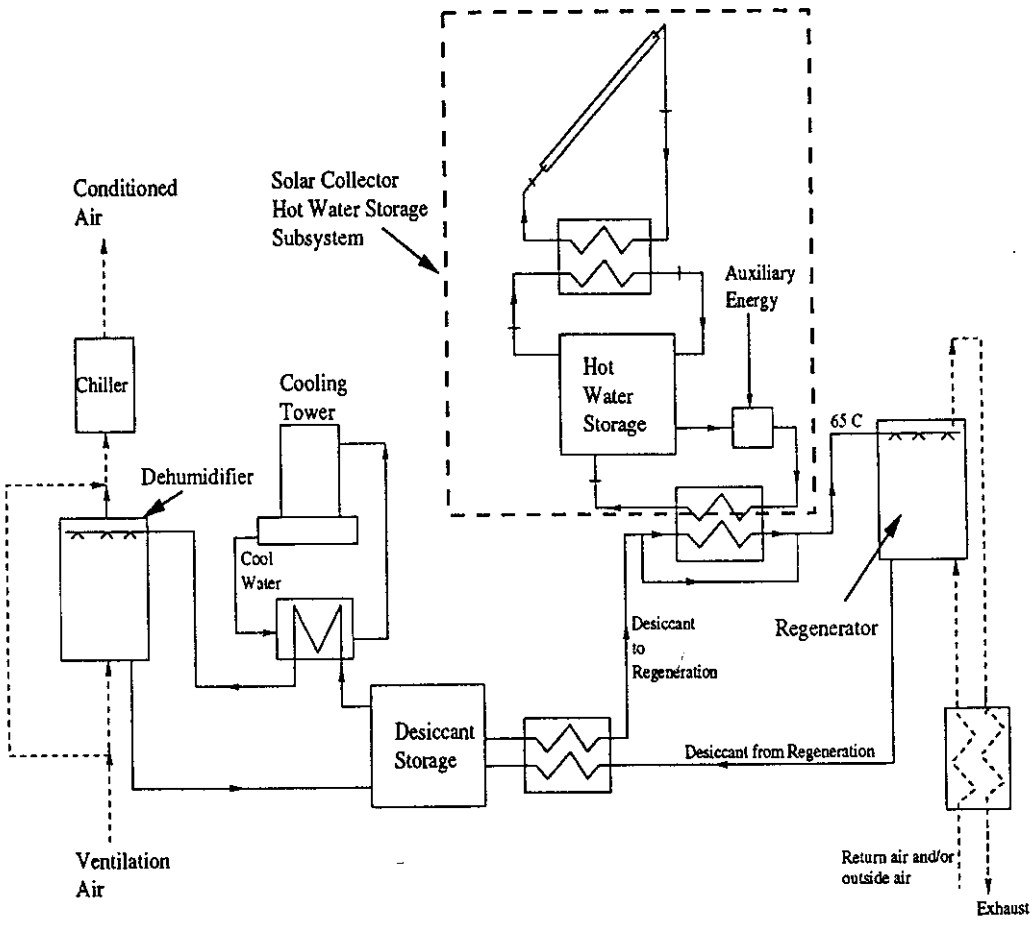

Figure 1. Solar hybrid liquid desiccant cooling system for ventilation air pre-conditioning.

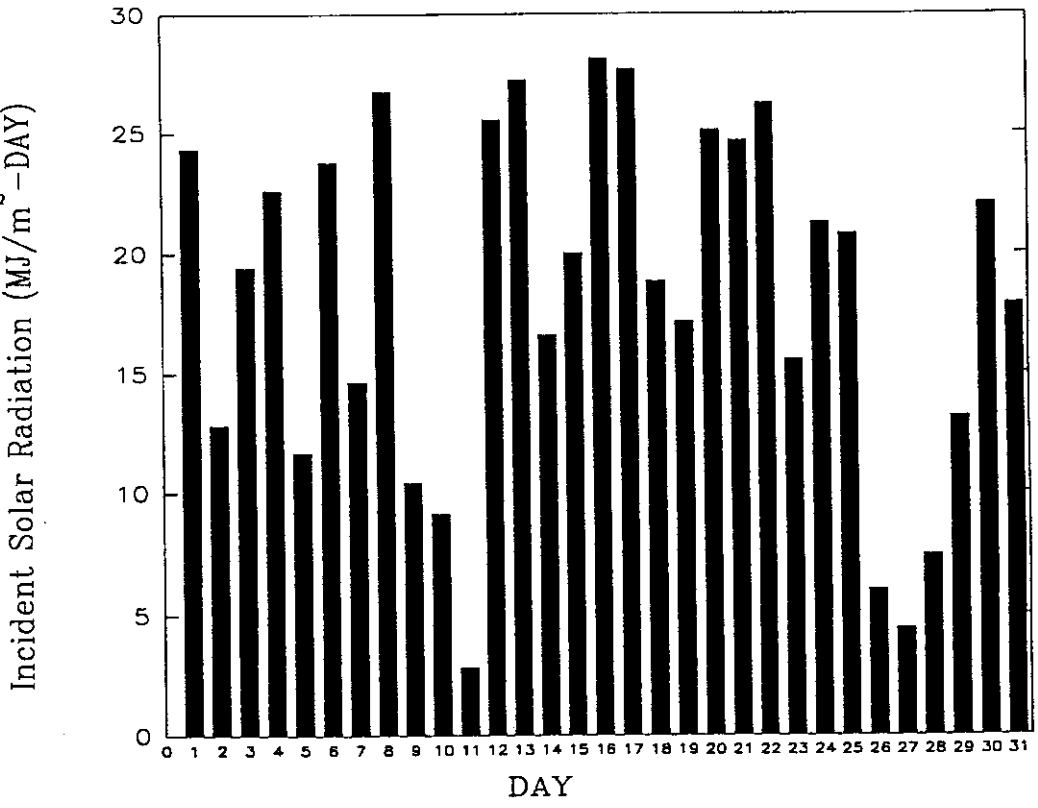

Figure 2. Daily solar radiation incident on the tilted collector surface for the month of August in Miami, Florida.

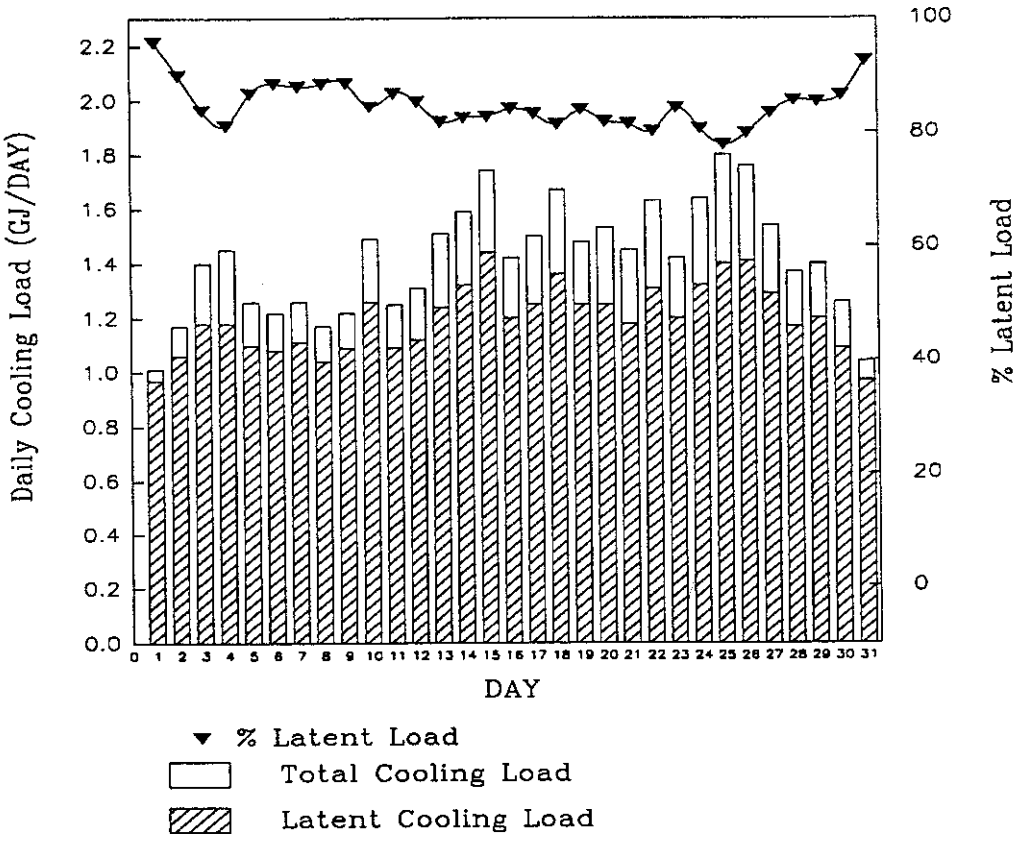

Figure 3. Daily total and latent cooling loads for pre-conditioning of 0.5 m^3/s ventilation air for the month of August in Miami, Florida.

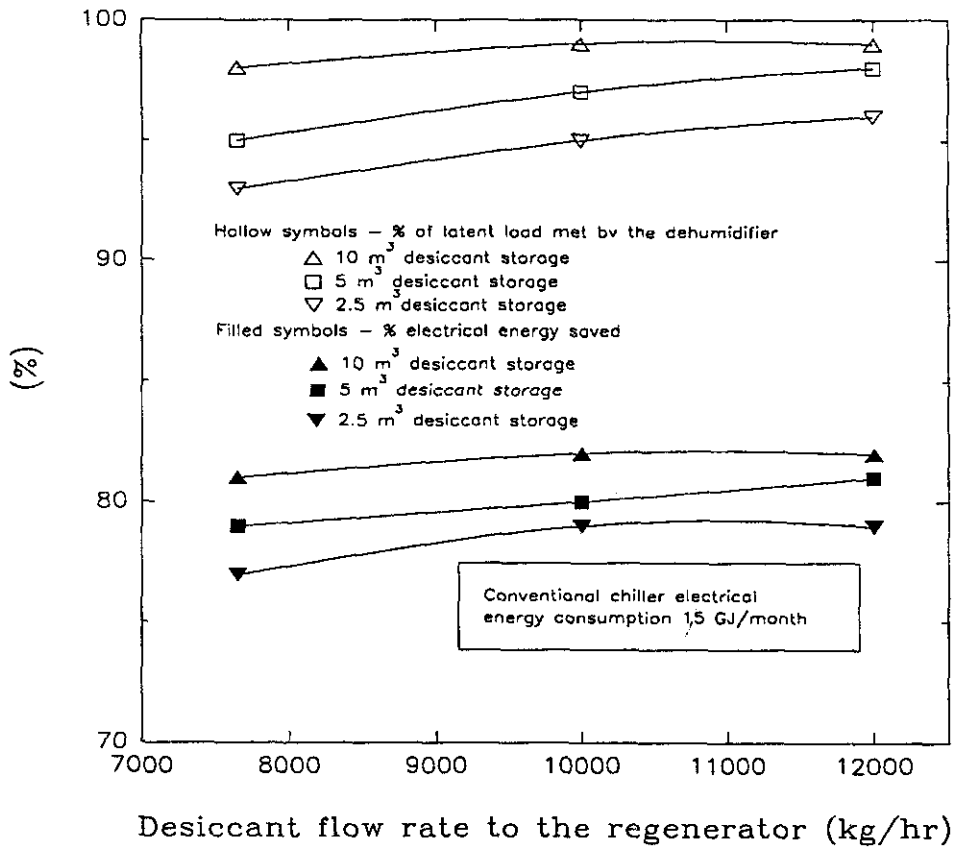

Figure 4. The influence of the desiccant storage size and the regenerator flow rate on the fraction of the latent load handled by the dehumidifier, and the percent electrical energy savings.

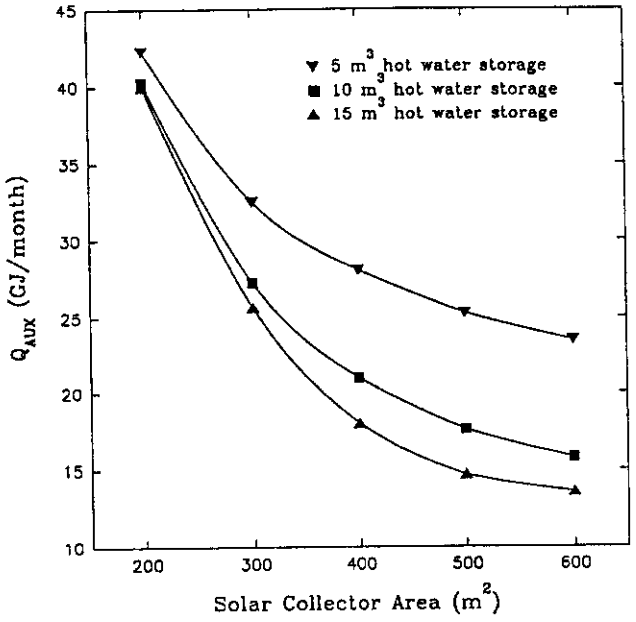

a.

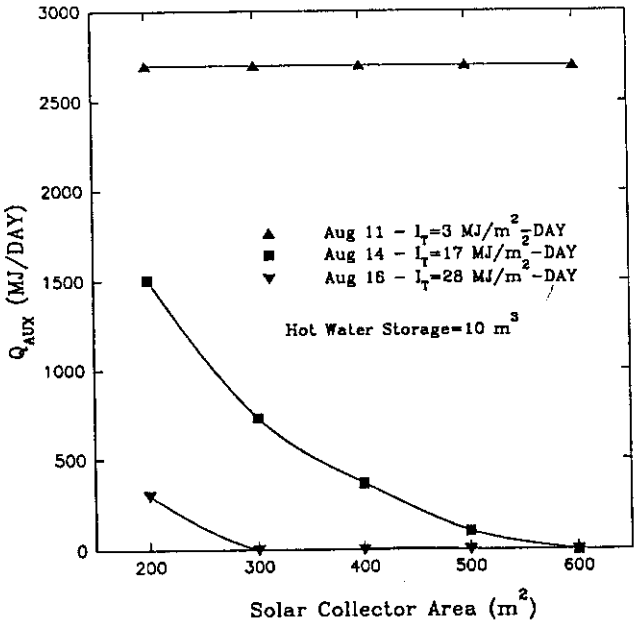

b.

Figure 5 Auxiliary energy requirement versus solar collector area - (a). monthly performance for various hot water storage sizes; (b). daily performance for a range of climatic conditions.

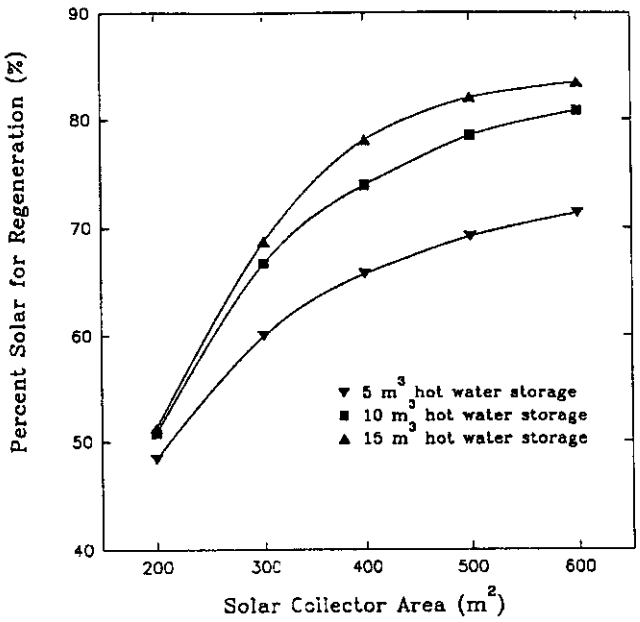

a.

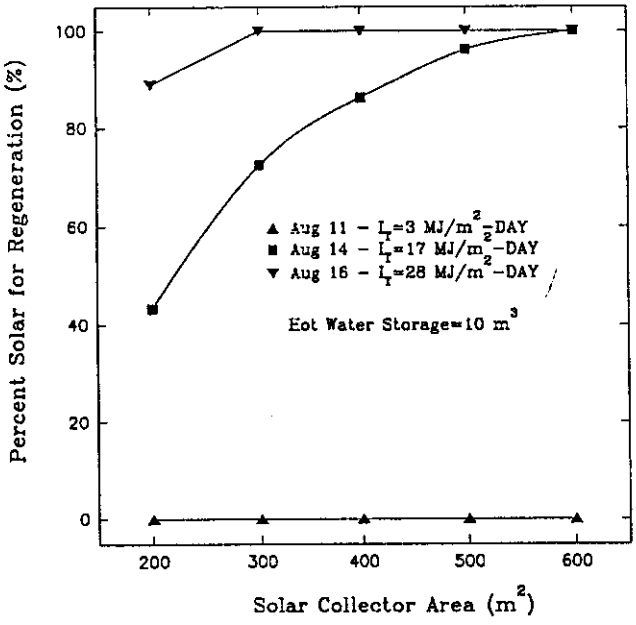

b.

Figure 6 Percent solar for regeneration versus solar collector area - (a). monthly performance for various hot water storage sizes; (b). daily performance for a range of climatic conditions.

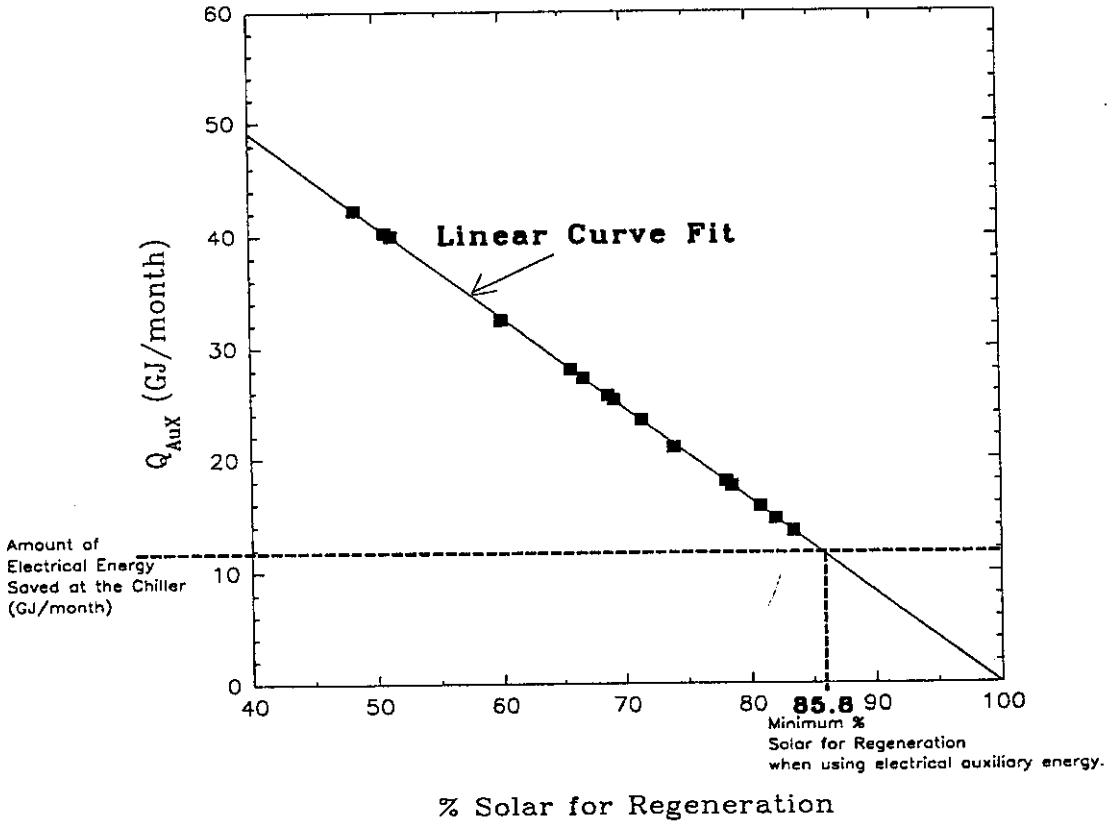

Figure 7. Auxiliary energy requirement versus percent solar for regeneration.

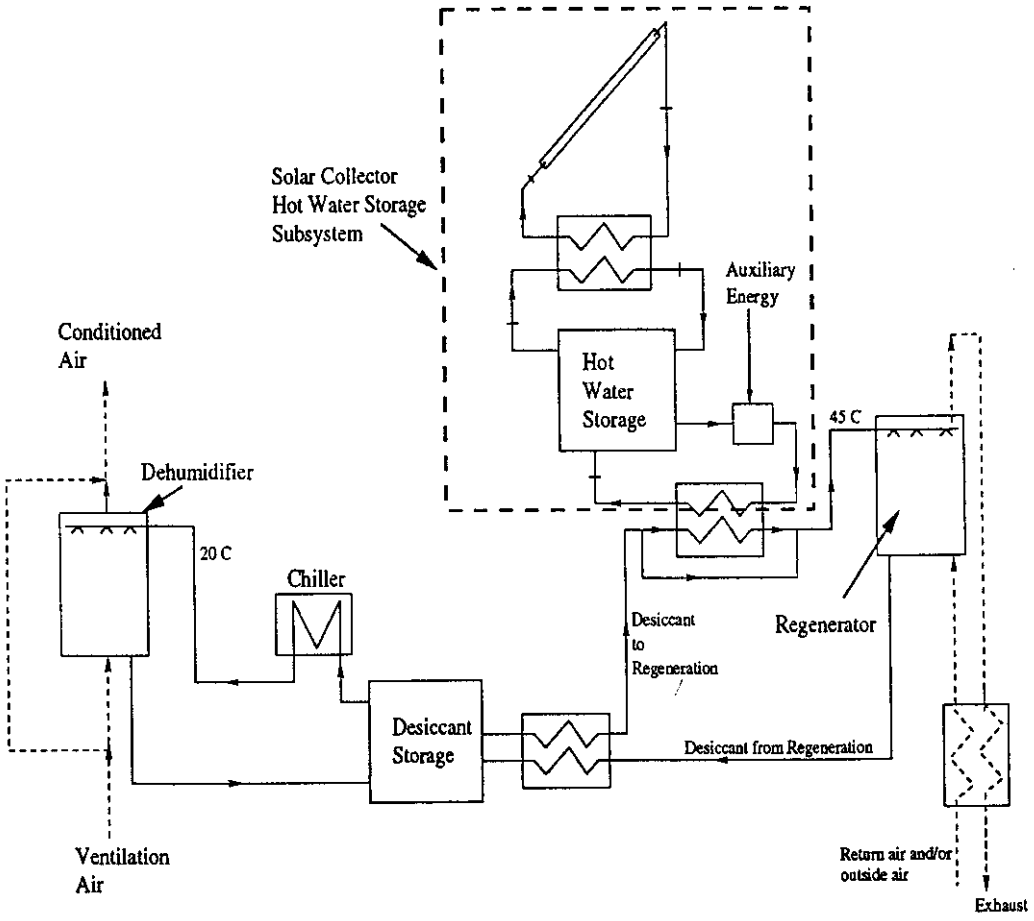

Figure 8. Solar hybrid liquid desiccant cooling system for ventilation air pre-conditioning, using a cool, dilute desiccant.

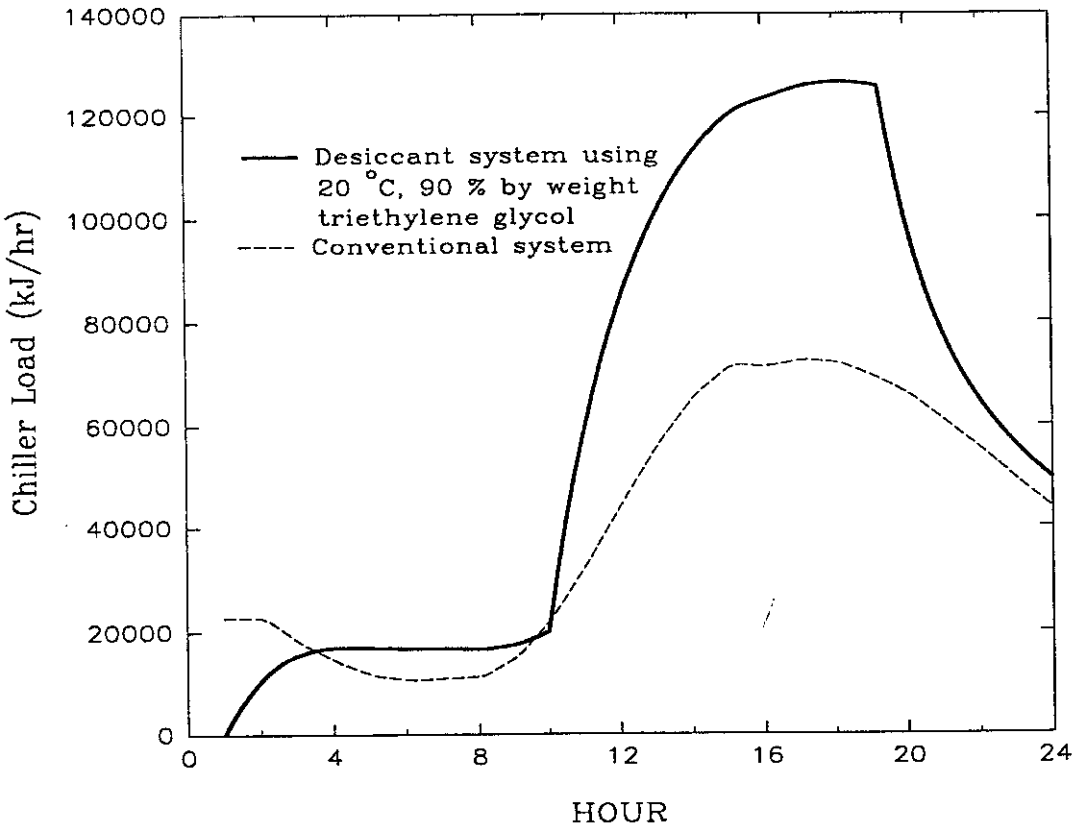

Figure 9. Hourly chiller load for a conventional and a low temperature desiccant system.

APPENDIX B

Laboratory Tests for Triethylene Glycol

Experimental Study of the Heat and Mass Transfer in a Packed Bed Liquid Desiccant Air Dehumidifier

V. Öberg and D.Y. Goswami[1]
Solar Energy and Energy Conversion Laboratory
Department of Mechanical Engineering
University of Florida
Gainesville, Florida 32611-6300

ABSTRACT

Desiccant cooling systems have the ability to provide efficient humidity and temperature control while reducing the electrical energy requirement for air conditioning as compared to a conventional system. Naturally, the desiccant air dehumidification process greatly influences the overall performance of the desiccant system. Therefore, the effects of variables such as air and desiccant flow rates, air temperature and humidity, desiccant temperature and concentration, and the area available for heat and mass transfer are of great interest. Due to the complexity of the dehumidification process, theoretical modeling relies heavily upon experimental studies. However, a limited number of experimental studies are reported in the literature. This paper presents results from a detailed experimental investigation of the heat and mass transfer between a liquid desiccant (triethylene glycol) and air in a packed bed absorption tower. A high performance packing that combines good heat and mass transfer characteristics with low pressure drop is used. The rate of dehumidification, as well as the effectiveness of the dehumidification process are assessed based on the variables listed above. Good agreement is shown to exist between the experimental findings and predictions from finite difference modeling. In addition, a comparison between the findings in the present study and findings previously reported in the literature is made. The results obtained from

this study make it possible to characterize the important variables which impact the system design.

1. INTRODUCTION AND BACKGROUND

Air conditioning requires efficient control of both temperature and humidity. In hot and humid climates, conventional vapor compression air conditioning systems cool the air below its dew point to reduce the moisture content, followed by reheat of the air to a comfortable temperature before it is introduced into the conditioned space. Hence, the evaporator in the vapor compression system operates at a lower temperature than what is required to meet the sensible cooling load, resulting in a lower coefficient of performance (COP). Furthermore, energy efficient vapor compression systems designed to operate at higher evaporator temperatures, have been found unable to maintain the indoor relative humidity within a comfortable range in hot and humid climates (Marsala et al., 1989). Therefore, separating the control of humidity and temperature by means of desiccants could result in energy savings, as well as improved humidity control. The largest energy requirement associated with the use of a desiccant dehumidifier is low temperature heat that could be provided by solar energy or waste heat.

The use of liquid desiccants may be advantageous compared to solid desiccants. For instance, the pressure drop through a liquid desiccant system is smaller than the pressure drop through a solid desiccant wheel (Howell, 1987). Also, the ability to pump the liquid makes it possible to connect several small dehumidifiers to one large regeneration unit (Harriman, 1992), which may be advantageous in large buildings. Finally, concentrated desiccant may be stored for use during the times when no suitable source of regeneration heat is available.

The driving force for mass transfer between the air and the desiccant is the difference in

vapor pressure between the air and the desiccant. Hence, the desiccant must have as low a vapor pressure as possible. Liquid desiccants commonly used are aqueous solutions of lithium bromide, lithium chloride, calcium chloride, salt mixtures, and triethylene glycol (TEG). As cool and concentrated desiccant is brought in contact with air, water vapor in the air is absorbed by the desiccant, i.e., water condenses into the desiccant. During this process, heat is evolved due to the latent heat of condensation of the water, and the heat of mixing. Equipment commonly employed in desiccant systems includes packed bed absorption towers (e.g., Gandhidasan, 1994, Kinsara et al., 1996, Sick et al., 1988, and Thornbloom and Nimmo, 1995) and spray chambers containing finned cooling coils (e.g., Johannsen, 1984, Mahmoud and Ball, 1988, Robison, 1977, and Scalabrin and Scaltriti, 1990). In a sprayed cooling coil dehumidifier, air is dehumidified as it is brought in contact with the desiccant film flowing over the coil. Cooling water or refrigerant flowing through the coil removes the heat evolved during the absorption, allowing for an isothermal process. Packed towers offer a larger area for heat and mass transfer per unit volume than coil dehumidifiers. However, the heat evolved is usually not removed with the result that the desiccant temperature may increase throughout the tower, reducing the potential for mass transfer. Pressure drop through a packed bed may also be higher than in a coil dehumidifier. However, modern packings are being designed for low pressure drop. The possibility of designing compact air dehumidifiers makes the packed bed absorption towers very attractive as a contact device. Thus, a packed bed absorption tower was chosen as the dehumidifier for this investigation.

Naturally, the effectiveness of the desiccant air dehumidification process greatly influences the overall performance of the desiccant system. Therefore, the the impact of variables such as air and desiccant flow rates, air temperature and humidity, desiccant temperature and concentration, and

the area available for heat and mass transfer on the performance of the dehumidifier is of great interest. A number of studies of the heat and mass transfer in the dehumidifier have been presented. The performance of a packed bed dehumidifier as a function of design variables has been modeled by Gandhidasan et al. (1987), Khan (1996 and 1994), and Ullah et al. (1988). Due to the complexity of the dehumidification process, theoretical modeling relies heavily upon experimental data. However, a limited number of studies which include experimental findings are reported in the literature. Chen et al. (1989), Chung et al. (1993), McDonald et al. (1992), and Patnaik et al. (1990) carried out experiments on packed bed dehumidifiers, using salt solutions as the desiccants. Chung et al. (1995) reported some experimental findings using triethylene glycol as the desiccant. The objective of the present investigation is to provide additional experimental data to aid in the design of desiccant systems. Therefore, a thorough experimental analysis was carried out, exploring the influence of all the variables previously listed. Due to its lower corrosivity and lower surface tension as compared to salt solutions, 95 % by weight triethylene glycol was chosen as the desiccant. The performance of the dehumidification process was evaluated in terms of the water condensation rate (i.e., the rate of moisture removal from the air), and the dehumidification effectiveness (concept introduced in a later section). The experimental findings were compared to those obtained from theoretical modeling, as well as other experimental findings reported in the literature.

2. EXPERIMENTAL PROCEDURE

The rate of moisture removal from the air (water condensation rate) as well as the effectiveness of the dehumidification process were studied experimentally as a function of the

following variables: air and desiccant flow rates; air temperature and humidity ratio; desiccant temperature and concentration; and the height of the packed bed.

A schematic of the experimental facility is shown in Figure 1. The packed bed absorption tower was constructed from a 25.4 cm (10 in) diameter acrylic tube to allow for flow visualization. The tower was made in sections so that the bed height could be varied without changing the distance from the liquid distribution to the top of the bed. The inner diameter of the tower was 0.24 m. The packing used was 2.54 cm (1 in) polypropylene Rauschert Hiflow® rings with a specific surface area of 210 m^2/m^3. Fresh, unused triethylene glycol was stored in a tank, and its temperature was adjusted by circulating cold or warm water through a submerged copper coil. Before each experiment, the desiccant was allowed to recirculate to remove any temperature and concentration gradients. Air was blown past an air heater and through a humidifying chamber to adjust its temperature and relative humidity before it entered the packed tower. When the desired air and desiccant conditions were obtained, the desiccant was allowed to flow through the tower. The desiccant was distributed over the packing by three spray heads evenly spaced in an equilateral triangular configuration. Once steady state was obtained, measurements were taken for 15 to 20 minutes using a pc-based data acquisition system. These measurements included inlet and outlet temperatures of the desiccant and the air using copper-constantan thermocouples, as well as inlet and outlet air relative humidities using Mamac Hu-224-2-MA humidity probes. In addition, samples of the desiccant entering and leaving the dehumidifier were taken during the experiment and analyzed for water content using Karl Fischer titration. The used desiccant was pumped over to a separate storage tank so that the inlet desiccant concentration did not change during the experiment. The liquid flow rate was set approximately using a Brooks Hi Pressure Thru-Flow Indicator.

However, it was measured accurately by a catch-bucket method. The air velocity was measured using an anemometer at the air outlet. Finally, the air pressure drop over the packed bed (not including the mist eliminating section) was determined by an air-over-oil manometer.

Experiments were conducted for each variable at three levels (low, intermediate, and high value) while keeping the other variables constant at their intermediate value. Three experiments were conducted at each level.

3. THEORETICAL MODEL OF THE PACKED BED ABSORPTION TOWER

For this study, a finite difference model similar to those used by Factor and Grossman (1980) and Gandhidasan et al. (1987) was utilized. This model is essentially based on the model for adiabatic gas absorption presented by Treybal (1969) with the exception that the resistance to heat transfer in the liquid phase is neglected. In summary, the assumptions made in this study are: adiabatic absorption; concentration and temperature gradients in the flow direction (Z-direction, referring to Figure 2) only; only water is transferred between the air and the desiccant; the interfacial surface area is the same for heat transfer and mass transfer, and it is equal to the specific surface area of the packing; the heat of mixing is negligible as compared to the latent heat of condensation of the water; and the resistance to heat transfer in the liquid phase is negligible.

Figure 2 a gives an overview of the packed bed absorption tower. For the finite difference model, the packed bed height Z is divided into small segments, dZ (Figure 2 b), and the mass and energy balances are solved for each segment, from the bottom to the top of the tower. The governing equations that describe the changes in air humidity and air temperature, desiccant

temperature and desiccant concentration, and desiccant flow rate across a segment are given below. A detailed derivation of these equations is given by Treybal (1969).

- Change in air humidity across the segment:

$$\frac{dY}{dZ} = -\frac{M_w F_G a_t}{G} \ln\left(\frac{1 - y_i}{1 - y}\right) \quad (1)$$

where the interfacial gas phase concentration is given by

$$y_i = 1 - (1 - y)\left(\frac{x}{x_i}\right)^{\frac{F_L}{F_G}} \quad (2)$$

The vapor-liquid equilibrium data for the triethylene glycol-water system (Dow Chemical Company, 1992) were used along with equation 2 to solve for the interface concentrations in the gas and liquid phases.

- Change in air temperature across the segment:

$$\frac{dT_a}{dZ} = \frac{-h_G a' (T_a - T_L)}{G (c_{p,a} + Y c_{p,v})} \quad (3)$$

where $h_G a'$ is the heat transfer coefficient corrected for simultaneous heat and mass transfer (equation 4).

$$h_G a' = \frac{-G c_{p,v} \frac{dY}{dZ}}{1 - \exp\left(\frac{G c_{p,v} \frac{dY}{dZ}}{h_G a_t}\right)} \quad (4)$$

- Change in desiccant temperature across the segment:

$$dT_L = \frac{G}{c_{p,L} L}\{(c_{p,a} + Y c_{p,v}) dT_a + [c_{p,v} (T_a - T_0) - c_{p,L} (T_L - T_0) + \lambda_0] dY\} \quad (5)$$

- Change in desiccant concentration across the segment:

$$dX = -\frac{G}{L} X \, dY \tag{6}$$

- Change in desiccant flow rate across the segment:

$$dL = G \, dY \tag{7}$$

Empirical correlations by Onda et al. (1968) were used for the gas and liquid phase heat and mass transfer coefficients (equations 8, 9, and 10).

$$k_L = 0.0051 \left(\frac{\mu_L g}{\rho_L}\right)^{1/3} \left(\frac{L}{a_w \mu_L}\right)^{2/3} \left(\frac{\rho_L D_L}{\mu_L}\right)^{1/2} (a_t d_p)^{0.4} \tag{8}$$

$$\frac{a_w}{a_t} = - \exp\left[-1.45 \left(\frac{\gamma_c}{\gamma_L}\right)^{0.75} \left(\frac{L}{a_t \mu_L}\right)^{0.1} \left(\frac{L^2 a_t}{\rho_L^2 g}\right)^{-0.05} \left(\frac{L^2}{\rho_L \gamma_L a_t}\right)^{0.2}\right] \tag{9}$$

$$k_G = 5.23 \frac{a_t D_G}{R T} \left(\frac{G}{a_t \mu_G}\right)^{0.7} \left(\frac{\mu_G}{\rho_G D_G}\right)^{1/3} (a_t d_p)^{0.2} \tag{10}$$

These k-type mass transfer coefficients can be converted to F-type coefficients by equations 11 and 12 (Treybal, 1969).

$$F_L = \frac{k_L \rho_L}{M_L} \tag{11}$$

$$F_G = k_G P \tag{12}$$

The gas phase heat transfer coefficient is found by applying the heat and mass transfer analogy (equation 13).

$$j_h = \frac{h_G}{c_{p,a}\, G} Pr^{\frac{2}{3}} = j_m = \frac{F_G\, M_a}{G} Sc^{\frac{2}{3}} \qquad (13)$$

A Fortran computer program was written to carry out the finite difference analysis with the bed height Z divided into 1000 segments. An under-relaxation iterative procedure was utilized to promote convergence. The criteria for convergence was ± 0.05 °C for the inlet desiccant temperature, and ± 0.0001 kg TEG/kg solution for the inlet desiccant concentration.

4. RESULTS AND DISCUSSION

The results from the experimental study and theoretical modeling are depicted graphically in Figures 3 to 9. These figures show the water condensation rate (moisture removal rate), m_{cond}, and the dehumidification effectiveness, ϵ_Y, as a function of air and desiccant flow rates and inlet temperatures, desiccant concentration, inlet air humidity ratio, and packed bed height. In each figure, error bars show the uncertainty of the experimental measurements. To cross-check the consistency of the data, a water mass balance across the dehumidifier was calculated, yielding ● 3 % deviation between the amount of water entering and leaving the dehumidifier. Similarly, an energy balance across the dehumidifier gave deviations of ± 6 %. Thus, the assumption of adiabatic absorption is satisfactory. The pressure drop across the packed bed varied between 30 and 210 Pa/m

packing, depending on the air flow rate.

The dehumidification effectiveness, ϵ_Y, is defined as the ratio of the actual change in moisture content of the air flowing through the dehumidifier to the maximum possible under the same operating conditions (Ullah et al., 1988).

$$\epsilon_Y = \frac{Y_{IN} - Y_{OUT}}{Y_{IN} - Y_{equ}} \tag{14}$$

Here, Y_{IN} and Y_{OUT} are the humidity ratios at the air inlet and outlet, respectively, and Y_{equ} is the humidity ratio in equilibrium with the desiccant at the local solution temperature and concentration. For counter flow arrangement, Y_{equ} would be the humidity ratio of the air in equilibrium with the desiccant at the desiccant inlet. Ullah et al. (1988) presented a curve fit for ϵ_Y as a function of the inlet desiccant and air temperatures, and the desiccant concentration for a given tower height, liquid and air flow rates, geometry, and desiccant. A more general correlation of ϵ_Y as a function of air and liquid flow rates, column and packing dimensions, and equilibrium properties of the desiccant was suggested by Chung (1994). This correlation was obtained using experimental data available in the literature. A parameter, π, representing the equilibrium properties of the desiccant was defined as the ratio of the vapor pressure depression to the vapor pressure of pure water (equation 15). The correlation by Chung (1994) is given in equation 16.

$$\pi = \frac{p_w - p_L}{p_w} \tag{15}$$

$$\epsilon_Y = \frac{1 - \left\{ \frac{0.205\left(\frac{G_{IN}}{L_{IN}}\right)^{0.174} \exp\left[0.985\left(\frac{T_{a,IN}}{T_{L,IN}}\right)\right]}{(aZ)^{0.184}\pi^{1.680}} \right\}}{1 - \left\{ \frac{0.152 \exp\left[-0.686\left(\frac{T_{a,IN}}{T_{L,IN}}\right)\right]}{\pi^{3.388}} \right\}} \qquad (16)$$

Results predicted with this correlation are shown together with the experimental findings from the present study in Figures 3 to 9.

The experimental findings agree well with the predictions from the finite difference model described in this study. Only a slight discrepancy can be seen, and the difference is consistently within the error bars of the experiments. In cases where a discrepancy is apparent, the finite difference model generally over-predicts the performance of the dehumidifier. This is presumably due to the assumption that the area available for heat and mass transfer is equal to the total specific surface area of the packing. Even though the liquid flow rates are high as compared to the air flow rate, complete wetting of the packing is difficult to obtain. Therefore, the mass transfer area is less than the packing surface area. Also, it should be kept in mind that the correlations used for the transfer coefficients are empirical, and they were obtained for liquid-gas systems and packings other than those used in the present study. Although the correlation by Chung (1994) predicted the performance of the dehumidifier within 10 % of the experimental findings, the finite difference model appears to predict the influence of design variables more accurately; i.e., trends shown by the experimental values were also predicted by the finite difference model. More specifically, the decrease in dehumidifier performance with increasing inlet air temperature (Figure 5) predicted by the correlation of Chung (1994) cannot be seen from the experiments or the finite difference model. Also, the correlation by Chung (1994) did not show a dependency on the inlet desiccant temperature

as was found from the experimental results and the finite difference model (Figure 6).

The present study revealed the following variables to have the most significant effect on the dehumidifier performance: air flow rate, inlet desiccant temperature, inlet air humidity ratio, inlet desiccant concentration, and the area available for heat and mass transfer, i.e., the height of the packed bed. The condensation rate increased with the air flow rate (Figure 3 a). The change in humidity ratio through the tower decreased with an increase in the air flow rate due to the reduced residence time for the air in the dehumidifier. Hence, the dehumidification effectiveness decreased with an increase in the air flow rate (Figure 3 b). Increasing the desiccant temperature decreased the condensation rate (Figure 6 a). A higher desiccant temperature gives a lower potential for mass transfer in the dehumidifier resulting in a lower condensation rate. However, the dehumidification effectiveness was not affected by the desiccant temperature (Figure 6 b). This is because the lowest possible humidity ratio that can be obtained at the air outlet, Y_{equ}, is directly dependent on $T_{L,IN}$, making the effectiveness somewhat normalized with respect to the desiccant temperature. Similarly, the condensation rate increased with the desiccant concentration, but the desiccant concentration did not change the effectiveness (Figure 8). An increase in the area available for heat and mass transfer, obtained by increasing the height of the packed bed, increased the condensation rate and the effectiveness (Figure 9). A taller bed makes it possible for the air to reach a humidity ratio closer to the equilibrium value, Y_{equ}, at the air outlet.

The influence of design variables is summarized in Table 1 along with the experimental findings previously reported in the literature. The table shows the desiccant used, the parameters describing the performance, the independent variables and the ranges examined. Under each independent variable, the influence of the variable on the performance parameter is indicated by up

and down arrows. As shown, the present study used liquid flow rates significantly higher than the previous studies with the exception of the work by Chung et al. (1995). Initial experiments at lower flow rates showed poor performance compared to the predictions from the theoretical model. This was presumably due to inadequate wetting of the packing. Therefore, it was decided to carry out the experiments at higher flow rates. Chung et al. (1995) had similar reasons for using high liquid flow rates. Indeed, Patnaik et al. (1990) and Chen et al. (1989) found the condensation rate to increase with liquid flow rate. They explained this partly by the increased wetting of the packing with increased flow rates. However, in the present study no dependency on the liquid flow rate was found. Hence, it may be concluded that the flow rates used in this study were sufficient to achieve maximum wetting for the present system.

Patnaik et al. (1990) found that the condensation rate decreased as the inlet air temperature increased. They explained this dependency on the increase in liquid temperature due to sensible heat transfer from the air to the desiccant. The present study showed no dependency of the condensation rate on the inlet air temperature. The reason for this observation is that the desiccant flow rate was significantly higher than the air flow rate. Therefore, the sensible heat transfer from the air to the desiccant was too small to increase the desiccant temperature significantly. Chen et al. (1989) found that the condensation rate increased with the inlet air temperature. This was probably due to the fact that they used relative humidity as a variable instead of humidity ratio. For a constant relative humidity, the warmer the air, the higher the humidity ratio, which gives a higher condensation rate.

Based on the comparison between the experimental and the theoretical results in this study, it is believed that the finite difference model described herein gives good predictions for design and performance simulation. This model is applicable to more general conditions than the correlations

given by Chen et al. (1989), McDonald et al. (1992), and Patnaik et al. (1990), which they obtained for specific operating conditions, and packings.

5. CONCLUSIONS

Design variables found to have the greatest impact on the performance of the dehumidifier are the air flow rate and the humidity ratio, the desiccant temperature and concentration, and the packed bed height. The liquid flow rate and the inlet air temperature did not have a significant effect on the dehumidifier performance; however, the liquid flow rate must be high enough to ensure wetting of the packing.

The results obtained in this study compare reasonably well with other experimental investigations. Contrary to the findings of this study, some studies suggest that the liquid flow rate and air temperature influence the performance. This is presumably due to the lower liquid flow rate used in those investigations.

The dehumidifier performance predicted with the finite difference model described in this paper shows a good agreement with the experimental findings. Thus, for a detailed study of the absorption process, this model gives accurate performance predictions based on fundamental equations, minimizing the assumptions and use of empirical correlations.

NOMENCLATURE

a_t	specific surface area of packing (m^2/m^3)
a_w	wetted surface area of packing (m^2/m^3)
COP	coefficient of performance
c_p	specific heat (kJ/kg-°C)
F_G	gas phase mass transfer coefficient (kmol/m^2-s)
F_L	liquid phase mass transfer coefficient (kmol/m^2-s)
G	superficial air (gas) flow rate (kg/m^2-s)
H	enthalpy (kJ/kg)
h_G	gas side heat transfer coefficient (kJ/m^2-s)
j_h	dimensionless heat transfer group (equation 13)
j_m	dimensionless mass transfer group (equation 13)
K_G	overall gas side mass transfer coefficient (kmol/m^2-s)
k_G	gas phase mass transfer coefficient (kmol/m^2-s-Pa)
k_L	liquid phase mass transfer coefficient (*m*/s)
L	superficial desiccant flow rate (kg/m^2-s)

M	molar mass (kg/kmol)
m	flow rate (kg/s)
N_v	molar vapor mass transfer flux (kmol/m^2-s)
P	total pressure (Pa)
Pr	Prandtl number
p	vapor pressure (Pa)
q	heat transfer flux (kW/m^2)
Sc	Schmidt number
T	temperature (°C)
TEG	triethylene glycol
X	desiccant concentration (kg TEG / kg solution)
x	desiccant mole fracion (kmol TEG /kmol solution)
Y	air humidity ratio (kg water/kg dry air or g water/kg dry air)
y	water mole fraction (kmol water / kmol air)
Z	tower height (m)
γ	surface tension (N/m)
ϵ	effectiveness
λ	latent heat of condensation/vaporization (kJ/kg)
μ	viscosity (Ns/m^2)
π	dimensionless vapor pressure difference (equation 15)
ρ	density (kg/m^3)

Subscripts

a	air
cond	water condensation
equ	equilibrium
G	gas phase
IN	inlet
L	desiccant or liquid phase
OUT	outlet
v	vapor
Y	air humidity ratio (kg water / kg dry air)
0	reference state

REFERENCES

Chen, L. C., Kuo, C. L., and Shyu, R. J., 1989, "The Performance of a Packed Bed Dehumidifier for Solar Liquid Desiccant Systems", Proceedings of the 11th Annual ASME Solar Energy Conference, Solar Engineering - 1989, San Diego, California, pp. 371-377.

Chung, T.-W., Ghosh, T. K., Hines, A. L., and Novosel, D., 1995 , "Dehumidification of Moist Air with Simultaneous Removal of Selected Pollutants by Triethylene Glycol Solutions in a Packed-Bed Absorber", Separation Science and Technology, 30(7-9), pp. 1807-1832.

Chung, T.-W., 1994, "Predictions of the Moisture Removal Efficiencies for Packed-Bed Dehumidification Systems", Gas Separation & Purification, 8 (4), pp. 265-268.

Chung, T.-W., Ghosh, T. K., and Hines, A. L., 1993, "Dehumidification of Air by Aqueous Lithium Chloride in a Packed Column", Separation Science and Technology, 28(1-3), pp. 533-550.

Dow Chemical Company, 1992, A Guide to Glycols, Dow Chemical Company, Midland, Michigan.

Factor, H. M., and Grossman, G., 1980, "A Packed Bed Dehumidifier/Regenerator for Solar Air Conditioning with Liquid Desiccants", Solar Energy, 24, pp. 541-550.

Gandhidasan, P., 1994, "Performance Analysis of an Open-Cycle Liquid Desiccant Cooling System using Solar Energy for Regeneration", International Journal of Refrigeration, 17 (7), pp. 475-480.

Gandhidasan, P., Ullah, M. R., and Kettleborough, C. F., 1987, "Analysis of Heat and Mass Transfer Between a Desiccant-Air System in a Packed Tower", Journal of Solar Energy Engineering, 109, pp. 89-93.

Harriman, L. G., 1992, The Dehumidification Handbook, 2nd edition, Munters Cargocaire, Amesbury, MA.

Howell, J. R., 1987, "A Survey of Active Solar Cooling Methods", Progress in Solar Engineering, Goswami, D. Y., editor, pp. 171- 182.

Johannsen, A., 1984, "Performance Simulation of a Solar Air-Conditioning System with Liquid Desiccant", International Journal of Ambient Energy, 5(2), pp. 59-89.

Khan, A. Y., 1996, "Parametric Analysis of Heat and Mass Transfer Performance of a Packed Type Liquid Desiccant Absorber at Part-Load Operating Conditions", ASHRAE Transactions, 102, pt. 1, pp. 349-357.

Khan, A. Y., 1994, "Sensitivity Analysis and Component Modeling of a Packed-Type Liquid

Desiccant System at Partial Load Operating Conditions", International Journal of Energy Research, 18, pp.643-655.

Kinsara, A. A., Elsayed, M. M., and Al-Rabghi, O. M., 1996, "Proposed Energy-Efficient Air-Conditioning System Using Liquid Desiccant", Applied Thermal Engineering, 16 (10), pp. 791-806.

Mahmoud, K. G., Ball, H. D., 1988, "Liquid Desiccant Systems for Cooling Applications", Proceedings of the Intersociety Energy Conversion Engineering Conference, Denver, Colorado, pp. 149-152.

Marsala, J., Lowenstein, A., and Ryan, W.A., 1989, "Liquid Desiccant for Residential Applications", ASHRAE Transactions, 95, pt. 1, pp. 828-834.

McDonald, B., Waugaman, D. G., and Kettleborough, C. F., 1992, "A Statistical Analysis of a Packed Tower Dehumidifier", Drying Technology, 10(1), pp. 223-237.

Onda, K., Takeuchi, H., and Okumoto, Y., 1968, "Mass Transfer Coefficients Between Gas and Liquid Phases in Packed Columns", Journal of Chemical Engineering of Japan, 1 (1), pp. 56-62.

Patnaik, S., Lenz, T. G., and Löf, G. O. G., 1990, "Performance Studies for an Experimental Solar Open-Cycle Liquid Desiccant Air Dehumidification System", Solar Energy, 44 (3), pp. 123-135.

Robison, H., 1977, "Liquid Sorbent Solar Air Conditioner", Alternative Energy Sources, 2, Veziroğlu, T. N., editor, Hemisphere Publishing Company, Washington, pp. 761-779.

Scalabrin, G. and Scaltriti, G., 1990, "A Liquid Sorption - Desorption System for Air Conditioning With Heat at Lower Temperature", Journal of Solar Energy Engineering, 112, pp. 70-75.

Sick, F., Buschulte, T. K., Klein, P., Northey, P., and Duffie, J. A., 1988, "Analysis of the Seasonal Performance of Hybrid Liquid Desiccant Cooling Systems", Solar Energy, 40, pp. 211-217.

Thornbloom, M., and Nimmo, B., 1995, "An Economic Analysis of a Solar Open Cycle Desiccant Dehumidification System", Proceedings of the 13th Annual ASME Conference, Solar Engineering - 1995, Hawaii, 1, pp. 705-709.

Treybal, R. E., 1969, "Adiabatica Gas Absorption and Stripping in Packed Towers", Industrial Engineering and Chemistry, 61 (7), pp. 36-41.

Ullah, M. R., Kettleborough, C. F., and Gandhidasan, P., 1988, "Effectiveness of Moisture Removal for an Adiabatic Counterflow Packed Tower Absorber Operating with $CaCl_2$-Air Contact System", Journal of Solar Energy Engineering, 110, pp. 98-101.

TABLE 1. PACKED BED DEHUMIDIFIER PERFORMANCE

Author	Desiccant	Performance Parameter	Independent Variables						
Öberg and Goswami (present study)	TEG		L (kg/m^2-s)	X_{IN} (kg/kg)	$T_{L,IN}$ (°C)	G (kg/m^2-s)	$T_{a,IN}$ (°C)	Y_{IN} (g/kg)	Z (m)
			4.5-6.5	0.94-0.96	25-35	0.5-2.0	25-35	11-22	0.4-0.8
		m_{cond}	↑↓	↑	↓	↑	↑↓	↑	↑
		ϵ_V	↑↓	↑↓	↑↓	↓	↑↓	↑↓	↑
Chen et al. (1989)	LiCl		L* (kg/m^2-s)	X_{IN} (kg/kg)	$T_{L,IN}$ (°C)	G* (kg/m^2-s)	$T_{a,IN}$ (°C)	Y_{IN} (g/kg)	Z (m)
			0.1-1.0	0.3-0.4	26-39	0.2-1.2	25-35	17-22	0.1-0.6
		m_{cond}	↑	↑	↓	↑	↑	↑	↑
Chung et al. (1995)	TEG		L* (kg/m^2-s)		X_{IN} (kg/kg)			G* (kg/m^2-s)	
			6-11		0.9-0.95			0.8-1.2	
		ϵ_V	↑		↑			↑	
		$K_G a$	↑		↑			↑	
McDonald et al. (1992)	mixture of LiCl and $CaCl_2$		L* (kg/m^2-s)	X_{IN} (kg/kg)	$T_{L,IN}$* (°C)	$T_{a,IN}$* (°C)	Y_{IN} (g/kg)	Z* (m)	
			1.5-3.9	0.4-0.45	28-43	31-36	21-41	0.5-1.4	
		$T_{a,OUT}$	↓	↑↓	↑	↑↓	↑	↑↓	
		Y_{OUT}	↓	↑↓	↑	↑↓	↑	↑↓	
Patnaik et al. (1990)	LiBr		L* (kg/m^2-s)	X_{IN} (kg/kg)	$T_{L,IN}$ (°C)	G* (kg/m^2-s)	$T_{a,IN}$ (°C)	Y_{IN} (g/kg)	
			0.6-1.7	0.45-0.58	24-32	1.3-1.9	24-36	9-22	
		m_{cond}	↑	↑	↑↓	↑↓	↓	↑	

* Values converted to this unit by present authors.
↑ performance parameter increases with increasing variable
↓ performance parameter decreases with increasing variable
↑↓ variable has no significant effect on the performance parameter

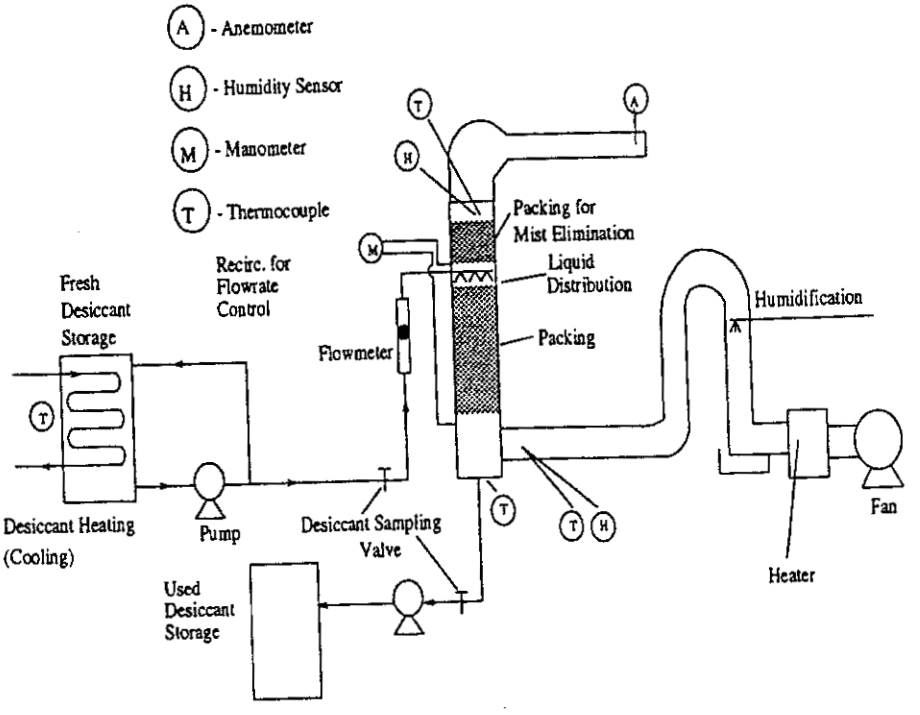

Figure 1. Experimental facility.

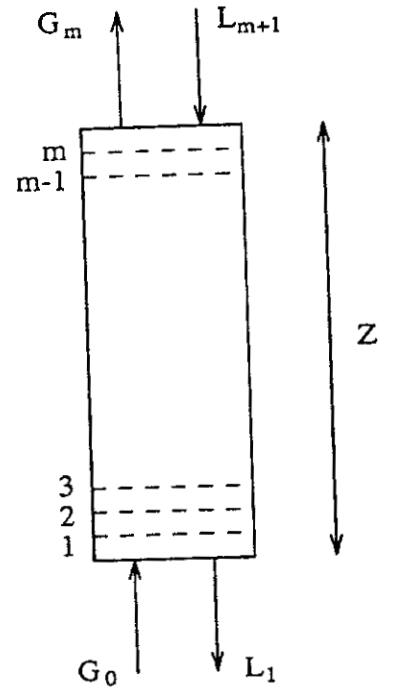

a.

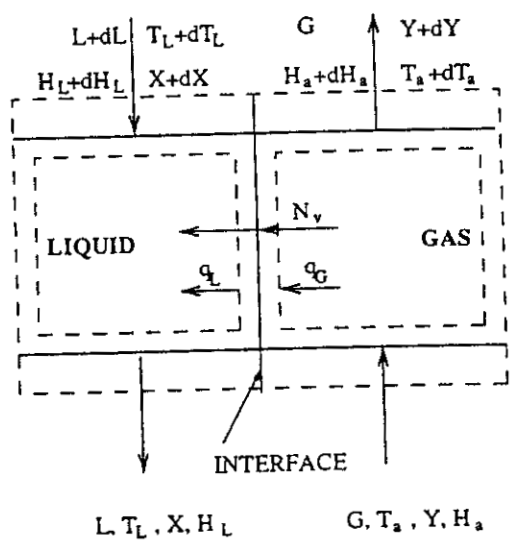

b.

Figure 2 a. Overview of the packed bed absorption tower. b. Differential segment of the packed bed absorption tower.

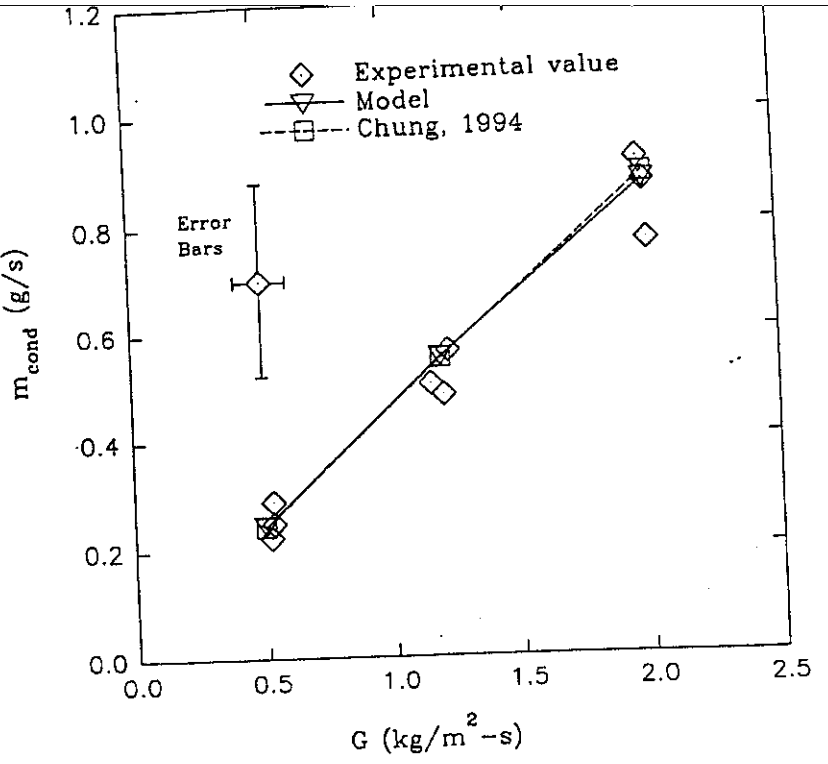

a.

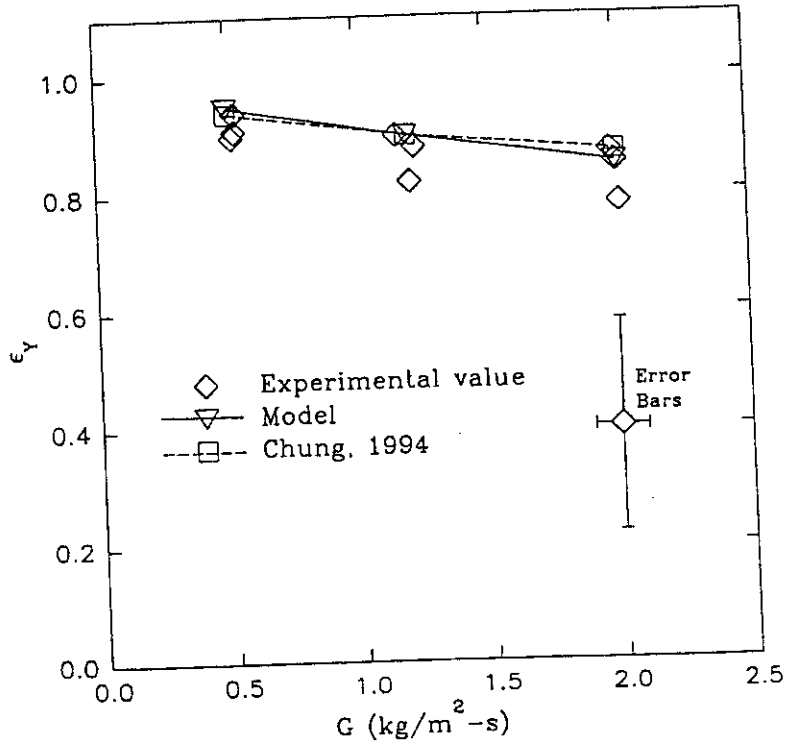

b.

Figure 3 a. Condensation rate versus air flow rate. b. Dehumidification effectiveness versus air flow rate.

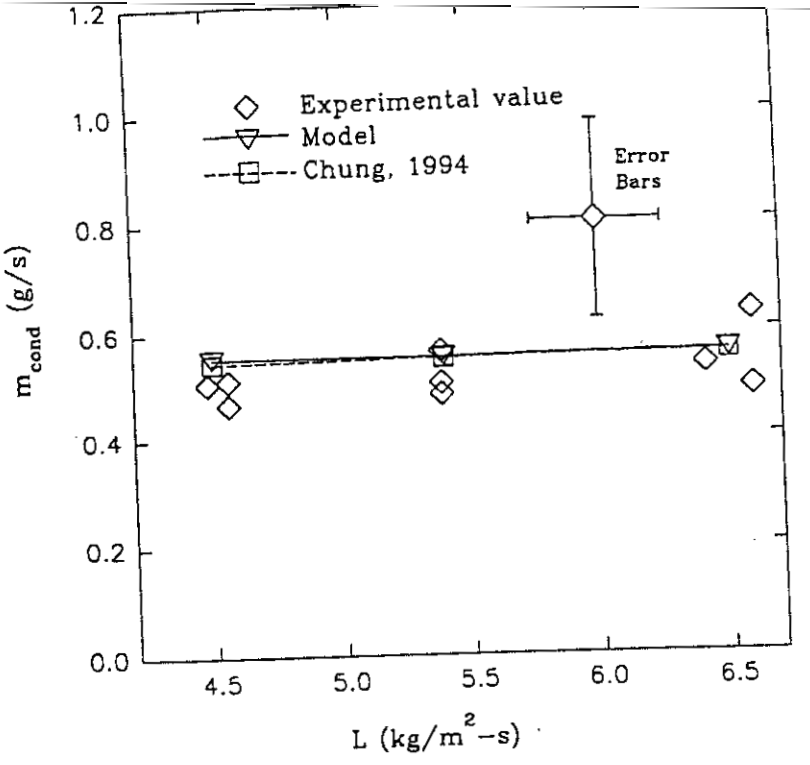

a.

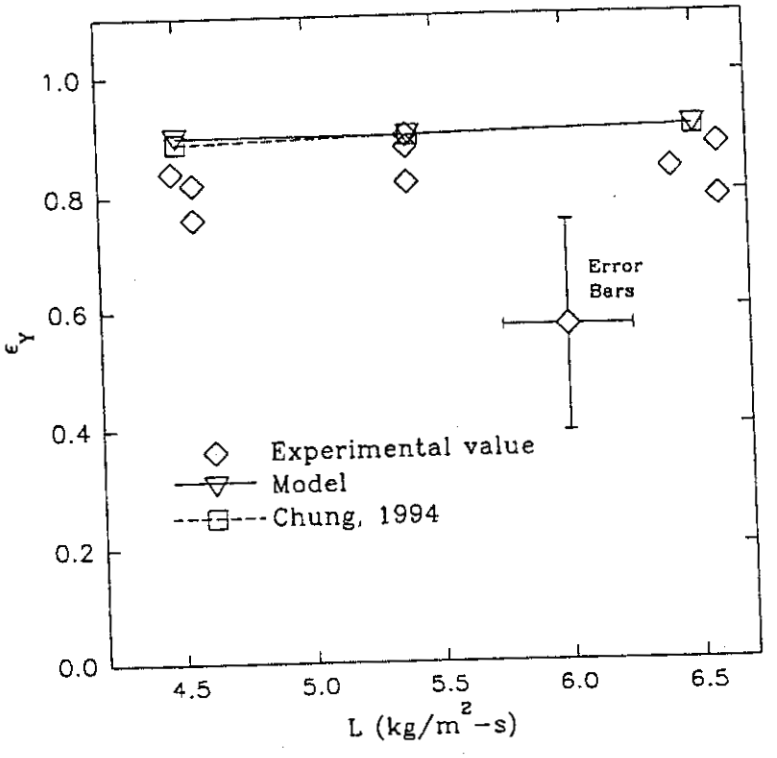

b.

Figure 4 a. Condensation rate versus desiccant flow rate. b. Dehumidification effectiveness versus desiccant flow rate.

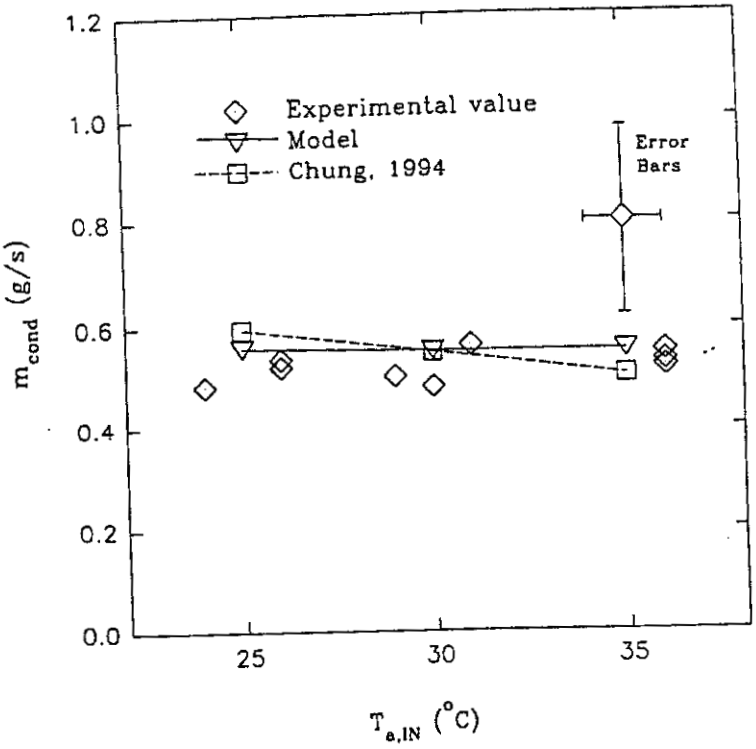

a.

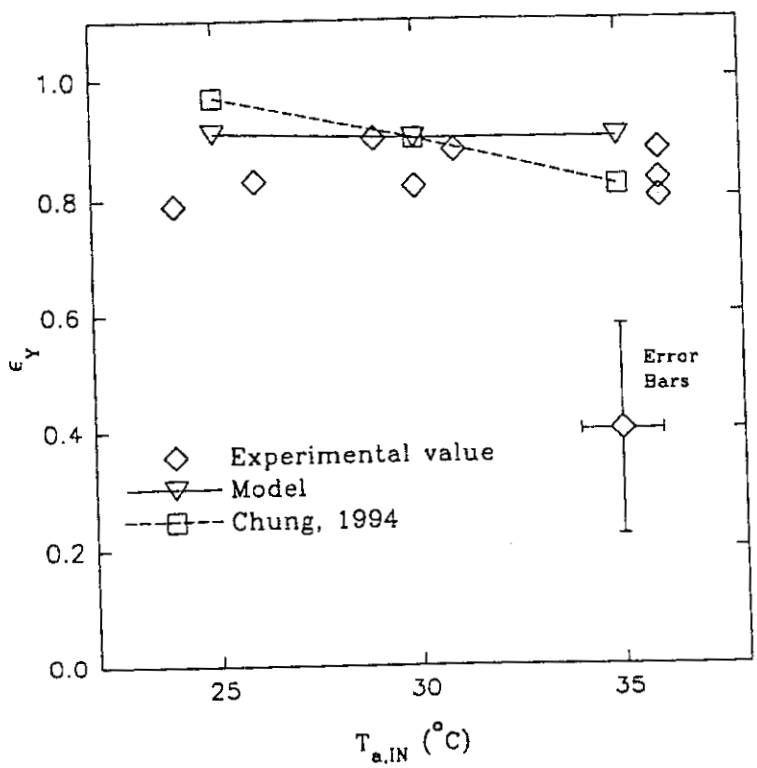

b.

Figure 5 a. Condensation rate versus inlet air temperature. b. Dehumidification effectiveness versus inlet air temperature.

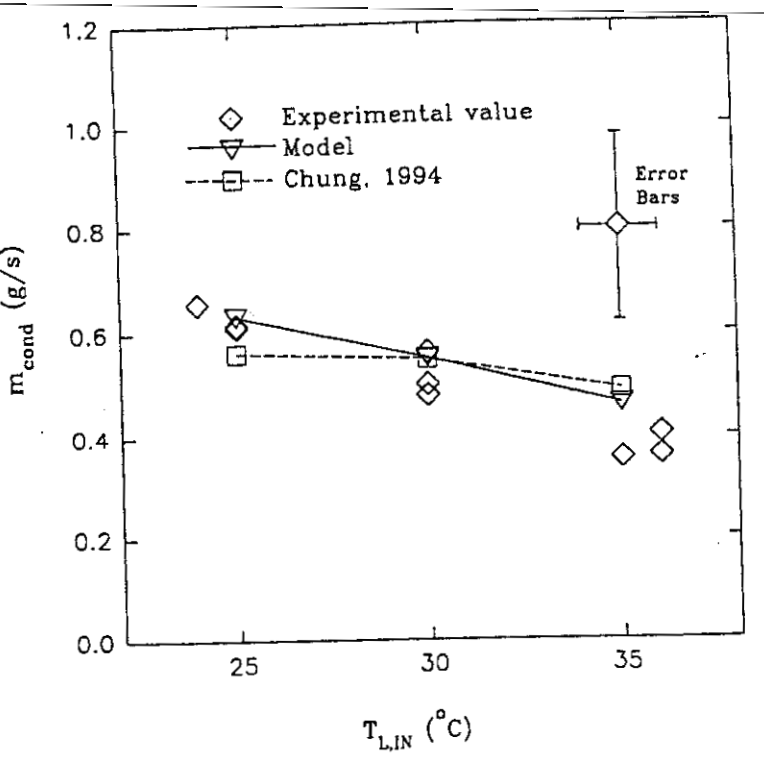

a.

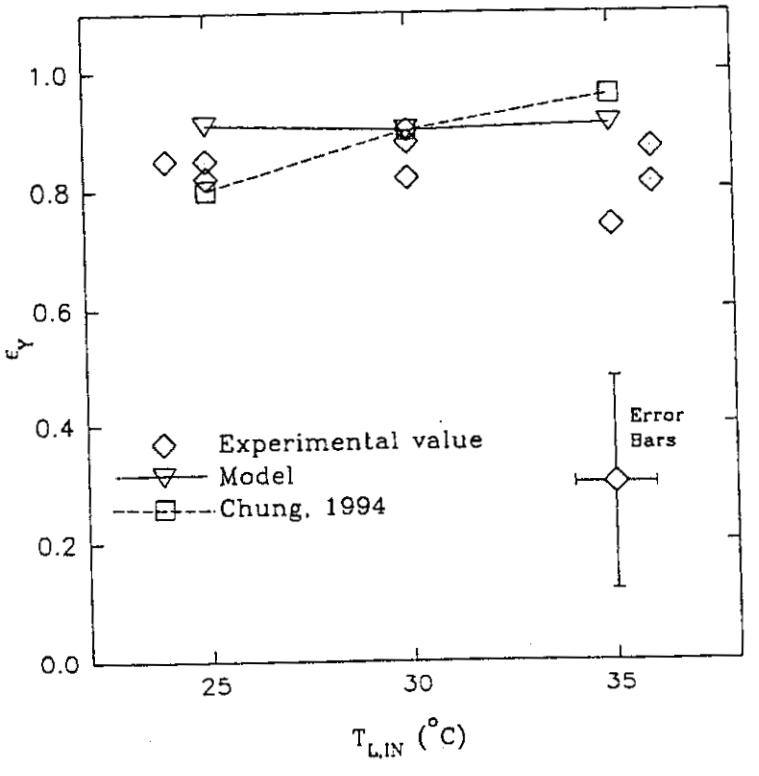

b.

Figure 6 a. Condensation rate versus inlet desiccant temperature. b. Dehumidification effectiveness versus inlet desiccant temperature.

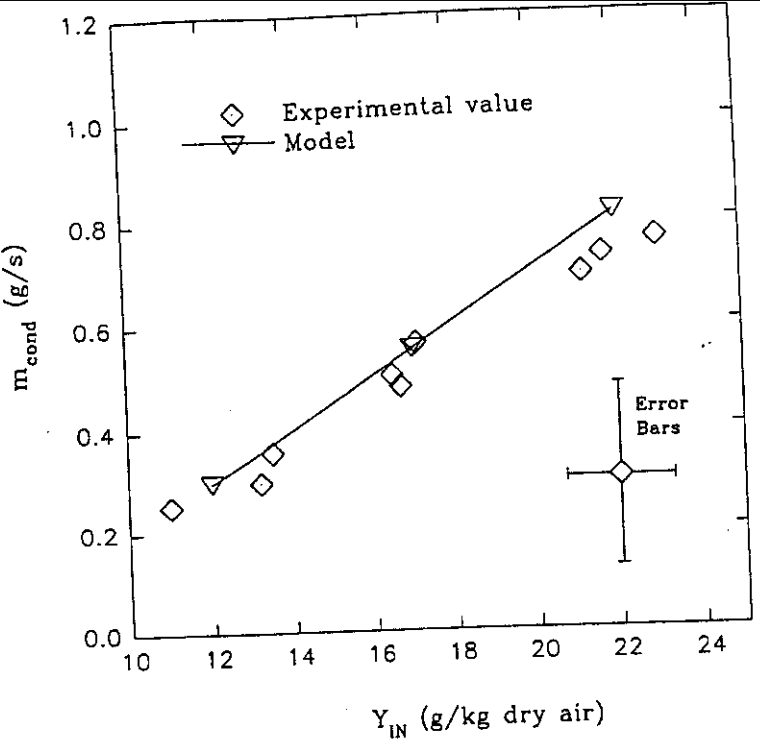

a.

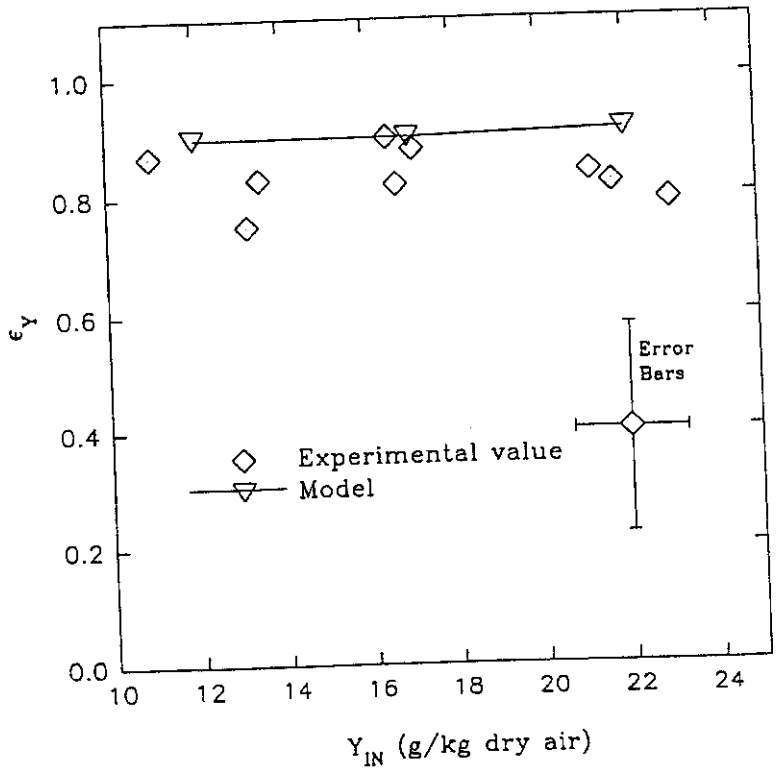

b.

Figure 7 a. Condensation rate versus inlet air humidity ratio. b. Dehumidification effectiveness versus inlet air humidity ratio.

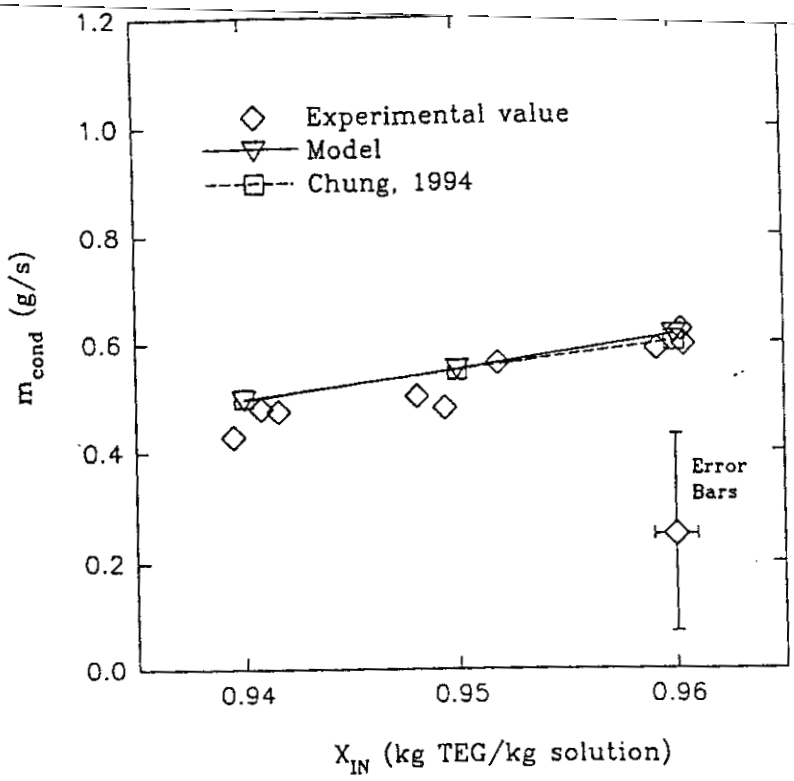

a.

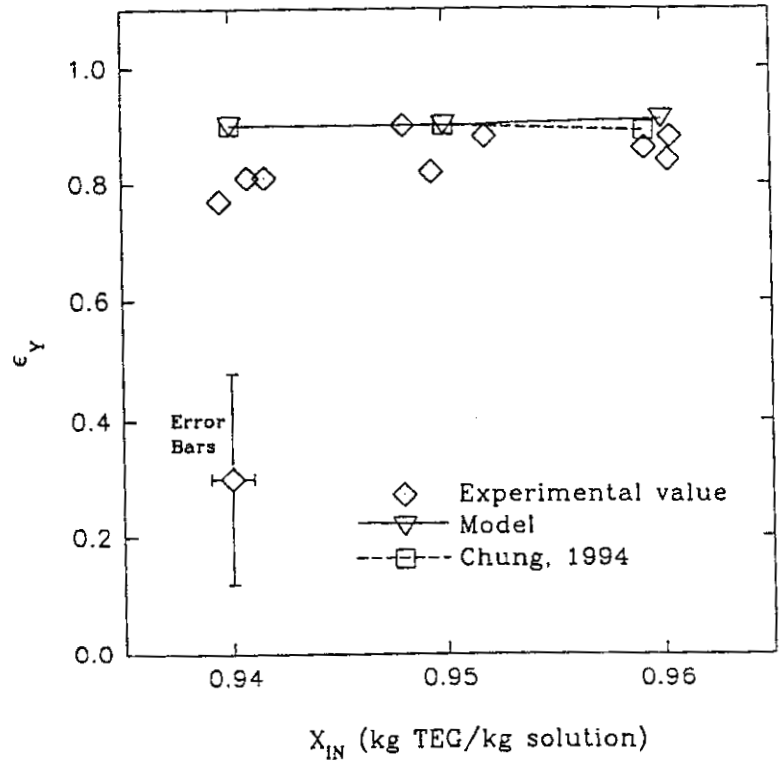

b.

Figure 8 a. Condensation rate versus inlet desiccant concentration. b. Dehumidification effectiveness versus inlet desiccant concentration.

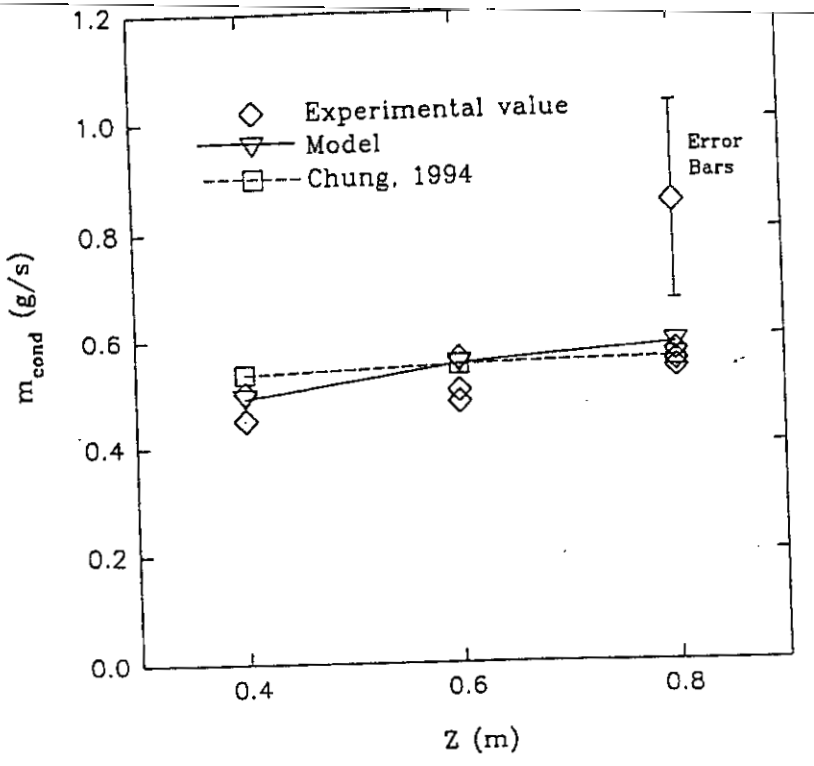

a.

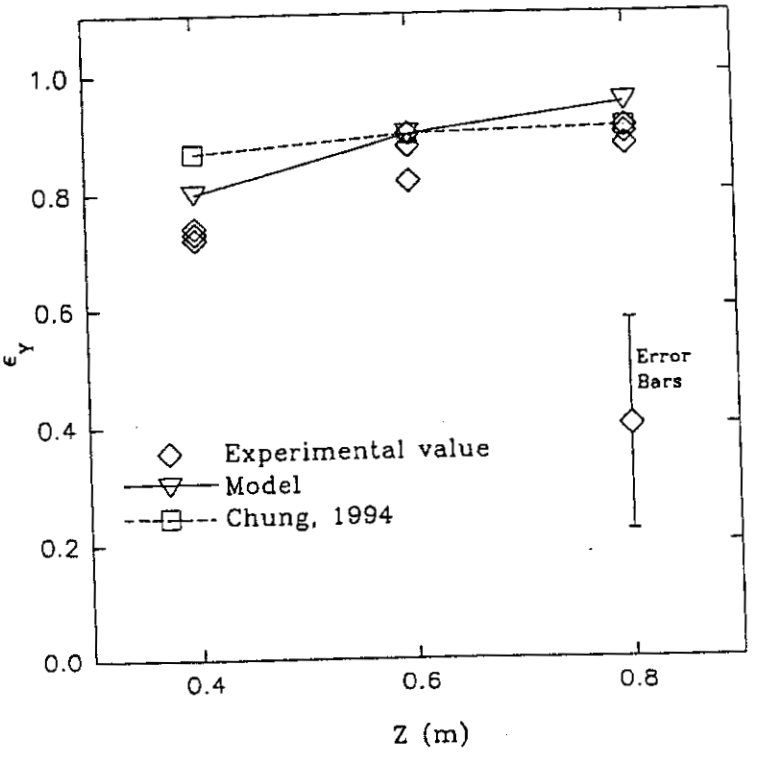

b.

Figure 9 a. Condensation rate versus packed bed height. b. Dehumidification effectiveness versus packed bed height.

Heat and Mass Transfer in Packed Bed Liquid Desiccant Regenerators - An Experimental Investigation

Viktoria Martin and D. Yogi Goswami [1]

Solar Energy and Energy Conversion Laboratory
Department of Mechanical Engineering
University of Florida
Gainesville, Florida 32611-6300

ABSTRACT

Liquid desiccant cooling can provide control of temperature and humidity, while at the same time lowering the electrical energy requirement for air conditioning. Since the largest energy requirement associated with desiccant cooling is low temperature heat for desiccant regeneration, the regeneration process greatly influences the overall system performance. Therefore, the effects of variables such as air and desiccant flow rates, air temperature and humidity, desiccant temperature and concentration, and the area available for heat and mass transfer on the regeneration process are of great interest. Due to the complexity of the regeneration process, which involves simultaneous heat and mass transfer, theoretical modeling must be verified by experimental studies. However, a limited number of experimental studies are reported in the literature. This paper presents results from a detailed experimental investigation of the heat and mass transfer between a liquid desiccant (triethylene glycol) and air in a packed bed regenerator using high liquid flow rates. To regenerate the desiccant, it is heated to temperatures readily obtainable from flat-plate solar collectors. A high performance packing that

combines good heat and mass transfer characteristics with low pressure drop is used. The rate of water evaporation, as well as the effectiveness of the regeneration process is assessed based on the variables listed above. Good agreement is shown to exist between the experimental findings and predictions from finite difference modeling. In addition, the findings in the present study are compared to findings previously reported in the literature. Also, the results presented here characterize the important variables that impact the system design.

NOMENCLATURE

a_t	specific surface area of packing (m^2/m^3)
c_p	specific heat (kJ/kg-°C)
F_G	gas phase mass transfer coefficient ($kmol/m^2$-s)
F_L	liquid phase mass transfer coefficient ($kmol/m^2$-s)
G	superficial air (gas) flow rate (kg/m^2-s)
h_G	gas side heat transfer coefficient (kJ/m^2-s)
L	superficial desiccant flow rate (kg/m^2-s)
M	molar mass (kg/kmol)
m	flow rate (kg/s) or (g/s)
N_v	molar vapor mass transfer flux ($kmol/m^2$-s)
p	vapor pressure (Pa)
Q	rate of heat transfer (W)
q	heat transfer flux (kW/m^2)

T	temperature (°C)
TEG	triethylene glycol
X	desiccant concentration (kg TEG / kg solution)
x	desiccant mole fraction (kmol desiccant / kmol solution)
Y	air humidity ratio (kg water/kg dry air or g water/kg dry air)
y	water mole fraction (kmol water / kmol air)
Z	tower height (m)
ε	effectiveness
λ	latent heat of condensation/vaporization (kJ/kg)
π	dimensionless vapor pressure difference (Equation 9)

Subscripts

a	air
equ	equilibrium
evap	water evaporation
G	gas phase
HE	heat exchanger
IN	inlet
i	interface
L	desiccant or liquid phase
OUT	outlet

v	vapor
w	water
Y	humidity
0	reference state

INTRODUCTION

Liquid desiccant cooling can provide control of temperature and humidity, while at the same time lowering the electrical energy requirement for air conditioning. The largest energy requirement associated with the use of desiccant cooling is low temperature heat for desiccant regeneration, and this heat can be provided by solar flat-plate collector system or by waste heat. However, the auxiliary energy requirement for desiccant regeneration can be large (Öberg and Goswami, 1998b), so that the effectiveness of the desiccant regeneration process greatly influences the overall performance of the desiccant system. Equipment commonly employed as regenerators in desiccant systems are: boilers (e.g., Marsala et al., 1989, and Albers et al., 1991); solar trickle collector regenerators (e.g., Thornbloom and Nimmo, 1995, and Gandhidasan, 1994); spray chambers containing a hot water finned coil (e.g, Robison, 1977, and Scalabrin and Scaltriti, 1990); and packed bed absorption towers (e.g, Kinsara et al., 1996, Öberg and Goswami, 1998b, and Sick et al., 1988). A more detailed review of liquid desiccant system configurations is given by Öberg and Goswami (1998a).

Peng and Howell (1984) have modeled the performance of desiccant regenerators. An open surface trickle solar collector regenerator, a glazed trickle solar collector regenerator, and a

regeneration chamber containing a finned tube heating coil were analyzed and compared. The authors concluded that an open solar collector regenerator was not practical for hot and humid climates. As opposed to a glazed trickle collector regenerator, the authors concluded that a regeneration chamber design would be compact, allow for steady operation, and it could be used with low-grade heat from sources other than solar. For these reasons a regeneration chamber was chosen for the present investigation. However, instead of using a finned tube heating coil as the extended heat and mass transfer surface, it was decided to use a packed bed tower since the packing provides very large surface area per unit volume, thus allowing for a compact design.

To advance solar-based liquid desiccant cooling technology, the impact of variables such as air and desiccant flow rates, air temperature and humidity, desiccant temperature and concentration, and the area available for heat and mass transfer on the performance of a packed bed regenerator is of great interest. Gandhidasan (1990) developed a simplified theoretical model for regeneration of a desiccant in a packed bed using solar heated air. Also, the performance of a packed bed regenerator was theoretically evaluated in terms of a humidity effectiveness and an enthalpy effectiveness by Khan (1994). However, desorption of water in a packed bed tower involves simultaneous heat and mass transfer with complex fluid flow patterns, so theoretical models must be verified by experimental studies. Regeneration of lithium chloride in a packed bed was examined experimentally by Löf et al. (1984). With the air providing the heat for the regeneration process, this study examined the overall heat and mass transfer coefficients as a function of flow rates and inlet temperatures. Patnaik et al. (1990) conducted experiments on a packed bed tower for the regeneration of aqueous lithium bromide. They

studied the influence of the type of liquid distribution system on the performance of the regenerator, and presented correlations based on experimental results for the rate of water evaporation as a function of inlet air temperature, humidity, inlet desiccant concentration and flow rate. A mixture of calcium chloride and lithium chloride in an aqueous solution was considered by Ertas et al. (1994) who investigated desiccant regeneration as a function of desiccant flow rate, inlet desiccant conditions, and inlet air humidity. Potnis and Lenz (1996) conducted an experimental study considering the influence of desiccant flow rate on the regeneration of aqueous lithium bromide in a packed bed regenerator (as well as air dehumidification in a packed bed). Based on the experimental findings, they developed dimensionless liquid-side mass transfer coefficients for both random and structured tower packings.

The objective of the present investigation is to provide additional experimental data for desiccant regeneration to aid in the design of solar-based desiccant systems. Therefore, a thorough experimental analysis was carried out exploring the influence of air and desiccant flow rates, air and desiccant inlet temperatures, inlet air humidity ratio, inlet desiccant concentration, and the area available for heat and mass transfer. Compared to the experimental studies listed above, higher liquid flow rates were used in the present investigation. A preliminary set of experiments showed these higher flow rates to be necessary to ensure adequate wetting of the packing. Compared to the study by Patnaik et al. (1990), the inlet air humidity ratio was significantly higher in the present investigation as it was varied in a range corresponding to outdoor conditions typically encountered in a humid climate. In a desiccant system, dry indoor

air may not always be available for the regeneration process. Due to its lower corrosivity and lower surface tension as compared to salt solutions, 95 % by weight triethylene glycol (TEG) was chosen as the desiccant. The performance of the regeneration process was evaluated in terms of the water evaporation rate and the humidity effectiveness (concept introduced in a later section). The effectiveness of desiccant regeneration in a packed bed has not been experimentally examined before. The experimental findings from the present study were also compared to those obtained from theoretical modeling, as well as other experimental findings reported in the literature.

HUMIDITY EFFECTIVENESS - A PERFORMANCE PARAMETER FOR A PACKED BED REGENERATOR

Analogous to the heat transfer effectiveness commonly used in heat exchanger analysis (ε_{HE}, Equation 1), the concept of effectiveness can be applied to the heat and mass transfer in a packed bed dehumidifier and regenerator.

$$\varepsilon_{HE} = \frac{Q_{actual}}{Q_{max}} \tag{1}$$

The humidity effectiveness of a packed bed dehumidifier/regenerator, ε_Y, is defined as the actual change in air humidity ratio across the packed bed, divided by the maximum possible change (Ullah et al., 1988).

$$\varepsilon_Y = \frac{Y_{IN} - Y_{OUT}}{Y_{IN} - Y_{equ}} \tag{2}$$

Here, Y_{IN} and Y_{OUT} are the humidity ratios at the air inlet and outlet, respectively, and Y_{equ} is the humidity ratio in equilibrium with the desiccant at the local solution temperature and concentration. For counter flow arrangement, Y_{equ} would be the humidity ratio of the air in equilibrium with the desiccant at the desiccant inlet.

Knowledge of the humidity effectiveness as a function of design variables gives a valuable design tool since for known inlet desiccant conditions, air humidity, and effectiveness, the outlet air humidity ratio can be found. Then, the outlet desiccant concentration (which is of most interest for the desiccant regeneration process) will follow from a water mass balance across the packed bed. Therefore, the influence of design variables on the humidity effectiveness has been investigated.

A correlation for ε_Y as a function of air and liquid flow rates, column and packing dimensions, and equilibrium properties of the desiccant derived by Chung (1994) is given by Equation 3.

$$\varepsilon_Y = \frac{1-\left\{\dfrac{0.205\left(\frac{G_{IN}}{L_{IN}}\right)^{0.174}\exp\left[0.985\left(\frac{T_{a,IN}}{T_{L,IN}}\right)\right]}{(aZ)^{0.184}\,\pi^{1.680}}\right\}}{1-\left\{\dfrac{0.152\exp\left[-0.686\left(\frac{T_{a,IN}}{T_{L,IN}}\right)\right]}{\pi^{3.388}}\right\}} \tag{3}$$

Here, the parameter, π, representing the equilibrium properties of the desiccant is defined as the ratio of the vapor pressure depression to the vapor pressure of pure water.

$$\pi = \frac{p_w(T_{L,IN}) - p_L(T_{L,IN}, X_{IN})}{p_w(T_{L,IN})} \tag{4}$$

Although this correlation was obtained from experimental data on desiccant air dehumidification in packed beds (absorption mode), its applicability for desiccant regeneration in a packed bed (desorption) is examined in the present study.

EXPERIMENTAL PROCEDURE

The rate of water evaporation from the desiccant as well as the humidity effectiveness of the regeneration process were studied experimentally as a function of the following variables: air and desiccant flow rates; air temperature and humidity ratio; desiccant temperature and concentration; and the height of the packed bed.

A schematic of the experimental facility is shown in Figure 1. The packed bed regenerator was constructed from a 25.4 cm (10 in) diameter acrylic tube to allow for flow visualization. The tower was made in sections so that the bed height could be varied without changing the distance from the liquid distribution to the top of the bed. The inner diameter of the tower was 0.24 m. The packing used was 2.54 cm (1 in) polypropylene Rauschert Hiflow® rings with a specific surface area of 210 m^2/m^3. Fresh, unused triethylene glycol was stored in a tank, and its temperature was adjusted by circulating hot water through a submerged copper coil. Before each experiment, the desiccant was allowed to recirculate to remove temperature and concentration gradients. Air was blown past an air heater and through a humidifying chamber to adjust its temperature and humidity before it entered the packed tower. At the air inlet, an air filter was installed to prevent airborne particles and water droplets from entering the regenerator. When the desired air and desiccant conditions were obtained, the desiccant was allowed to flow

through the tower. The desiccant was distributed over the packing by three spray heads evenly spaced in an equilateral triangular configuration. A section of packing (20 cm) was placed above the spray heads, before the air outlet to minimize the loss of desiccant through the air outlet. Once steady state was obtained, measurements were taken for 15 to 20 minutes using a PC-based data acquisition system. These measurements included inlet and outlet temperatures of the desiccant and the air using copper-constantan thermocouples, as well as inlet and outlet air relative humidities using electrical relative humidity transducers. In addition, samples of the desiccant entering and leaving the regenerator were taken during the experiment and analyzed for water content using Karl Fischer titration. The used desiccant was pumped over to a separate storage tank so that the inlet desiccant concentration did not change during the experiment. The liquid flow rate was set approximately using a flow indicator. However, it was measured accurately by a catch-bucket method. The air velocity was measured using a vane anemometer at the air outlet. Finally, an air-over-oil manometer determined the air pressure drop over the packed bed (not including the mist eliminating section).

Experiments were conducted for each variable at three levels (low, intermediate, and high value) while keeping the other variables constant at their intermediate value. Three experiments were conducted at each level to reveal the repeatability of the experimental measurements.

FINITE DIFFERENCE MODEL FOR THE PACKED BED REGENERATOR

For theoretical modeling of the desiccant regeneration process in a packed bed, a finite difference model based on a model for adiabatic gas absorption presented by Treybal (1969) was

used. Figure 2 shows an overview of the packed bed, as well as a small segment, dZ, of the packed bed. In summary, the assumptions made in this model are: adiabatic absorption; concentration and temperature gradients in the flow direction (Z-direction, referring to Figure 2) only; only water is transferred between the air and the desiccant; the interfacial surface area is the same for both heat and mass transfer, and it is equal to the specific surface area of the packing; the heat of mixing is negligible as compared to the latent heat of condensation of water; and the resistance to heat transfer in the liquid phase is negligible.

In the finite difference model, the packed bed height Z is divided into small segments, dZ (Figure 2b), and the mass and energy balances are solved for each segment, from the bottom to the top of the tower, resulting in the governing equations given below. These governing equations include the changes in air humidity, air temperature, desiccant temperature, desiccant concentration, and desiccant flow rate across the segment dZ. A detailed derivation of these equations is given elsewhere (Treybal, 1969, and Öberg, 1998).

The mass flux of water vapor across the interface (Figure 2b), taken positive from the gas to the liquid, is

$$N_v M_w a_t dZ = F_G M_w a_t dZ \ln\left(\frac{1-y_i}{1-y}\right) = F_L M_w a_t dZ \ln\left(\frac{x}{x_i}\right) = -G dY \qquad (5)$$

Equation (5) gives the change in air humidity across the segment as

$$\frac{dY}{dZ} = -\frac{M_w F_G a_t}{G} \ln\left(\frac{1-y_i}{1-y}\right) \qquad (6)$$

where the interfacial gas phase concentration is given by:

$$y_i = 1 - (1 - y)\left(\frac{x}{x_i}\right)^{\frac{F_L}{F_G}} \tag{7}$$

Equation (7) is the result of equating the molar vapor mass transfer flux, N_v, as calculated with respect to the gas phase to the molar flux calculated with respect to the liquid phase (Equation 5). The vapor-liquid equilibrium data for the triethylene glycol-water system (Dow Chemical Company, 1992) were used along with Equation 3 to solve iteratively for the interface concentrations in the gas and liquid phases. The equilibrium concentrations are a function of the liquid desiccant temperature and concentration. Empirical correlations for the mass transfer coefficients obtained for packed bed desiccant regenerators are available in the literature. Potnis and Lenz (1996) presented dimensionless liquid-side mass transfer correlations based on experimental results on packed bed liquid desiccant contactors using a lithium bromide solution as the desiccant. However, since the present investigation used TEG as the desiccant, it was decided to use the empirical correlations by Onda et al. (1968) for the gas and liquid phase heat and mass transfer coefficients (h_G, F_G, and F_L). These correlations have predicted data within ± 20 % for a range of operating and system conditions, using organic solvents as well as water (Onda et al., 1968).

The air temperature gradient across the segment is found from an energy balance across the gas phase (control volume I, Figure 2b).

$$\frac{dT_a}{dZ} = \frac{-h_G a' (T_a - T_L)}{G (c_{p,a} + Y c_{p,v})} \tag{8}$$

Here $h_G a'$ is the heat transfer coefficient corrected for simultaneous heat and mass transfer.

$$h_G a' = \frac{-G\, c_{p,v} \dfrac{dY}{dZ}}{1 - \exp\left(\dfrac{G\, c_{p,v} \dfrac{dY}{dZ}}{h_G a_t} \right)} \tag{9}$$

An energy balance over the entire segment (control volume III, Figure 2b) gives the change in desiccant temperature:

$$dT_L = \frac{G}{c_{p,L} L} \left\{ \left(c_{p,a} + Y c_{p,v} \right) dT_a + \left(c_{p,v} \left[T_a - T_0 \right] - c_{p,L} \left[T_L - T_0 \right] + \lambda_0 \right) dY \right. \tag{10}$$

A water mass balance across the segment (control volume III, Figure 2b) yields the change in desiccant concentration.

$$dX = -\frac{G}{L} X\, dY \tag{11}$$

Finally, an overall mass balance over control volume III (Figure 2) gives the change in desiccant flow rate.

$$dL = G\, dY \tag{12}$$

A FORTRAN computer program was written to carry out the finite difference analysis with the bed height Z divided into 1000 segments. An under-relaxation iterative procedure was utilized to promote convergence. The criteria for convergence was ± 0.05 °C for the inlet desiccant temperature, and ± 0.0001 kg TEG/kg solution for the inlet desiccant concentration.

RESULTS AND DISCUSSION

The results from the experimental study and theoretical modeling are shown graphically

in Figures 3 to 9. These figures show the water evaporation rate, m_{evap}, and the humidity effectiveness, ε_Y, as a function of air and desiccant flow rates and inlet temperatures, desiccant concentration, inlet air humidity ratio, and packed bed height. In addition, performance predictions from Chung's correlation (Equation 3) are shown along with the experimental results.

Uncertainties of the experimental measurements were calculated using the method by Kline and McClintock (1953). Error bars obtained from these uncertainty calculations are shown in the figures. Further details on the uncertainty analysis are given elsewhere (Öberg, 1998). The repeatability of the experimental measurements is also indicated in the figures as three experimental data points are shown for each set of variables. To further cross-check the consistency of the data, a water mass balance across the regenerator was calculated, yielding ± 5 % deviation between the amount of water entering and leaving the regenerator. Similarly, an energy balance across the regenerator gave deviations of ± 10 %.

The pressure drop across the packed bed varied between 30 and 210 Pa/m packing, depending on the air flow rate. Typically, packed bed absorbers/desorbers are designed for a pressure drop between 200 and 400 Pa/m packing (Treybal, 1980). Hence, even at the highest air flow rate, the regenerator operated at the lower end of the typical design conditions.

The finite difference model presented herein has previously been found to give good performance predicitions for air dehumidification in a packed bed (Öberg and Goswami, 1998c). Figures 3 to 9 show that the experimental findings for desiccant regeneration also agree well with the predictions from the finite difference model. Only a slight discrepancy can be seen (approximately ± 15 %), and the difference is within the error bars of the experiments. Also, the

repeatability of the experiments for each set of variables is better than what the error bars indicate. In cases where there is a discrepancy, the finite difference model generally over-predicts the performance of the regenerator. One explanation for this is the assumption that the area available for heat and mass transfer is equal to the total specific surface area of the packing. Even though the liquid flow rate is high as compared to the air flow rate, complete wetting of the packing is difficult to obtain. Therefore, the mass transfer area is less than the packing surface area. Also, it should be kept in mind that the correlations used for the transfer coefficients are empirical, and they were obtained for liquid-gas systems and packings other than those used in the present study.

Chung's correlation greatly overpredicts the performance of the regenerator, and the influence of design variables is not accurately shown from this correlation. For instance, the humidity effectiveness obtained from the finite difference model and the experiments shows a larger dependency on the air flow rate and packed bed height than what is predicted by Chung's correlation (figures 3b and 9b). Since this correlation was obtained from experimental data on packed bed dehumidifiers, accurate predictions on desiccant regeneration would not be expected.

The experimental study on the packed bed regeneration tower showed the following variables to significantly influence the regeneration performance: air flow rate, inlet desiccant temperature, inlet air humidity ratio, inlet desiccant concentration, and the packed bed height. The water evaporation rate increases with the air flow rate (Figure 3a). However, the humidity effectiveness decreases with the air flow rate (Figure 3b) since the change in humidity ratio across the tower decreases as the air flow rate increases.

In the regeneration process, the water vapor pressure in the liquid is higher than the vapor pressure in the air so that water is evaporated from the desiccant to the air. Therefore, as the liquid vapor pressure increases with the desiccant temperature, the potential for mass transfer increases. Hence, the water evaporation rate increases with the liquid temperature (Figure 6a). However, the effectiveness shows only a slight dependency on the inlet desiccant temperature (Figure 6b). This is because the highest possible humidity ratio that can be obtained at the air outlet, Y_{equ}, is dependent on $T_{L,IN}$, making the effectiveness somewhat normalized with respect to the desiccant temperature.

By similar reasoning it may be explained why the water evaporation rate decreases with increasing desiccant inlet concentration, X_{IN}, while the desiccant concentration did not influence the humidity effectiveness significantly (Figure 8). Increasing X_{IN} decreases the driving force for mass transfer, and thus lowers the water evaporation rate. On the other hand, Y_{equ} is dependent on X_{IN} so that the humidity effectiveness is normalized with respect to the desiccant concentration. Therefore, the humidity effectiveness is not significantly influenced by X_{IN}.

An increase in the inlet humidity ratio increases the vapor pressure in the air, decreasing the potential for mass transfer between the desiccant and the air. Therefore, the water evaporation rate decreases with increasing inlet air humidity (Figure 7a). By definition, the humidity effectiveness is already normalized with respect to the inlet humidity ratio (Equation 2). This explains why the humidity effectiveness is not significantly dependent on the inlet humidity ratio as shown in Figure 7b.

Increasing the bed height increases the water evaporation rate, as well as the effectiveness

(Figure 9). This is because a taller bed increases the area for heat and mass transfer so that a humidity ratio closer to the equilibrium value, Y_{equ}, may be reached at the air outlet.

A comparison between the findings in this investigation and experimental findings from studies previously reported in the literature is given in Table 1. The table shows the desiccant used, the parameters describing the performance, the independent variables and the ranges examined. Under each variable, up- and down-arrows indicate the influence of the variable on the performance parameter. Table 1 shows that a limited amount of experimental data on packed bed regenerators is available in the literature. Thus, the present detailed investigation provides valuable insights into the design of the desiccant regeneration process, especially for the use of triethylene glycol as the desiccant.

In general, findings from all the studies agree well. However, Ertas et al. (1994), Patnaik et al. (1990), and Potnis and Lenz (1996) found that the water evaporation rate increases with desiccant flow rate, whereas the present study found only a slight dependency on the desiccant flow rate. Patnaik et al. (1990) and Potnis and Lenz (1996) explained the large dependency on desiccant flow rate as being due to the large resistance to mass transfer in the liquid phase. In the present investigation TEG was used as the desiccant whereas salt solutions were used in the other investigations, and it may be that the resistance to mass transfer in the liquid phase is not as important in the TEG-water-air system. Also, Patnaik et al. (1990) explained part of the dependency on the desiccant flow rate as being due to increased wetting of the packing with increasing flow rate. That is, if the liquid flow rate is low, an increase may provide better wetting of the packing, and therefore increase the performance of the regenerator. In the present

study, higher desiccant flow rates were used than in the other studies. At a certain desiccant flow rate, maximum wetting of the packing is obtained and a further increase of the flow rate will not improve the wetting. Therefore, in addition to a large resistance to mass transfer in the liquid phase, the performance improvement reported in the previous investigations (Ertas et al.,1994, Patnaik et al., 1990, and Potnis and Lenz, 1996) is also explained by the increased wetting of the packing with increasing flow rate. Since no significant dependency was obtained in the present investigation, it may be concluded that the flow rates used were sufficient to obtain maximum wetting in the system used here.

In the study by Patnaik et al. (1990), the evaporation rate increases with air temperature. In the present study, no dependency on the air temperature was obtained. Again, this discrepancy can be explained by the higher desiccant flow rates used in the present study. The performance of the regeneration process will increase with increased heat addition since this will increase the average temperature in the regenerator, which in turn increases the driving force for mass transfer. With a higher desiccant flow rate, the relative amount of heat added to the regenerator by the air stream is lower. Thus, the inlet air temperature is not as important when using high desiccant flow rates.

Finally, provided that the desiccant flow rate is high enough to ensure adequate wetting of the packing, only the air flow rate, G, and the tower height, Z, significantly influence the humidity effectiveness, ε_Y. Hence, the knowledge of a functional relationship between ε_Y, G, and Z opens up the possibility for a greatly simplified model of the desiccant regeneration in a packed bed. However, such a model would be system specific and would only apply to the

specific packing, desiccant, etc., for which the relationship was obtained.

CONCLUSIONS

As the largest energy requirement associated with desiccant cooling is low temperature heat for desiccant regeneration, the performance of the regeneration process greatly influences the overall system performance. Therefore, to advance solar-based liquid desiccant cooling technology, the many design variables affecting the performance of a packed bed regenerator have been experimentally investigated. In addition, performance predictions from a theoretical model, and empirical correlations previously available in the literature, have been compared to the experimental findings.

Design variables found to have the greatest impact on the performance of the regenerator are the air flow rate and the humidity ratio, the desiccant temperature and concentration, and the packed bed height. The liquid flow rate and the inlet air temperature did not have a significant effect on the regenerator performance; however, the liquid flow rate must be high enough to ensure wetting of the packing. In this study, the liquid flow rate was higher as compared to the flow rates used in the studies previously reported.

The results obtained in this study compare reasonably well with other experimental investigations. Contrary to the findings of this study, some studies have found that the liquid flow rate and air temperatures influence the performance. One explanation for this is the lower liquid flow rate used in those investigations.

The regenerator performance predicted with the finite difference model described in this

paper shows a good agreement with the experimental findings. Thus, for a detailed study of the regeneration process, the finite difference model gives accurate performance predictions based on fundamental equations, minimizing the assumptions and use of empirical correlations.

Correlations for the effectiveness of the absorption/desorption process in a packed bed dehumidifier/regenerator as a function of design variables are very useful for quick performance estimates, and for incorporating into system simulation models. The most general correlation currently available in the literature is the one by Chung (1994) which is based on experimental data for air dehumidification in a packed bed. From the present study it is evident that this correlation is not applicable to desiccant regeneration in a packed bed. Hence, it would be valuable if correlations valid for both dehumidification and regeneration were derived.

REFERENCES

Albers, W. F., Beckman, J. R., Farmer, R. W., Gee, K. G., 1991, "Ambient Pressure, Liquid Desiccant Air Conditioner," ASHRAE Transactions, Vol. 97, pt. 2, pp. 603-608.

Chung, T.-W., 1994, "Predictions of the Moisture Removal Efficiencies for Packed-Bed Dehumidification Systems," Gas Separation & Purification, Vol. 8 (4), pp. 265-268.

Dow Chemical Company, 1992, A Guide to Glycols, Dow Chemical Company, Midland, Michigan.

Ertas, A., Gandhidasan, P., Kiris, I., and Anderson, E. E., 1994, "Experimental Study on the Performance of a Regeneration Tower for Various Climatic Conditions," Solar Energy, Vol. 53(1), pp. 125-130.

Gandhidasan, P., 1994, "Performance Analysis of an Open-Cycle Liquid Desiccant Cooling System Using Solar Energy for Regeneration," International Journal of Refrigeration, Vol. 17 (7), pp. 475-480.

Gandhidasan, P., 1990, "Reconcentration of Aqueous Solutions in a Packed Bed: A Simple Approach," Journal of Solar Energy Engineering, Vol. 112, pp. 268-272.

Khan, A. Y., 1994, "Sensitivity Analysis and Component Modeling of a Packed-Type Liquid Desiccant System at Partial Load Operating Conditions," International Journal of Energy Research, Vol. 18, pp.643-655.

Kinsara, A. A., Elsayed, M. M., and Al-Rabghi, O. M., 1996, "Proposed Energy-Efficient Air-Conditioning System Using Liquid Desiccant," Applied Thermal Engineering, Vol. 16 (10), pp. 791-806.

Kline, S. J., and McClintock, F. A., 1953, "Uncertainties in Single-Sample Experiments," Mechanical Engineering, Vol. 75, pp. 3-8.

Löf, G. O. G, Lenz, T. G., and Rao, S., 1984, "Coefficients of Heat and Mass Transfer in a Packed Bed Suitable for Solar Regeneration of Aqueous Lithium Chloride Solutions," Journal of Solar Energy Engineering, Vol. 106, pp. 387-392.

Marsala, J., Lowenstein, A., and Ryan, W.A., 1989, "Liquid Desiccant for Residential Applications,"ASHRAE Transactions, Vol. 95, pt. 1, pp. 828-834.

Öberg, V., 1998, Heat and Mass Transfer Study of a Packed Bed Absorber/Regenerator for Solar Desiccant Cooling, Ph.D. Dissertation, University of Florida, Gainesville, Florida.

Öberg, V., and Goswami, D. Y., 1998a, "A Review of Liquid Desiccant Cooling," Advances in Solar Energy, Vol. 12, Karl W. Böer, editor, American Solar Energy Society, Boulder, Colorado, pp. 346-385.

Öberg, V., and Goswami, D. Y., 1998b, "Performance Simulation of Solar Hybrid Liquid Desiccant Cooling for Ventilation Air Preconditioning," accepted for publication in Solar Engineering - 1998, Proceedings of the 16th Annual ASME Conference, New Mexico, pp. 176-182.

Öberg, V., and Goswami, D. Y., 1998c, "Experimental Study of the Heat and Mass Transfer in a Packed Bed Liquid Desiccant Air Dehumidifier," Journal of Solar Energy Engineering, Vol. 120, pp. 289-297.

Onda, K., Takeuchi, H., and Okumoto, Y., 1968, "Mass Transfer Coefficients Between Gas and Liquid Phases in Packed Columns," Journal of Chemical Engineering of Japan, Vol. 1 (1), pp. 56-62.

Patnaik, S., Lenz, T. G., and Löf, G. O. G., 1990, "Performance Studies for an Experimental Solar Open-Cycle Liquid Desiccant Air Dehumidification System," Solar Energy, Vol. 44 (3), pp. 123-135.

Peng, C. S. P., and Howell, J. R., 1984, "The Performance of Various Types of Regenerators for Liquid Desiccants," Journal of Solar Energy Engineering, Vol. 106, pp. 133-141.

Potnis, S. V., and Lenz, T. G., 1996, "Dimensionless Mass Transfer Correlations for Packed-Bed Liquid-Desiccant Contactors," Industrial and Engineering Chemistry Research, Vol. 35, 4185-4193.

Robison, H., 1977, "Liquid Sorbent Solar Air Conditioner," Alternative Energy Sources, Vol. 2, Veziro_lu, T. N., editor, Hemisphere Publishing Company, Washington, DC, pp. 761-779.

Scalabrin, G. and Scaltriti, G., 1990, "A Liquid Sorption-Desorption System for Air Conditioning With Heat at Lower Temperature," Journal of Solar Energy Engineering, Vol. 112, pp. 70-75.

Sick, F., Buschulte, T. K., Klein, P., Northey, P., and Duffie, J. A., 1988, "Analysis of the Seasonal Performance of Hybrid Liquid Desiccant Cooling Systems," Solar Energy, Vol. 40, pp. 211-217.

Thornbloom, M., and Nimmo, B., 1995, "An Economic Analysis of a Solar Open Cycle Desiccant Dehumidification System," Solar Engineering - 1995, Proceedings of the 13th Annual ASME Conference, Hawaii, Vol. 1, pp. 705-709.

Treybal, R. E., 1980, Mass Transfer Operations, third edition, McGraw-Hill, New York.

Treybal, R. E., 1969, "Adiabatic Gas Absorption and Stripping in Packed Towers," Industrial and Engineering Chemistry, Vol. 61 (7), pp. 36-41.

Ullah, M. R., Kettleborough, C. F., and Gandhidasan, P., 1988, "Effectiveness of

Moisture Removal for an Adiabatic Counterflow Packed Tower Absorber Operating with $CaCl_2$-Air Contact System," Journal of Solar Energy Engineering, Vol. 110, pp. 98-101.

Table 1. Packed Bed Regenerator Performance

Reference	Desiccant	Performance Parameter	Independent Variable						
			L (kg/m^2-s)	X_{IN} (kg/kg)	$T_{L,IN}$ (°C)	G (kg/m^2-s)	$T_{a,IN}$ (°C)	Y_{IN} (g/kg)	Z (m)
present study	TEG		4.2-6.5	0.93-0.95	60-70	0.4-2.0	30-50	10-25	0.4-0.8
		m_{evap}	↑↓	↓	↑	↑	↑↓	↓	↑
		ε_Y	↑↓	↑↓	↑↓	↓	↑↓	↑↓	↑
Ertas et al. (1994)	mixture of LiCl and $CaCl_2$		L^* (kg/m^2-s)		X_{IN} (kg/kg)		$T_{L,IN}$ (°C)	Y_{IN}^* (g/kg)	
			0.8-3.1		0.32-0.46		60-90	18-25	
		X_{OUT}	↓		↑		↑	↓	
		$T_{L,OUT}$	↑		↑		↑	↑	
Löf et al. (1984)	LiCl		G^* (kg/m^2-s)						
			0.7-0.74						
		h_Ga	↑						
Patnaik et al. (1990)	LiBr		L^* (kg/m^2-s)		$T_{L,IN}$ (°C)	X_{IN} (kg/kg)	$T_{a,IN}$ (°C)		Y_{IN} (g/kg)
			1.1-1.5		40-56	0.57-0.60	55-75		5-9
		m_{evap}	↑		↑	↓	↑		↓
Potnis and Lenz (1996)	LiBr		L^* (kg/m^2-s)						
			1-3						
		m_{evap}	↑						

* Values converted to this unit by present authors.
↑ performance parameter increases with increasing variable
↓ performance parameter decreases with increasing variable
↑↓ variable has no significant effect on the performance parameter

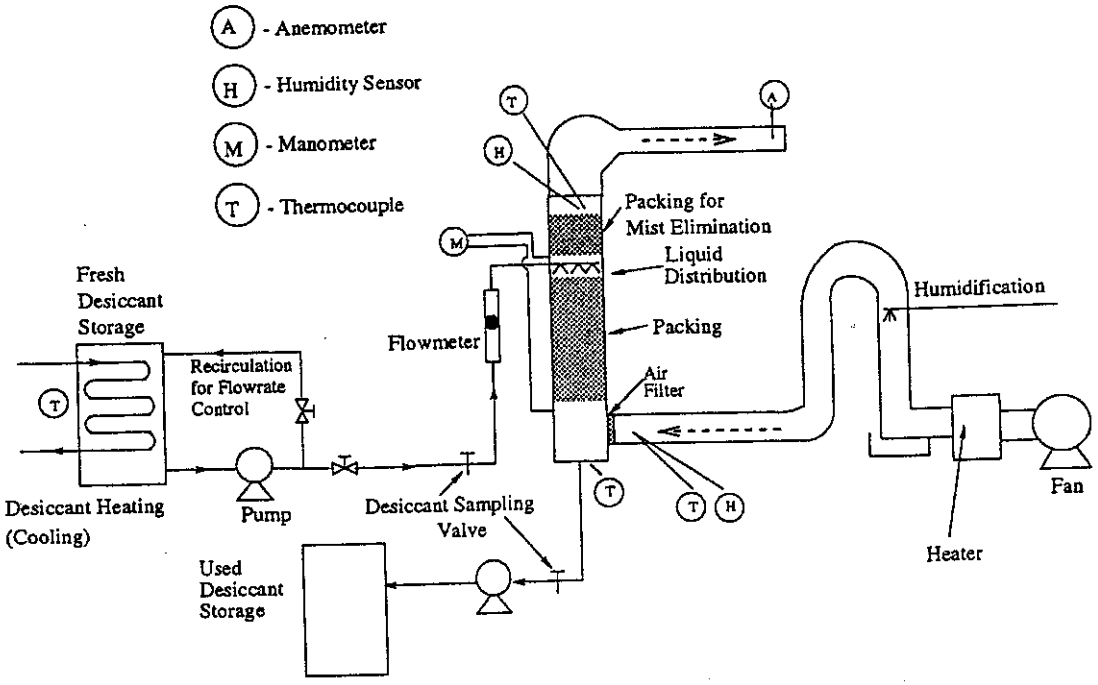

Figure 1. Experimental Facility

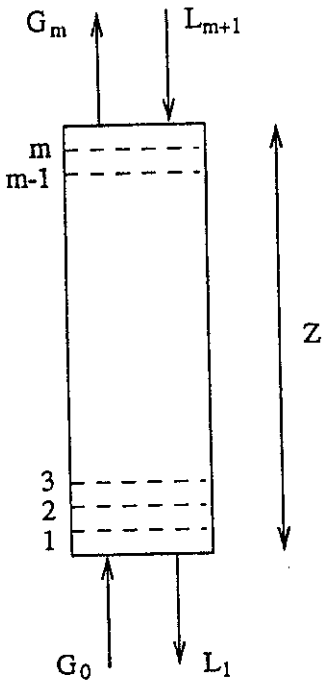

(a)

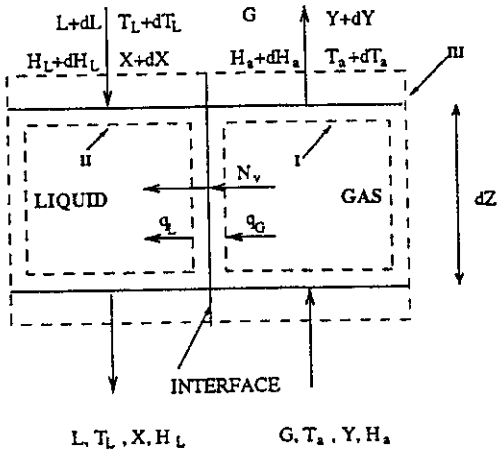

(b)

Figure 2. Packed Bed Regeneration Tower - (a) Tower Overview; (b) Differential Segment

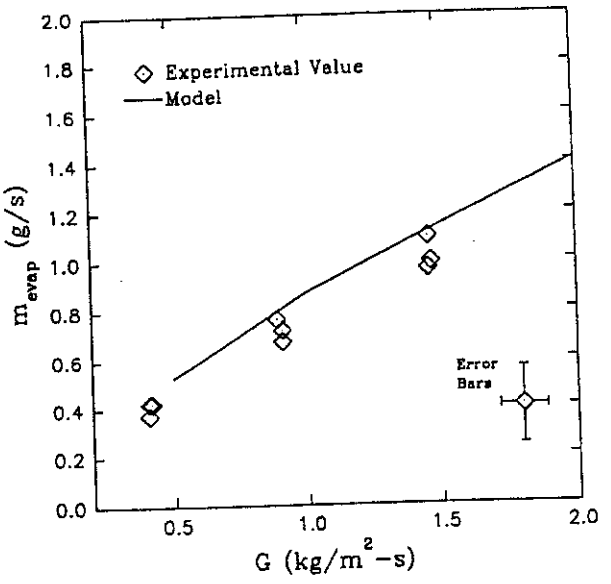

(a)

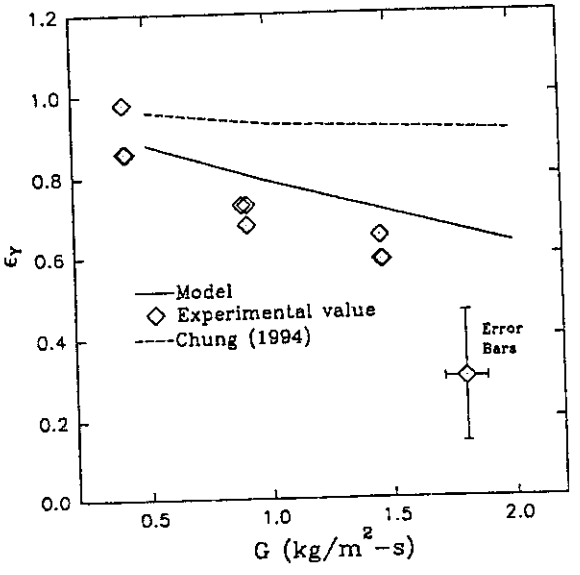

(b)

Figure 3. Influence of Air Flow Rate On: (a) Water Evaporation Rate; (b) Humidity Effectiveness

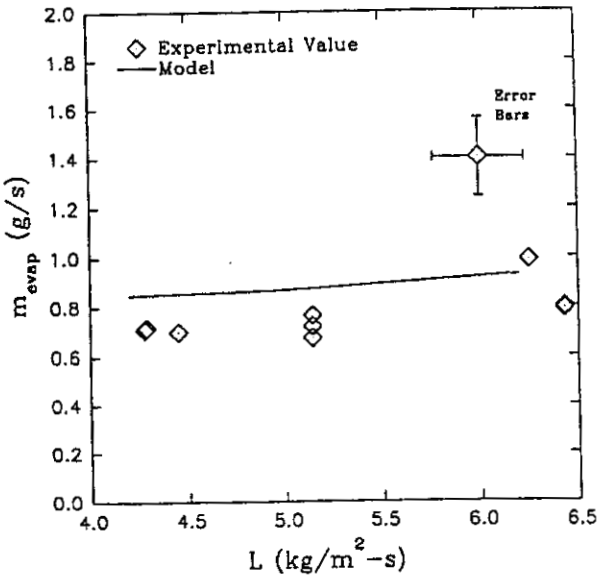

(a)

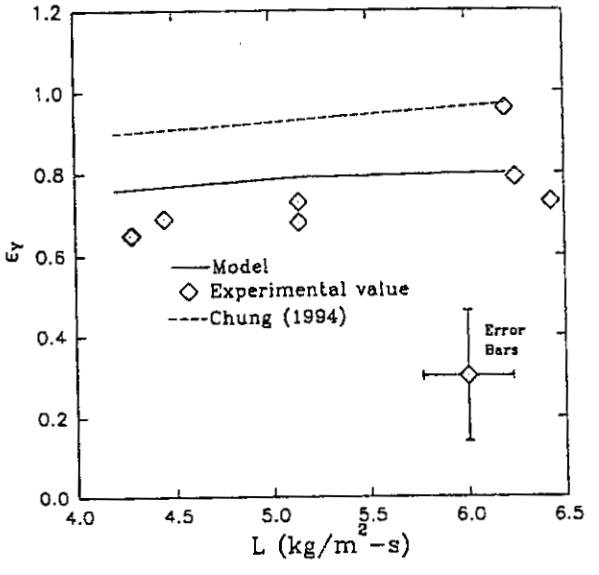

(b)

Figure 4. Influence of Desiccant Flow Rate On: (a) Water Evaporation Rate; (b) Humidity Effectiveness

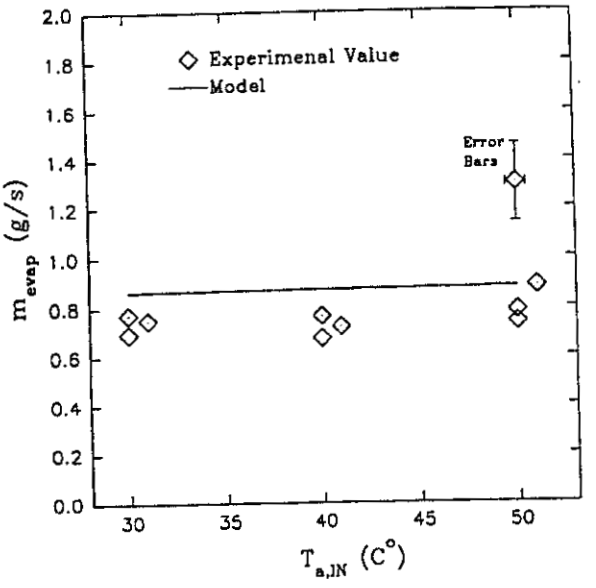

(a)

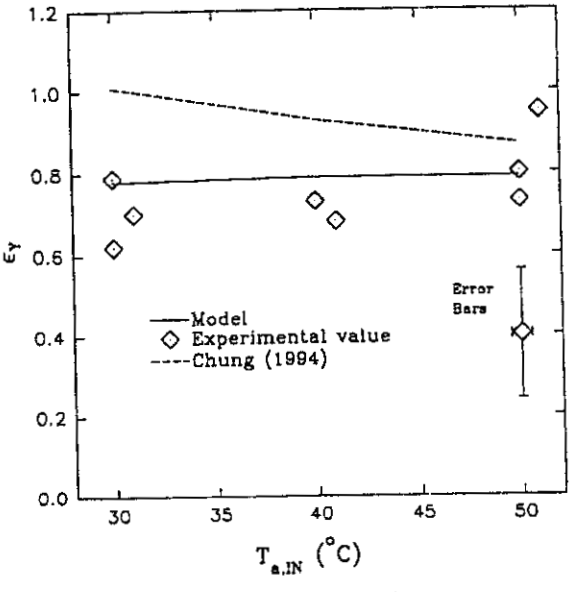

(b)

Figure 5. Influence of Inlet Air Temperature On: (a) Water Evaporation Rate; (b) Humidity Effectiveness

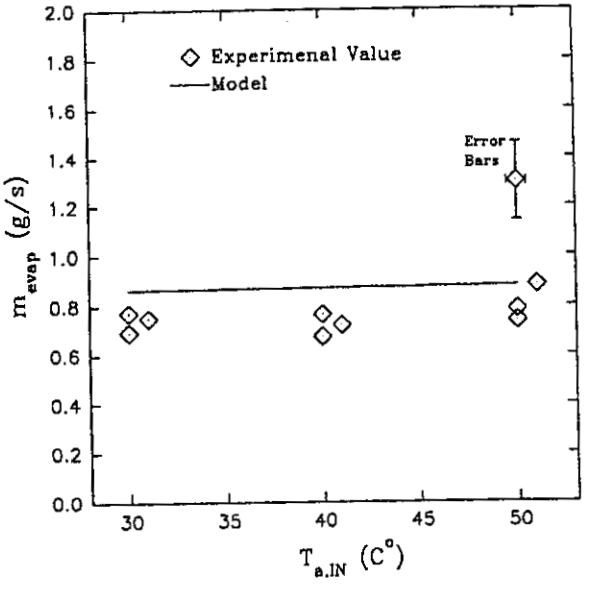

(a)

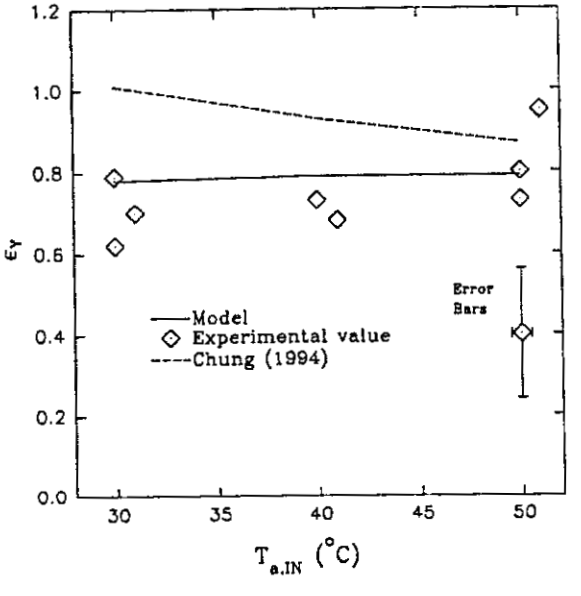

(b)

Figure 5. Influence of Inlet Air Temperature On: (a) Water Evaporation Rate; (b) Humidity Effectiveness

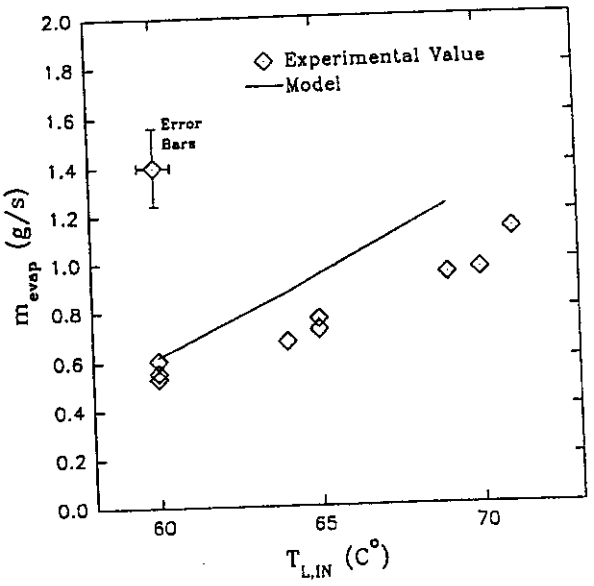

(a)

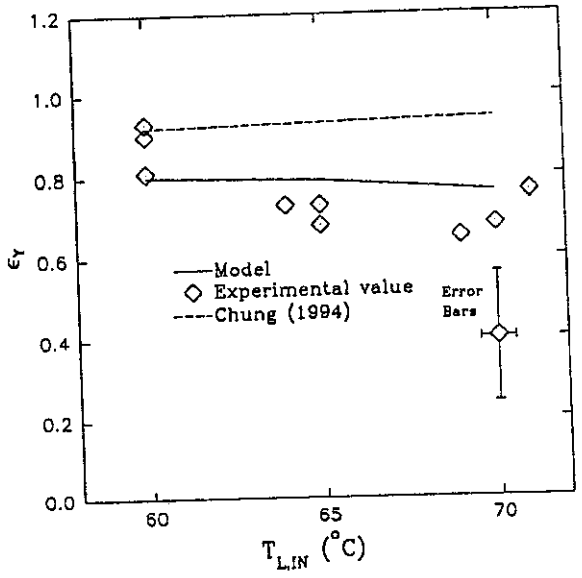

(b)

Figure 6. Influence of Inlet Desiccant Temperature On: (a) Water Evaporation Rate; (b) Humidity Effectiveness

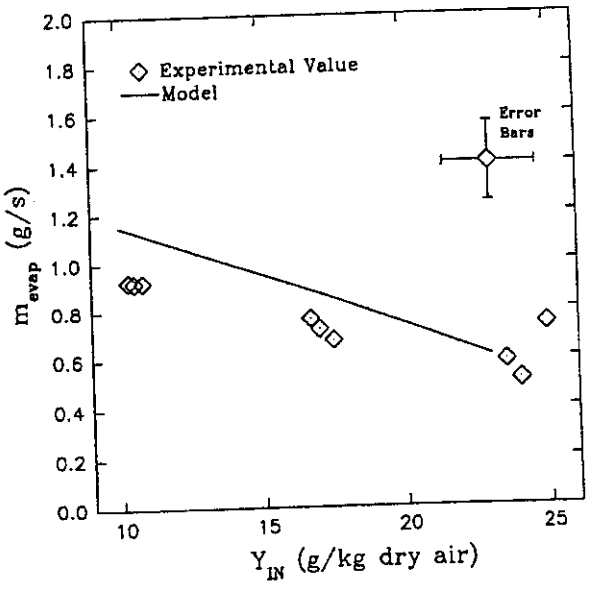

(a)

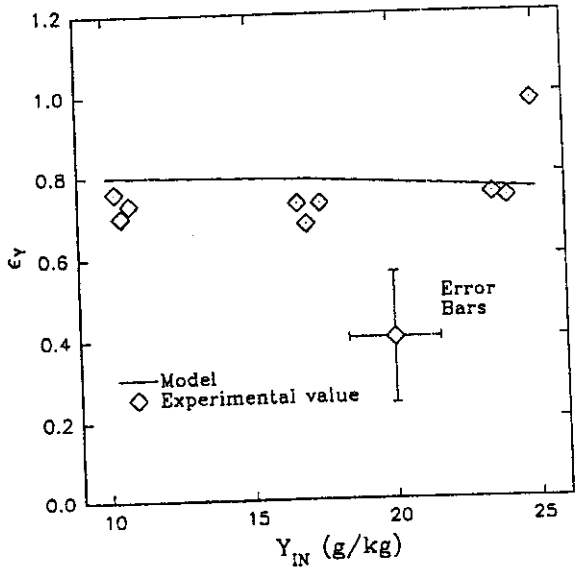

(b)

Figure 7. Influence of Inlet Air Humidity Ratio On: (a) Water Evaporation Rate; (b) Humidity Effectiveness

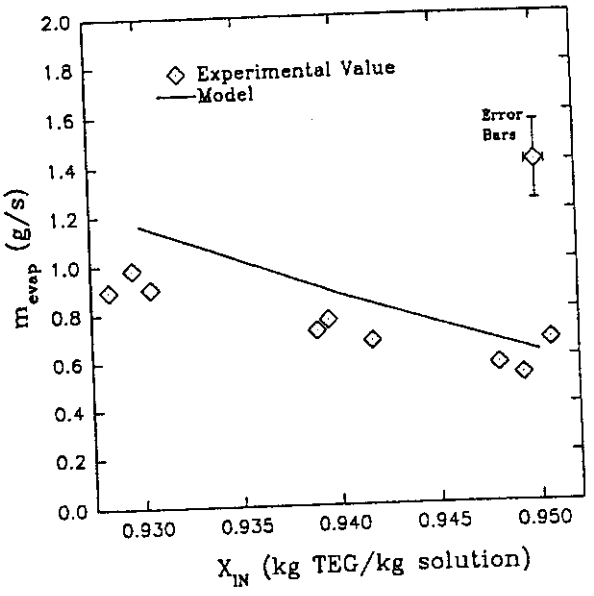

(a)

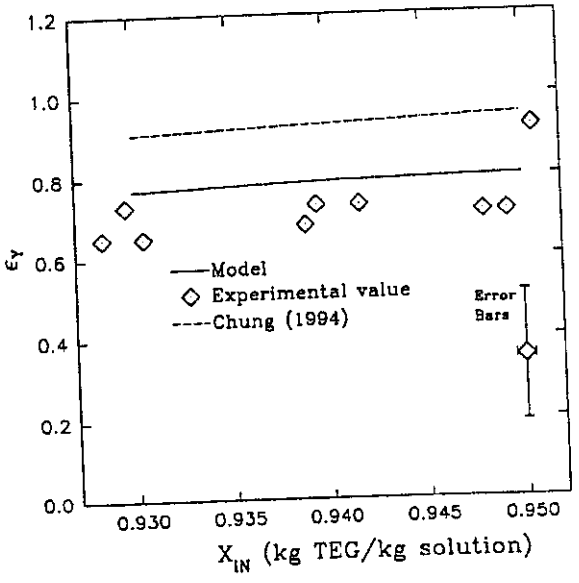

(b)

Figure 8: Influence of Inlet Desiccant Concentration On: (a) Water Evaporation Rate; (b) Humidity Effectiveness

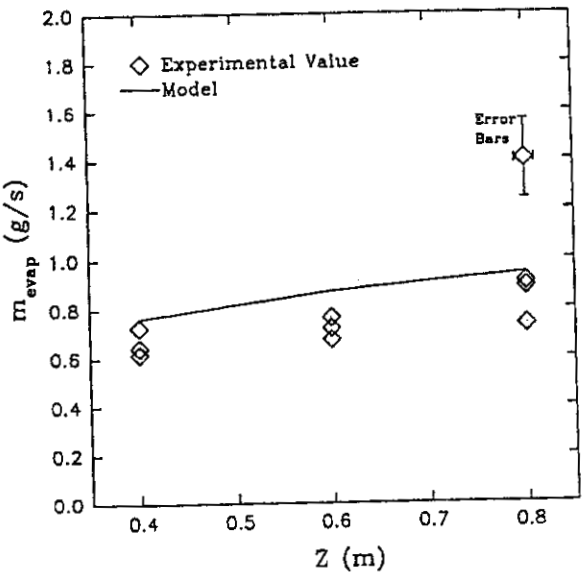

(a)

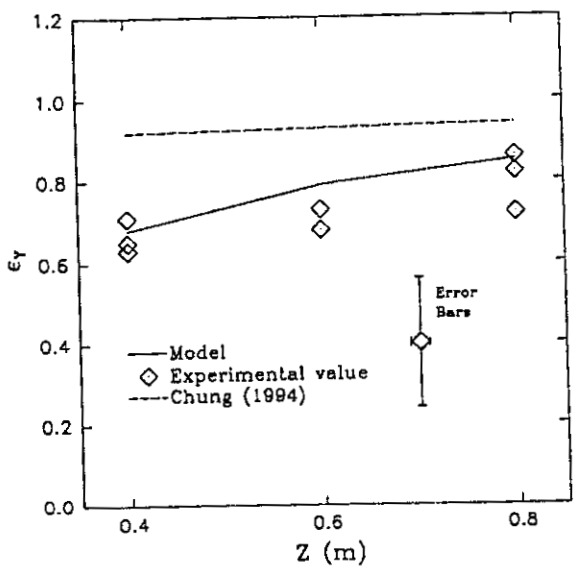

(b)

Figure 9. Influence of Packed Bed Height On: (a) Water Evaporation Rate; (b) Humidity Effectiveness

APPENDIX C

Laboratory Test for Lithium Chloride

Experimental Facility and Procedure

Experimental facility: A schematic of the experimental facility is shown in figure c-1. The facility is basically the same used by Öberg [1998] with some modifications to avoid corrosion and contact with the desiccant. The packed absorption tower was constructed from a 25.4 cm diameter (24 cm inner diameter) acrylic tube to allow for flow visualization. The packing used was 1 inch polypropylene Rauschert Hiflow® rings with a specific surface area of 210 m^2/m^3. The desiccant was distributed over the packing by three spray heads evenly spaced in an equilateral triangular configuration. To adjust the temperature of the inlet desiccant, cold and warm water was circulated through a submerged stainless steel coil. To adjust the temperature and humidity of the inlet air, an electrical heater and water spray nozzle were installed between the blower and the tower.

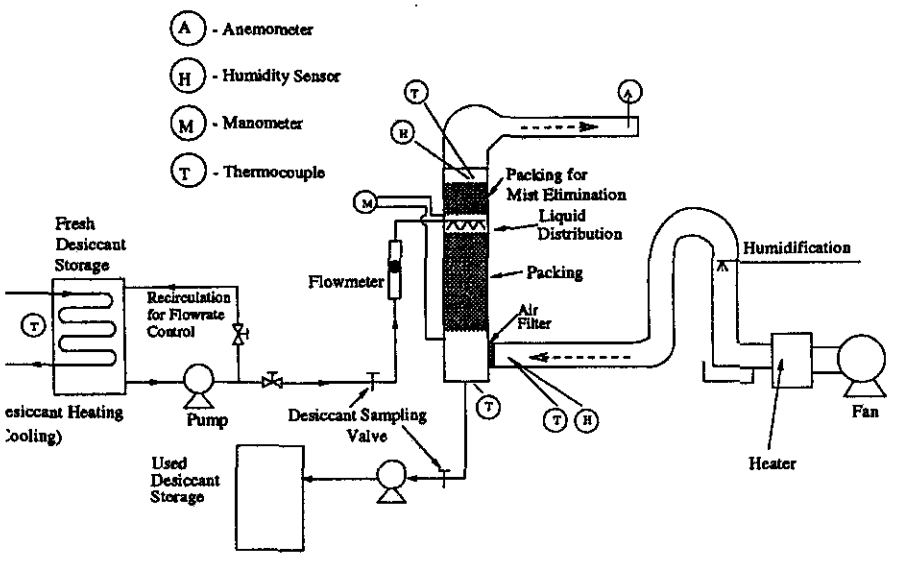

Figure c-1. Experimental facility.

The desiccant that passed through the tower was pumped to another tank so as not to affect the conditions of the inlet desiccant. Temperature was measured by copper-constantan thermocouples. Relative humidity was measured by Mamac Hu-224-2-MA humidity probes. Air velocity was measured by a vane anemometer installed at the air outlet.. The air pressure drop in the packed tower was determined by an air-over-oil manometer. For liquid

flow rate, a flow meter was used to set approximately the desired value and measured by a catch-bucket method. Desiccant concentration was determined by ***the Karl Fischer titration method.***

Experimental procedure: The rate of water condensation for dehumidification and the rate of water evaporation for regeneration were studied for the following variables: air flow rate, temperature of the air at the inlet, humidity of the air at the inlet, desiccant flow rate, temperature of the desiccant at the inlet, and desiccant concentration at the inlet. Each variable was studied for three different values, low, medium, high, while the others were held constant. For a constant tower height of 0.6 m, three experiments were done for each set of variables, and the final result given as the average of the results for the three experiments.

For each experiment the inlet desiccant temperature was set using the water (cold/warm) coil while the desiccant was allowed to recirculate to remove any temperature and concentration gradient. Air was blown through the electrical heater and humidifier to adjust the temperature and humidity to the desired values. When the inlet conditions for the desiccant and air were adjusted to the desired levels, the desiccant was allowed to flow through the tower. Once steady state was obtained, measurements were taken for 5 to 10 minutes using a PC-based data acquisition system. The variables measured with the data acquisition system were: the temperature of the desiccant, the temperature of the inlet and outlet air, and the humidity levels of the inlet and outlet air. During the experiment the air velocity was measured at the outlet of the tower. Samples of the inlet desiccant were taken for concentration measurement.

Results for Air Dehumidification

The results from the experimental study for air dehumidification are shown in figure c-2 to c-7 and table c-1. As mentioned in section earlier, the final results are the average of three experiments. Table c-1 gives the full set of values for the variables measured. Figures c-2 to c-7 show the water condensation rate, m_{cond}, from the experiments and theoretical model, as a function of superficial air and desiccant mass velocities (G, L), inlet air and desiccant temperatures (Ta, T_L), inlet air humidity ratio (Y), and inlet desiccant concentration (X). In each figure, error bars show the uncertainty of the experimental measurements.

Figure c-2 shows that the water condensation rate increases with the air flow rate. It may be explained that a high air flow rate will remove the dehumidified air more rapidly from the interface reducing the humidity gradient between the interface and air bulk, consequently the driving force is less affected.

Figure c-3 shows that the water condensation rate is stable with the change of inlet air temperature if it is around the desiccant temperature. In the temperature range of interest the water vapor pressure in air may be considered independent of temperature, consequently the driving force will remain constant. If the air temperature is too high, the desiccant temperature will increase because of heat transfer, which will cause an increase of the desiccant vapor pressure and certainly a decrease of the driving force. In fact, the results show that for temperatures around 40°C or higher, there is a slight reduction in the water condensation rate due to the increase of the desiccant temperature.

Figure c-4 shows that the water condensation rate increases with the inlet air humidity ratio. It happens because a higher humidity ratio implies higher air vapor pressure and consequently higher driving force.

Figure c-5 shows that the water condensation rate is stable with the change of desiccant flow rate. This result can be explained as follows. The rate of water condensed does not reduce the desiccant concentration enough to affect its vapor pressure significantly, and if the liquid flow rate is sufficient to wet the packing, there is not an appreciable variation in any property that can affect the driving force.

Kim et al [1997] investigated the performance of LiCl for absorber design using vertical film. They results about the effect of the desiccant flow rate on water condensation rate agree with the results of the present investigation. Kavasogullari et al [1991], investigated the performance of LiCl in a dehumidifying packed tower. They results shows that the effect of desiccant flow rate on water condensation rate is greater than the results of this investigation. The higher effect of the desiccant flow rate in Kavasogullari' s results could be the effect of an unwetted packing. This assumption can be justified when is compared the ratio of air flow rate to liquid desiccant flow rate, G/L. For Kavasogullari et al, $2.96 \leq G/L \leq 7.4$, and for the present study $0.15 \leq G/L \leq 0.2$.

Figure c-6 shows that the water condensation rate decreases considerably with the desiccant temperature. Vapor pressure of the desiccant is highly dependent on temperature, the higher the temperature the higher the vapor pressure, and consequently the lower the driving force. Results from Kim et al, Kavasogullari et al and the present study agree.

Figure c-7 shows that the water condensation rate increases with the desiccant concentration. Vapor pressure of the desiccant is dependent on the concentration, the higher the concentration the lower the vapor pressure, and consequently the higher the driving force.

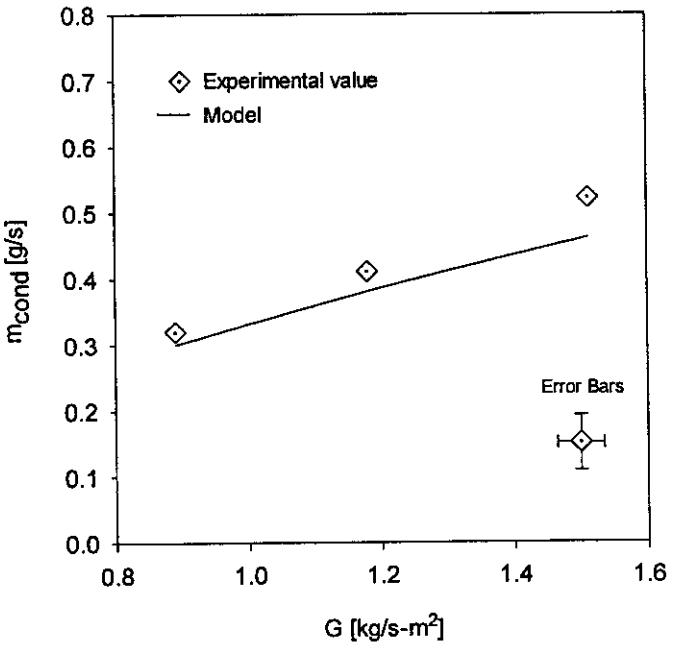

Figure c-2: Influence of air flow rate on water condensation rate.

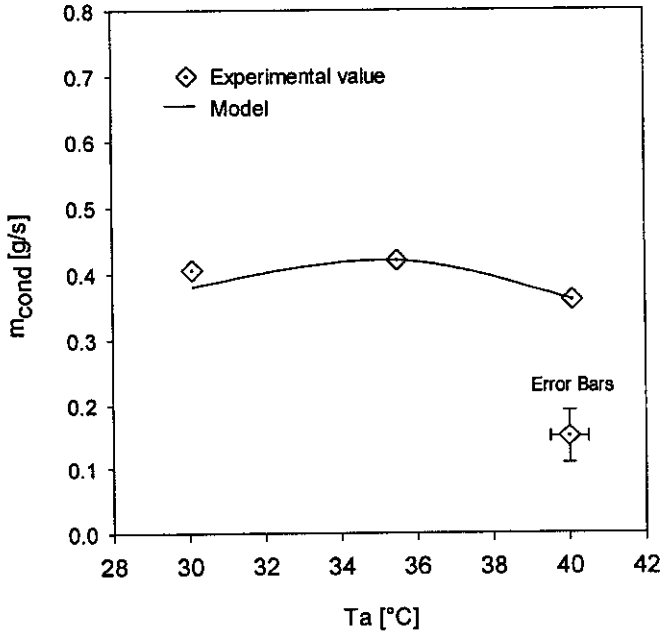

Figure c-3: Influence of inlet air temperature on water condensation rate.

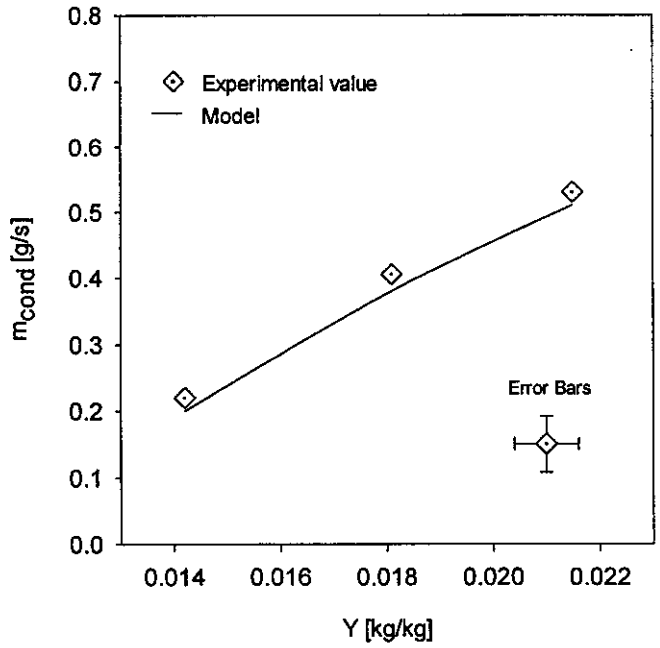

Figure c-4: Influence of inlet air humidity ratio on water condensation rate.

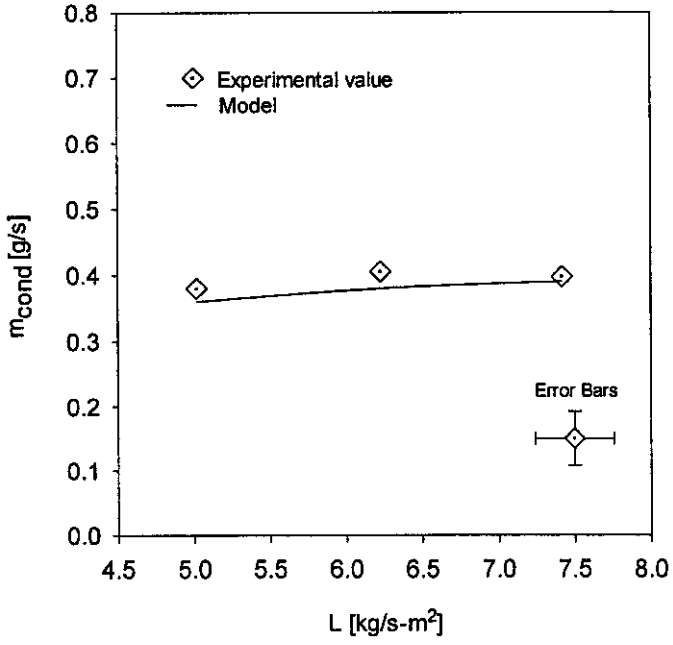

Figure c-5: Influence of desiccant flow rate on water condensation rate.

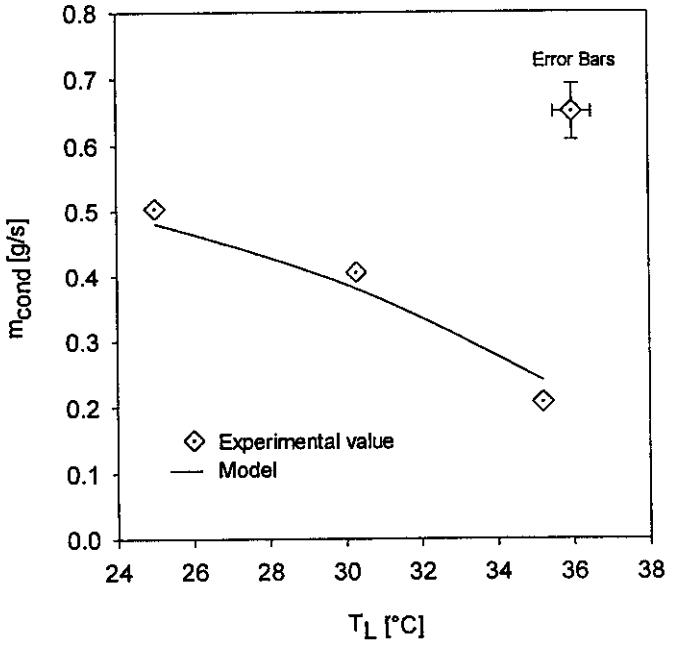

Figure c-6: Influence of inlet desiccant temperature on water condensation rate.

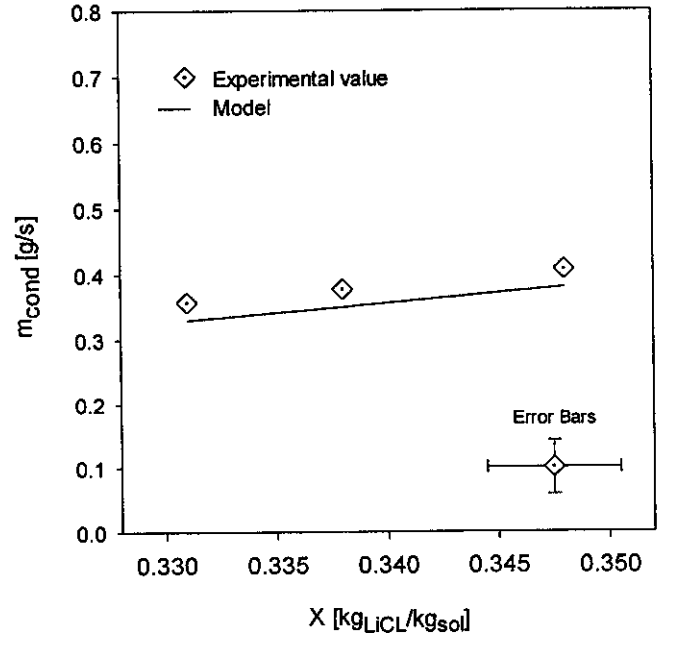

Figure c-7: Influence of inlet desiccant concentration on water condensation rate.

Table c-1: Experimental results for air dehumidification.

INLET						OUTLET				
G	Ta	Y	L	TL	X	Ta	Y	TL	X	m_{cond}
0.890	30.1	0.0180	6.124	30.1	34.6	31.3	0.0104	32.3	34.5	0.32
1.180	30.1	0.0181	6.227	30.3	34.7	32.2	0.0108	32.6	34.6	0.40
1.513	30.2	0.0181	6.113	30.0	34.3	32.2	0.0108	32.7	34.1	0.52
1.189	35.5	0.0188	6.290	30.3	34.5	32.8	0.0112	32.6	33.7	0.42
1.183	40.1	0.0180	6.287	30.5	34.4	33.1	0.0115	32.9	34.3	0.36
1.214	30.3	0.0142	6.273	30.1	33.9	31.1	0.0103	31.5	33.8	0.23
1.187	29.9	0.0215	6.272	30.3	33.9	33.4	0.0120	33.1	33.7	0.53
1.190	30.1	0.0180	5.019	30.2	34.4	32.2	0.0113	32.7	34.2	0.38
1.182	30.2	0.0181	7.420	30.2	34.4	32.0	0.0110	32.5	34.3	0.39
1.198	29.9	0.0177	6.269	25.0	34.7	28.2	0.0088	28.4	34.5	0.50
1.176	29.9	0.0178	6.309	35.2	34.9	35.7	0.0140	36.2	34.8	0.21
1.182	29.9	0.0179	6.164	30.1	33.1	32.4	0.0114	32.2	33.0	0.36
1.192	29.9	0.0179	6.267	30.2	33.8	32.5	0.0112	32.6	33.7	0.38
1.176	30.0	0.0181	6.206	30.2	34.8	32.0	0.0107	32.5	34.7	0.41

Results for Desiccant Regeneration

The results from the experimental study for desiccant regeneration are shown in figures c-8 to c-13 and table c-2. As mentioned before, these results are the averages of three experiments. Table c-2 gives the full set of values for the variables measured. Figures c-8 to c-13 show the water evaporation rate, m_{evap}, from the experiments and theoretical model, as a function of superficial air and desiccant mass velocities (G, L), inlet air and desiccant temperature (Ta, T_L), inlet air humidity ratio (Y), and inlet desiccant concentration (X). In each figure, error bars show the uncertainty of the experimental measurements.

Figure c-8 shows that the water evaporation rate increases with the air flow rate. Since a high air flow rate rapidly removes the higher moist air from the interface, it reduces thehumidity gradient between the interface and bulk air, consequently the driving force is less affected. Therefore, as the air flow increases, the water evaporation also increases.

Figure c-9 shows that the water evaporation rate increases slightly with the inlet air temperature. In the temperature range of interest the water vapor pressure in air may be considered independent of temperature,

therefore there is not a direct change of the driving force due to air temperature. But, at higher air temperature there will be less reduction of the liquid temperature. Consequently a higher average desiccant temperature gives a higher average driving force for regeneration which increases the water evaporation rate.

As expected, figure c-10 shows that the water evaporation rate decreases with the inlet humidity ratio, since a higher humidity ratio implies a higher air vapor pressure and consequently less driving force.

Figure c-11 shows that the water evaporation rate increases with the desiccant flow rate. At higher desiccant flow rates there will be less reduction of the liquid

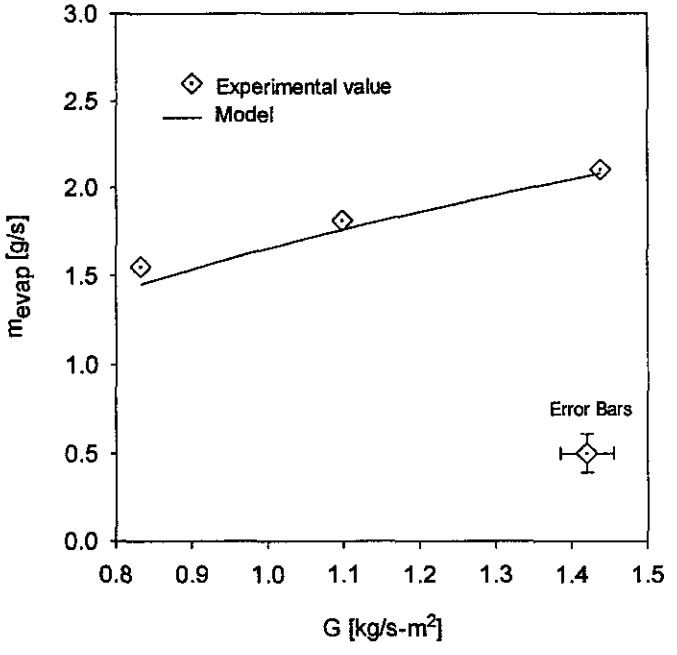

Figure c-8: Influence of air flow rate on water evaporation rate.

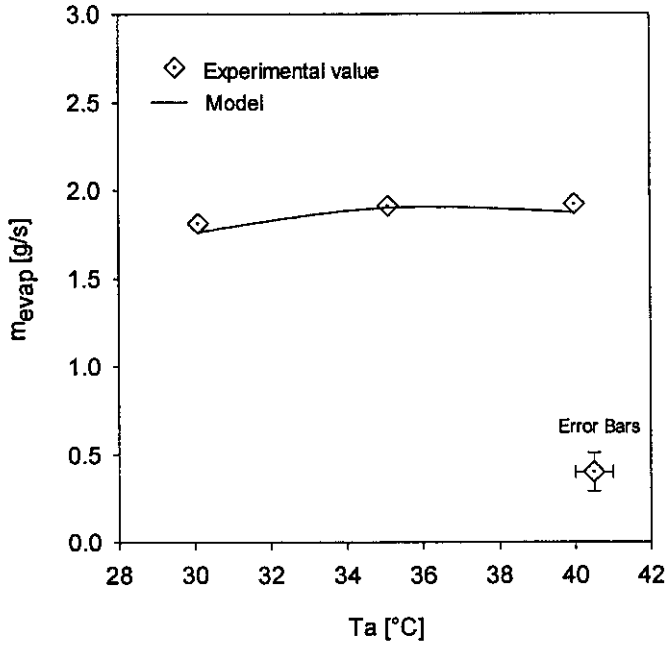

Figure c-9: Influence of inlet air temperature on water evaporation rate.

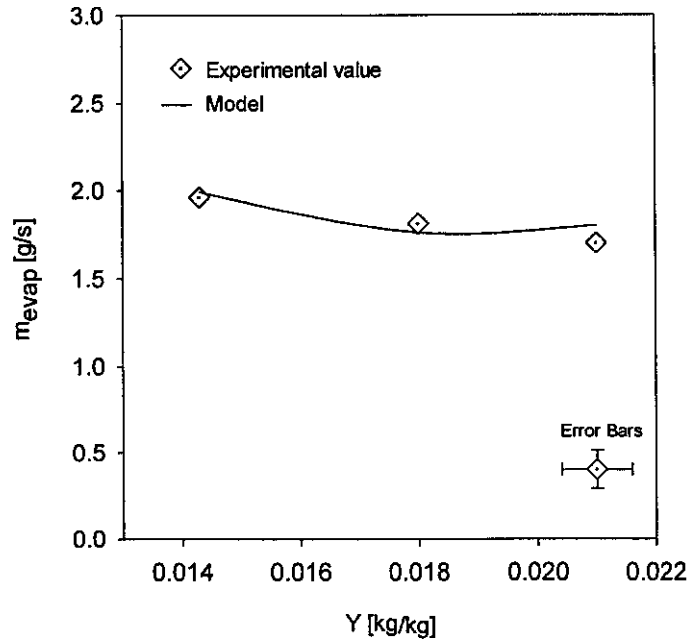

Figure c-10: Influence of inlet air humidity ratio on water evaporation rate.

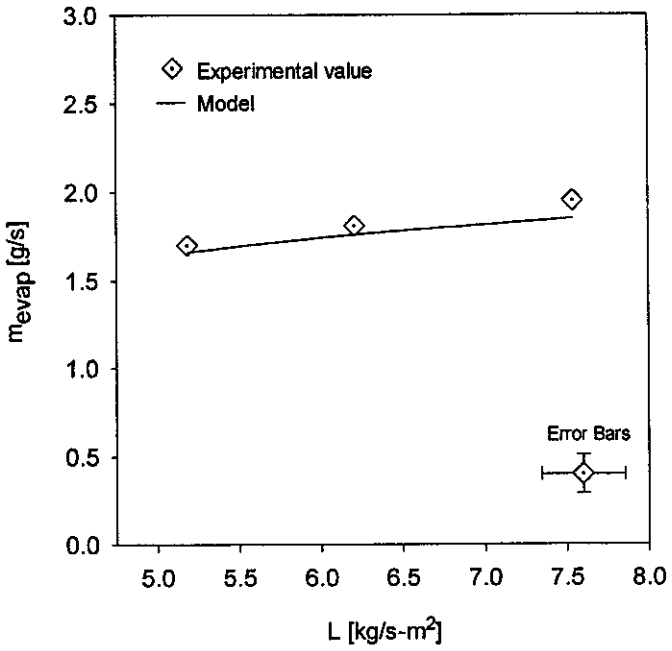

Figure c-11: Influence of desiccant flow rate on water evaporation rate.

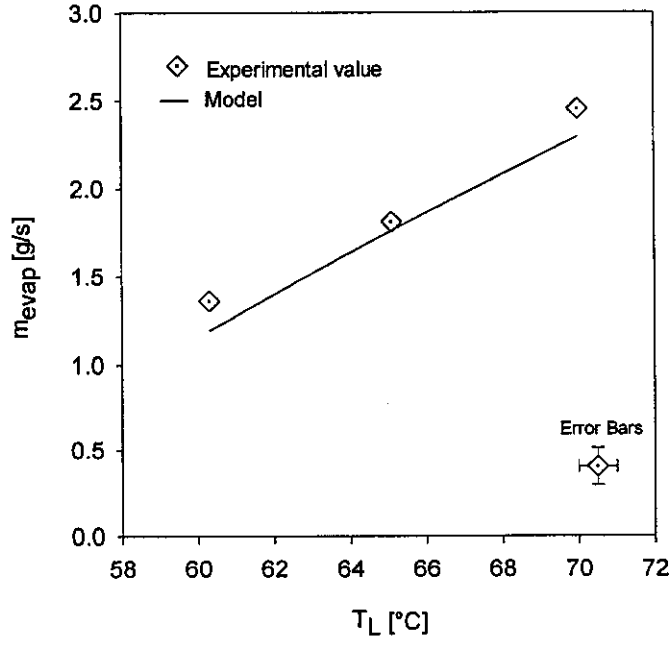

Figure c-12: Influence of inlet desiccant temperature on water evaporation rate.

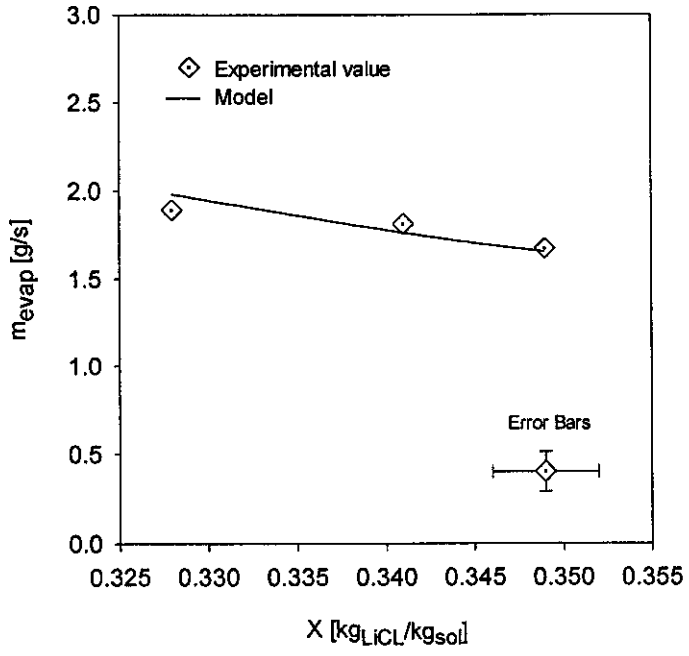

Figure c-13: Influence of inlet desiccant concentration on water evaporation rate.

temperature. Consequently a higher average desiccant vapor pressure or a higher average driving force is maintained which increases the water evaporation rate.

Figure c-12 shows that the water evaporation rate increase considerably with the inlet desiccant temperature. Since vapor pressure of the desiccant is highly dependent on the temperature, the higher the temperature the higher the vapor pressure, and consequently higher the driving force.

Figure c-13 shows that the water evaporation rate decreases with the inlet desiccant concentration. This may be explained from the fact that vapor pressure of the desiccant is a function of the concentration. Therefore, the higher the concentration, the lower the vapor pressure, and consequently lower the driving force, for water evaporation.

Table c-2: Experimental results for desiccant regeneration.

INLET						OUTLET				
G	Ta	Y	L	TL	X	Ta	Y	TL	X	m_{evap}
0.833	30.4	0.0183	6.463	65.0	34.0	58.9	0.0579	58.6	34.5	1.55
1.098	30.1	0.0180	6.206	65.1	34.1	59.3	0.0532	57.8	34.8	1.81
1.438	29.8	0.0177	6.479	65.1	34.5	57.5	0.0488	56.6	35.2	2.10
1.097	35.1	0.0180	6.349	65.1	33.4	58.5	0.0551	57.4	34.1	1.91
1.102	40.0	0.0178	6.354	65.0	33.6	58.9	0.0548	57.6	34.2	1.91
1.132	30.2	0.0143	6.370	65.2	34.0	57.6	0.0513	57.2	34.7	1.97
1.097	29.4	0.0210	6.440	65.5	33.6	58.5	0.0541	58.3	34.2	1.70
1.116	30.3	0.0182	5.185	65.4	34.4	57.6	0.0507	57.0	34.9	1.71
1.101	29.9	0.0180	7.541	65.2	34.3	59.0	0.0556	57.9	34.9	1.95
1.111	30.0	0.0187	6.245	60.3	34.4	55.8	0.0447	54.2	34.8	1.36
1.084	29.7	0.0184	6.315	70.0	34.5	62.6	0.0666	60.0	35.3	2.45
1.099	29.7	0.0177	6.400	64.8	32.8	57.6	0.0542	56.8	33.4	1.89
1.116	30.3	0.0182	6.428	65.0	34.9	57.9	0.0501	57.5	35.4	1.67

Absorber/Regenerator Efficiency

The efficiencies of the absorption and regeneration systems were evaluated using the humidity effectiveness, ϵ_Y, defined as the ratio of the actual change in moisture of the air flowing through the tower to the maximum possible change in moisture content for a given set of operating conditions. Therefore, the column efficiency or humidity effectiveness can be expressed as

$$\epsilon_Y = \frac{Y_{IN} - Y_{OUT}}{Y_{IN} - Y_{equ}} \qquad \text{(c-1)}$$

For this relation, Y_{IN} and Y_{OUT}, are the humidity ratio of the air at the inlet and outlet of the tower, respectively. Y_{equ} is the humidity ratio of the air, which is in equilibrium with the desiccant solution at the local solution temperature and concentration. Since the system operates in counter-flow, Y_{equ} would be the humidity ratio of the air in equilibrium with the desiccant at the inlet.

One of the objectives of this investigation was to verify if the empirical correlation for humidity effectiveness proposed by Öberg [1998], may be used to predict

the experimental results for the new system using LiCl as desiccant. Öberg's correlation is defined as

$$\epsilon_Y = 1 - C_1 \left(\frac{L}{G}\right)^a \left(\frac{h_{a,IN}}{h_{L,IN}}\right)^b \left(a_t \cdot Z\right)^c \qquad \text{(c-2)}$$

where

$$a = k_1 \frac{\gamma_L}{\gamma_C} + m_1 \qquad \text{(c-3)}$$

$$c = k_2 \frac{\gamma_L}{\gamma_C} + m_2 \qquad \text{(c-4)}$$

and constant values as:

C_1	b	k_1	m_1	k_2	m_2
48.34456	-0.75103	0.3959	-1.57311	0.03312	-0.90589

The material critical surface tension, γ_C, for polypropylene (packing material) is 29E-3 N/m.

The inlet air enthalpy is calculated as

$$h_{a,IN} = T_a + Y(2501.3 + 1.86T) \ [kJ/kg] \qquad \text{(c-5)}$$

The inlet desiccant enthalpy is calculated as

$$h_{L,IN} = c_{P,L} \cdot T_L \ [kJ/kg] \qquad \text{(c-6)}$$

with $c_{P,L}$ as a function of temperature and concentration.

Calculations of the humidity effectiveness using this correlation gave deviations between 30 and 60%, which are much higher than the 15% stated by Öberg. Although she used data from Chung et al [1993] for lithium chloride, Chung's equilibrium humidity values are considerably lower than those obtained from a curve fit of the vapor pressure suggested in this study.

Using the experimental data from this study and the data from Chung et al [1993], a curve fit was done to find the new constants to be used in equation c-2 for lithium chloride. To calculate the experimental humidity effectiveness, the values of humidity equilibrium obtained from the vapor pressure curve fit suggested in this study

were used. Equation c-6 was redefined in order to account for the integral heat of solution, Δh_S°, which is a function only of concentration:

$$h_{L,IN} = 420 + \Delta h_S^\circ + c_{P,L} \cdot T_L \ \left[kJ/kg\right] \qquad \text{(c-7)}$$

where Δh_S° is calculated using the curve fit equation proposed by Buschulte [1984]:

$$\Delta h_S^\circ = -0.8759 - 839.9X - 61.54X^2 + 1978.6X^3 \ \left[kJ/kg\right] \qquad \text{(c-8)}$$

with concentration, X, in kilograms of lithium chloride per kilograms of solution.

The quantity 420 kJ/kg in equation c-7 is a reference enthalpy to avoid negative values. Enthalpies calculated in this way will be similar to those given by Uemura [1967].

The new constants for equations c-2 to c-4 are

C_1	b	k_1	m_1	k_2	m_2
0.00021	-1.2047	-0.0942	0.029	0.2532	0.3856

For the redefined correlation, humidity effectiveness for each experiment was calculated, and the values are shown in figures c-2 to c-4 together with the experimental values.

Absorber: Figures c-14 to c-19 show the influence of the design variables on the humidity effectiveness for the absorber. Humidity effectiveness for the absorber remains stable and around 80% for the change of the variables in the range studied. An exception is the liquid temperature, which yields a lower $\in_Y$ for the desiccant temperatures over 33°C. This is understandable because as the desiccant temperature goes up, the desiccants ability to absorb moisture reduces until it goes to zero and finally when the temperature is high enough direction of mass transfer is reversed. For a middle value of the variables studied, G=1.2 kg/s-m^2, Ta=30°C, Y=0.018 kg/kg, L=6.2 kg/s-m^2 and X=35%, using the mathematical model it was found that at a desiccant temperature around 43°C no net mass transfer will occur.

Chung et al [1992] investigated the efficiency and mass transfer coefficient for dehumidification of air by LiCl in a packed tower. Chung et al used the humidity effectiveness, $\in_Y$, to evaluate the efficiency of the absorber, presenting the effect of the air flow rate and liquid flow rate on the tower efficiency. For these two variables the results in both, Chung and present study, show that for an increase of air flow rate the humidity effectiveness decreases, while for an increase of the desiccant flow rate the humidity effectiveness increases.

Regenerator: Figures c-20 to c-25 show the influence of the design variables on the humidity effectiveness for the regenerator. Humidity effectiveness for the regenerator is in the range of 0.7 and 0.9, and is more sensitive to changes in the variables than the humidity effectiveness for the absorber. Two defined tendencies can be seen from the figures. One tendency is the apparent lineal decrease of ϵ_Y for an increase in the air flow rate. This can be explained because for a higher air flow rate the air will be in contact with the liquid for a shorter period of time, giving a higher humidity ratio at the exit, while the condition of the liquid and consequently the equilibrium humidity ratio will remain approximately constant. The second defined tendency is the apparent lineal increase of ϵ_Y with the increase of desiccant flow rate. This can be explained from the result seen earlier that the water evaporation rate is proportional to the desiccant flow rate. Therefore, for a higher desiccant flow rate, the humidity at the outlet will be higher; while, the desiccant condition and consequently the equilibrium humidity will remain almost constant. Chung et al [1992, 1993] also found these tendencies.

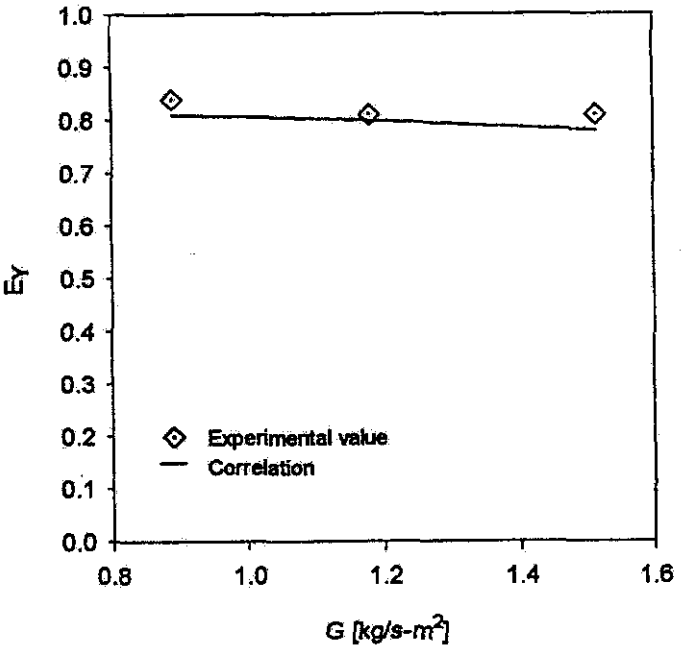

Figure c-14: Influence of air flow rate on absorber humidity effectiveness.

Figure c-15 shows that using the redefined correlation for humidity effectiveness, 90% of the experimental results for this study and that of Chung et al can be predicted within ±15% and the total number of experiments within ±30%.

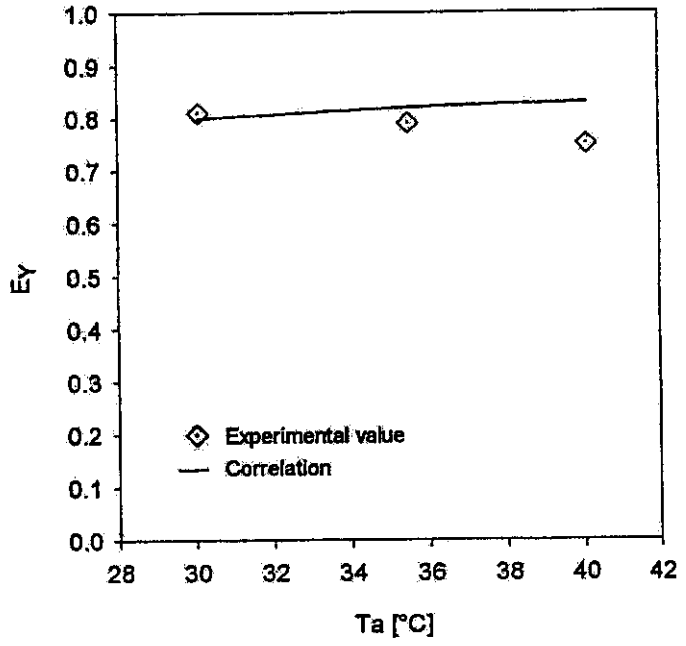

Figure c-15. Influence of inlet air temperature on absorber humidity effectiveness.

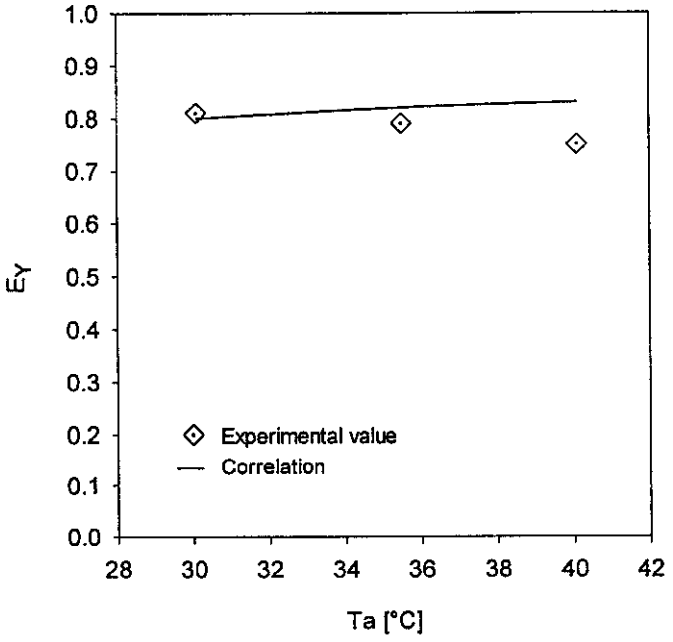

Figure c-16: Influence of humidity ratio on absorber humidity effectiveness.

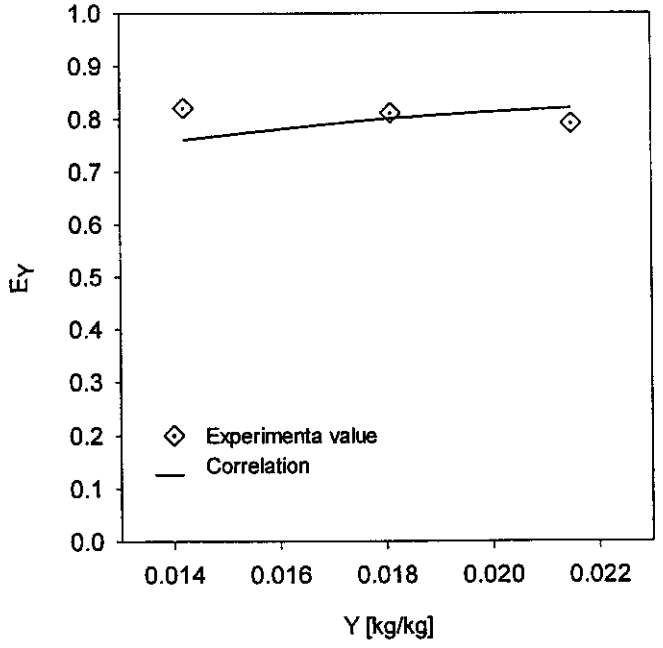

Figure c-17: Influence of desiccant flow rate on absorber humidity effectiveness.

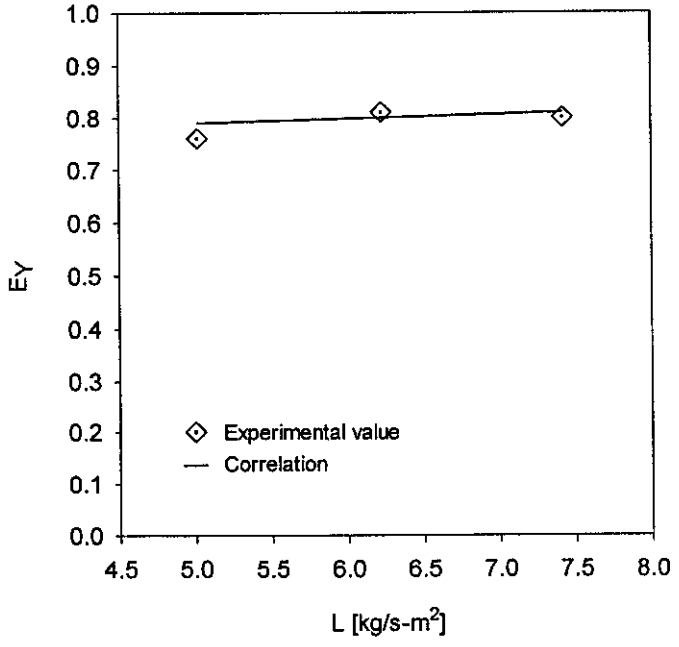

Figure c-18: Influence of desiccant flow rate on absorber humidity effectiveness.

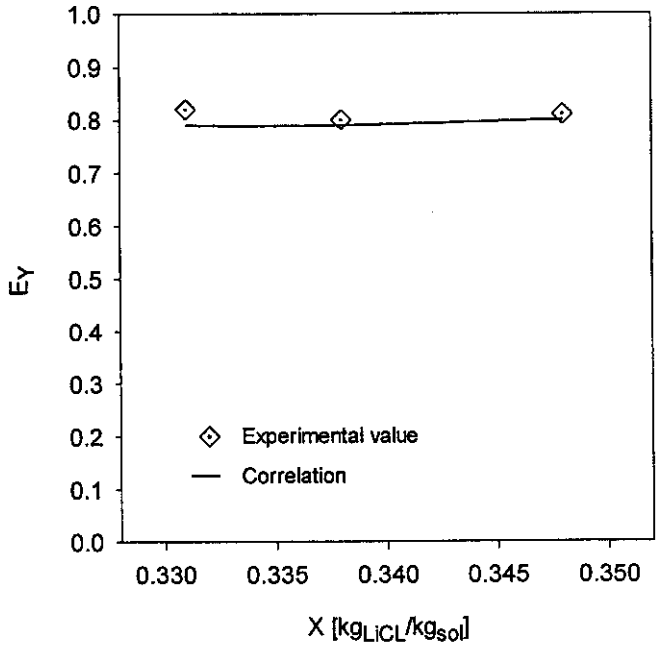

Figure c-19: Influence of inlet desiccant concentration on absorber humidity effectiveness.

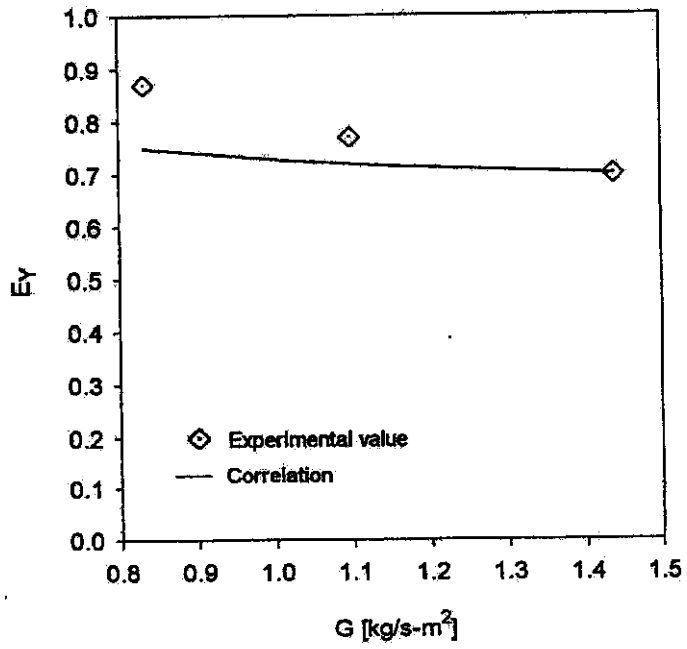

Figure c-20: Influence of air flow rate on regenerator humidity effectiveness.

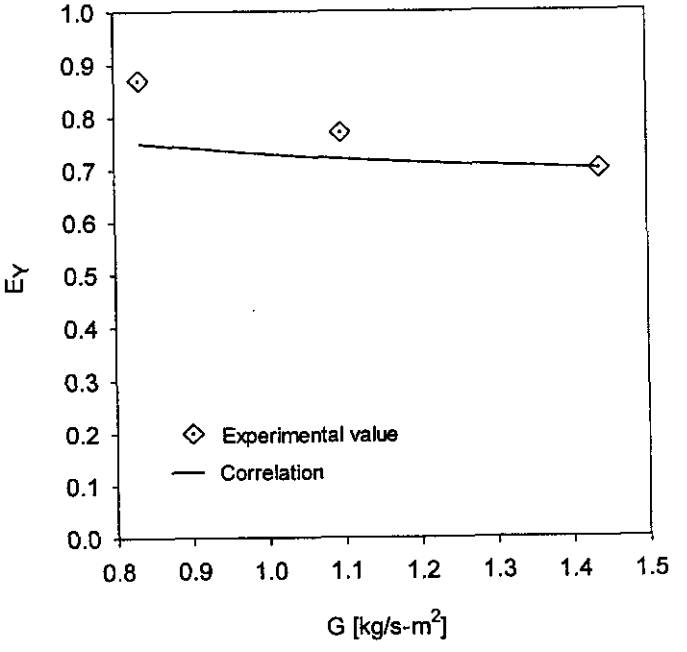

Figure c-21: Influence of inlet air temperature on regenerator humidity effectiveness.

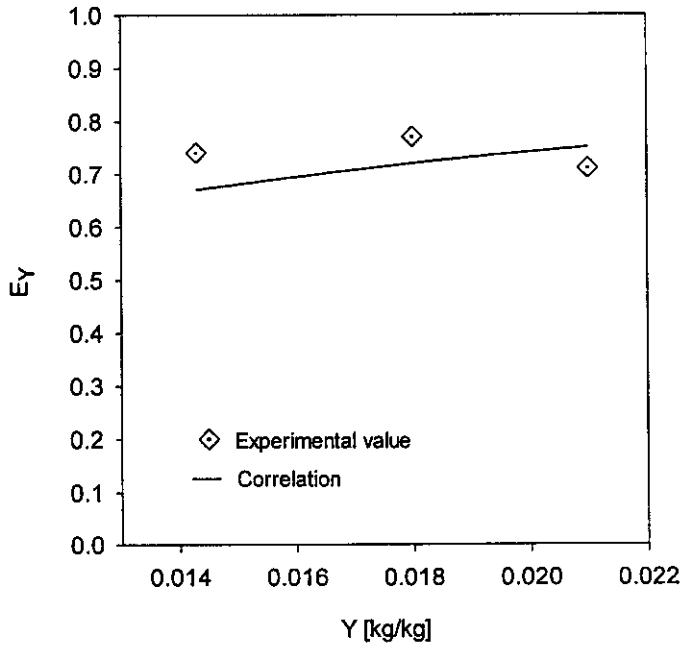

Figure c-22: Influence of air humidity ratio on regenerator humidity effectiveness.

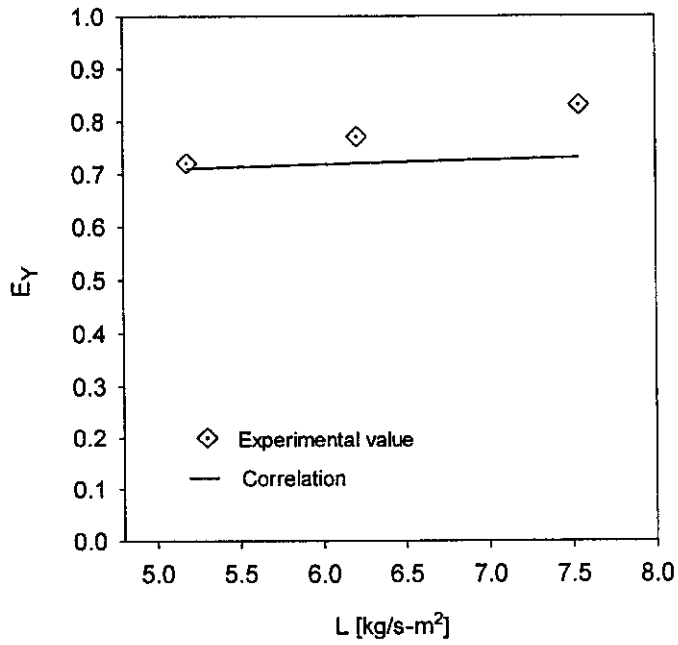

Figure c-23: Influence of desiccant flow rate on regenerator humidity effectiveness.

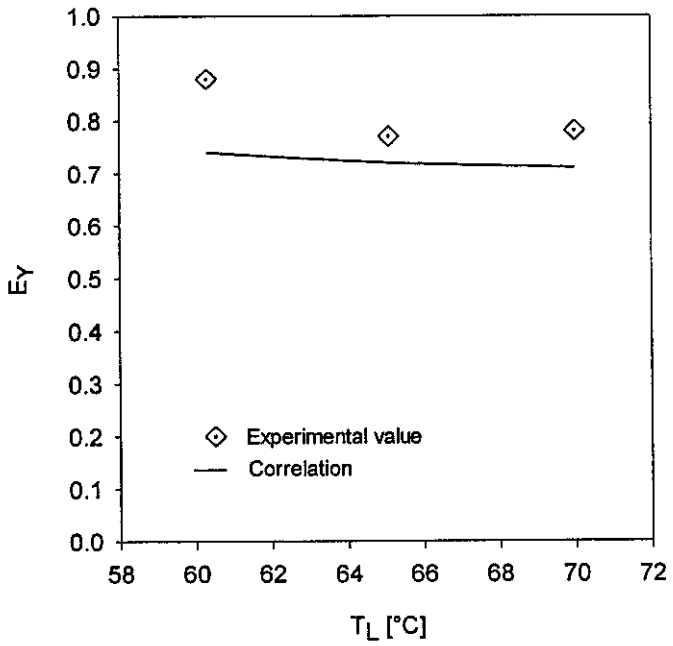

Figure c-24: Influence of inlet desiccant temperature on regenerator humidity effectiveness.

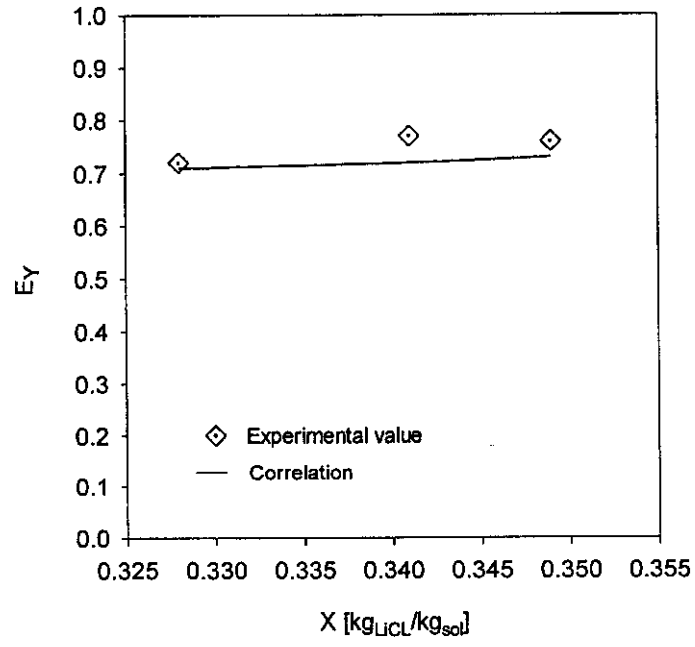

Figure c-25: Influence of inlet desiccant concentration on the humidity effectiveness.

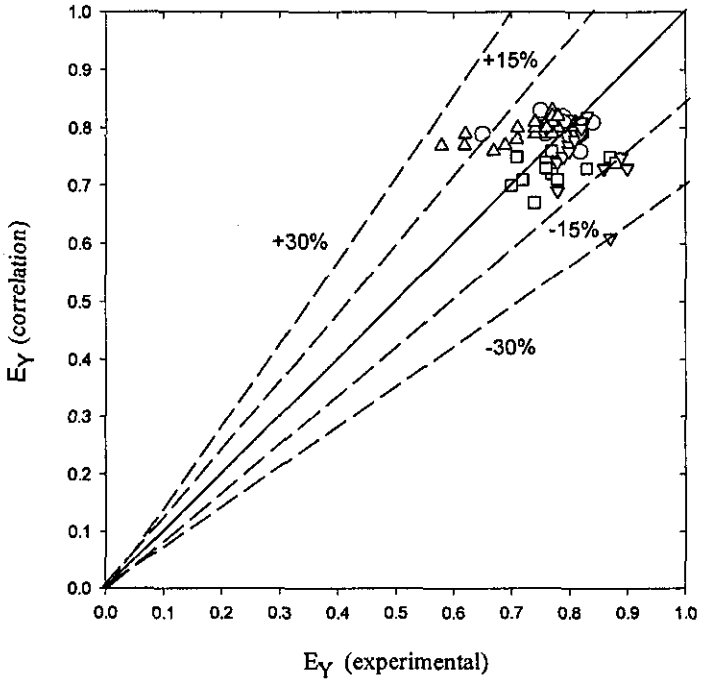

O present study - dehumidification, LiCL
25 mm Polypropylene Hiflow Rings.
present study - regeneration, LiCL
25 mm Polypropylene Hiflow Rings.

Δ Chung [1] - dehumidification, LiCL
16 mm Polypropylene Flexi Rings.

∇ Chung [2] - dehumidification, LiCL
16 mm Polypropylene Flexi Rings.

Figure c-26: Correlation for humidity effectiveness, $\in_Y$.

CONCLUSIONS

Reliable sets of data for air dehumidification and desiccant regeneration were obtained. Different values of properties for the inlet air and inlet desiccant were used to investigate the performance of the absorber/regenerator. For air dehumidification, influences of the variation of the variables studied on the variation of water condensation rates are

Air flow rate ≈	1.1 to 1
Humidity ratio ≈	1.7 to 1
Desiccant temperature ≈	1 to 1 (decreasing)
Desiccant concentration ≈	1 to 3

The variations in air temperature and desiccant flow rate do not cause significant variations in the water condensation rate for the ranges studied. For desiccant regeneration, influences of the variables studied on the variation of water evaporation rates are

Air flow rate ≈	1 to ½
Desiccant temperature ≈	1 to 5
Desiccant concentration ≈	1 to 2

The other variables cause a variation equal or higher of 3.3 to 1.

An aqueous solution of lithium chloride can be regenerated at temperatures below 60°C, which makes this liquid desiccant a viable candidate for low cost solar cooling desiccant applications.

For the absorber the humidity effectiveness stays approximately constant for the change of the variables in the range studied. For the regenerator the humidity effectiveness is more sensitive to the change in the variables. Unfortunately, clear trends were observed only for air flow rate and desiccant flow rate. Humidity effectiveness decreases with air flow rate; and humidity effectiveness increases with desiccant flow rate.

Theoretical computer programs were developed for the absorber/regenerator. The results predicted from these programs agree with the experimental results. Only 8% of the predicted values were slightly outside of the uncertainty limits, which is more than satisfactory considering that the correlation used for the heat and mass transfer coefficients are empirical, and these were obtained for liquid-gas systems and packings other than those used in the present study.

A redefined empirical correlation for humidity effectiveness is proposed for lithium chloride. With this correlation, more than 90% of the experimental results from this study and Chung et al [1992] were predicted within ±15%, and the other results within ±30%.

APPENDIX D

FIELD TESTS

FIELD TESTS

Field tests of a hybrid solar liquid desiccant cooling system were conducted at the Solar House at the University of Florida's Energy Research and Education Park. These tests consisted of operating the air conditioning system in two configurations–the conventional vapor compression system, and the hybrid desiccant system. Figures D1a and D1b show the air conditioning configuration with a vapor compression system only and Figures D2a and D2b show the configuration with a hybrid desiccant air conditioning system. The system was operated in the two modes (vapor compression system with and without the liquid desiccant system) and the data was collected to compare the performance of both arrangements. In each of the modes, the system was operated with: (a) recirculation air; and (b) 100% ventilation air. Figures D1a and D2a show the arrangement for recirculation air for the two systems, and Figures D1b and D2b show the arrangement for 100% ventilation air for the two systems.

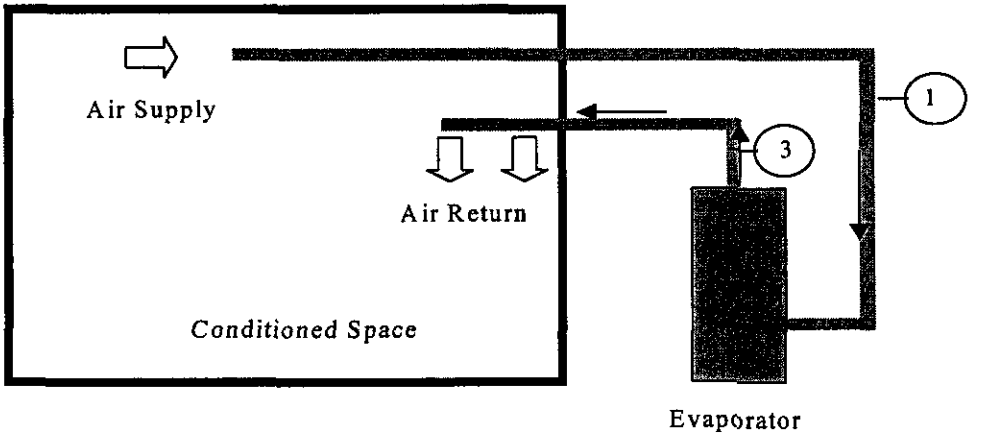

Figure D1a. Vapor compression system with recirculating air.

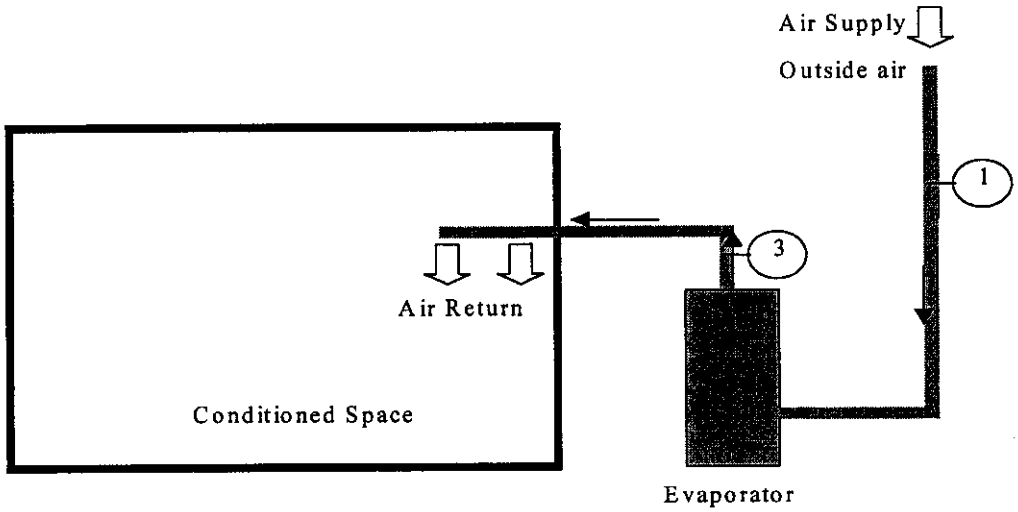

Figure D1b: Vapor compression system with 100% fresh air.

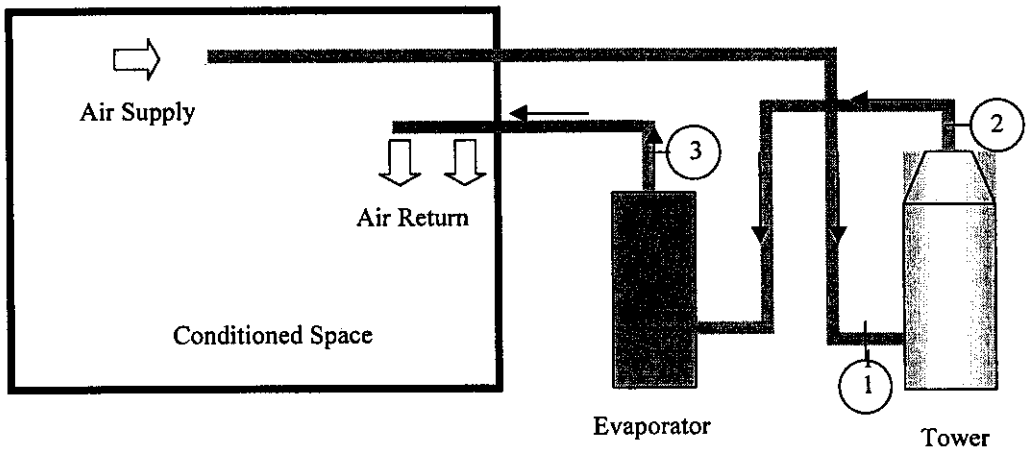

Figure D2a: Liquid desiccant system with recirculating air.

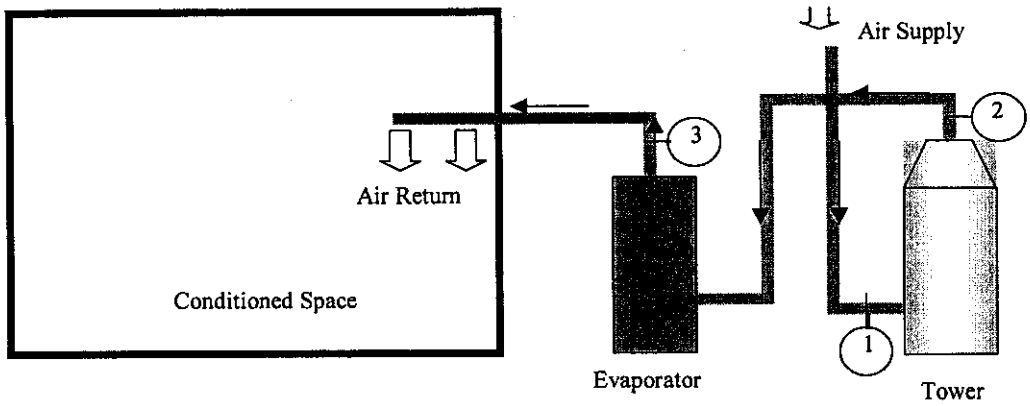

Figure D2b. Liquid desiccant system with 100% fresh air.

FIELD TEST RESULTS

The air conditioning system in the field test house was run in both configurations – the hybrid desiccant system and the conventional vapor compression system, in order to compare their performances. The systems were also run for various air flow rates, inlet air temperatures and desiccant temperatures of these experiments and an analysis of the results is described in the next section. Some typical results are described in this section. Tables D1 and D2 show the typical performance results for the vapor compression system and the hybrid liquid desiccant system respectively. The performance was measured for both the systems, the recirculation (Experiment A) and the 100% fresh air (Experiment B) modes.

Table D1. Performance for the Vapor Compression System

	Entrance				Exit				Change of Enthalpy of Air
System Mode	Temp. °C	RH %	Hum. Ratio	Enthalpy KJ/Kg	Temp. °C	RH %	Hum. Ratio	Enthalpy KJ/Kg	KJ/Kg
A Recirculation	26	53	0.011	54.4	17	80	0.0097	41.5	12.8
B 100% Fresh Air	33	51	0.016	74.4	27	63	0.014	62.5	11.7

Table D2. Liquid Desiccant Cooling System

System Mode	Conditions of Air at Entrance of Desiccant Tower				Conditions of Air at Exit of Vapor Compression System			
	Temp. °C	RH %	Hum. Ratio	Enthalpy KJ/Kg	Temp. °C	RH %	Hum. Ratio	Enthalpy KJ/Kg
A: Recirculation	26	53	0.011	54.4	27	40	0.009	49.7
B: 100% Fresh Air	33	51	0.016	74.4	34	40	0.013	68.2

Table D2. Liquid Desiccant Cooling System, continued

System Mode	Change in Enthalpy of Air		
	Desiccant Tower	Vapor Compression System	System Total
	KJ/Kg	KJ/Kg	KJ/Kg
A: Recirculation	4.2	11.8	16.0
B: 100% Fresh Air	6.2	13.3	19.5

Experiment A was done with recirculation of the air in the house, and experiment B was done using 100% fresh air. Comparing experiment A for both cases, we can see that using the hybrid liquid desiccant cooling system the total change of enthalpy in the system was 16 KJ/Kg, while for the vapor compression system, it was 12.8 KJ/Kg. Therefore, the hybrid liquid desiccant system was able to remove 3.2 KJ/Kg more enthalpy from the air than the conventional vapor compression system. It shows that the capacity of the equipment to extract heat from the air is higher using the liquid desiccant cooling system. Also the change of humidity ratio using liquid desiccant cooling system was almost twice that of the change using the vapor compression system only and the temperature dropped by one degree Celsius.

Comparing Experiment B for both cases we can see that using the liquid desiccant cooling system the total change of enthalpy in the system was 19.5 KJ/Kg as compared to 11.7 kJ/kg for the vapor compression system. The change in enthalpy increased by 6.6 KJ/Kg in the desiccant system only. This result shows that the liquid desiccant cooling system offers more advantage when 100% fresh air is required. It is because the fresh air is much more humid than the recirculation air, and the main function of using the liquid desiccant is to reduce the humidity before the air enters the evaporator. Also, the change in humidity ratio is more than twice with the liquid desiccant system than without it.

Based on these results it is concluded that the hybrid desiccant system improves the air conditioning performance in the field house by decreasing the outlet humidity and temperature of the air. However, the size of the present desiccant system is too small since the vapor compression system has to condense some moisture in addition to sensible cooling of the air. Ideally, in a hybrid desiccant cooling system, the desiccant system should do all of the dehumidification and the vapor compression system should provide only the sensible cooling. The present desiccant tower height is 0.6m. The following analysis of the electricity consumption is done for the present desiccant tower height of 0.2m and for an increased height of 2.5 m.

ADDITIONAL EXPERIMENTAL RESULTS

The variables studied in the experiments for dehumidification of the air were: air mass velocity (airflow rate), temperature of the air at the inlet, humidity ratio (air humidity) and liquid mass velocity (desiccant flow rate). Experiments were done using re-circulating air and one hounded percent fresh air. Each variable was studied for three different values, while the others were held constant. Each experiment was done three times and the final result was the average of them.

Experiment 1. This experiment was conducted to study the influence of airflow rate over different parameters in the system. The airflow rates used were 0.6, 0.65 and 0.70 kg/s and the other conditions were held constant.

Table D3. Inlet Conditions for Experiment 1 for Both Systems.

Vapor-Compression System		Hybrid Liquid-Desiccant Cooling System				
Inlet Air Conditions		Inlet Air Conditions		Desiccant Conditions		
T_a (°C)	RH_a (%)	T_a (°C)	RH_a (%)	T_L (°C)	X (%)	V (l/s)
26	53	26	53	27	35	0.423

Table D4. Results for Vapor-Compression System in Experiment 1.

	Inlet Air Conditions		Outlet Air Conditions		System		
Air flow rate Kg/s	T (°C)	HR (%)	T (°C)	HR (%)	Change of humidity ratio	Change of enthalpy (kW)	Rate of condensation g/s
0.60	26	53	13.9	92	0.00204	10.50	1.22
0.65	26	53	14.8	88.3	0.00188	10.5	1.22
0.70	26	53	15.6	84.8	0.00177	10.6	1.24

Table D5. Results for Hybrid Liquid Desiccant Cooling System in Experiment 1.

Air Flow Rate	Inlet Air Conditions Desiccant Tower		Outlet Air Conditions Desiccant Tower		Outlet Air Conditions System	
Kg/s	T °C	HR %	T °C	HR %	T °C	HR %
0.60	26	53	27.6	39.5	12.3	99.5
0.65	26	53	26.7	39	12.4	97.8
0.70	26	53	27.6	39.3	13.6	90

Table D5. Continuation.

Change of Humidity Ratio			Change of Enthalpy kW			Rate of Condensation g/s		
Tower	Evapor.	System	Tower	Evapor.	System	Tower	Evapor.	System
0.0020	0.0002	0.0023	2.34	10.49	12.82	1.33	0.15	1.48
0.0022	0.0002	0.0024	2.53	10.38	12.91	1.41	0.13	1.54
0.0021	0.0003	0.0024	2.62	10.51	13.12	1.47	0.21	1.69

Figure D3 shows the influence of airflow rate on the water condensation rate. This figure shows that the water condensation rate is constant in the vapor-compression system for the range analyzed. As seen from the data in Table D4 the change of humidity ratio decreases with the airflow rate, however the product of the airflow rate and the change of humidity ratio remains constant. In the hybrid-desiccant cooling system the rate of condensation increases with the airflow rate.

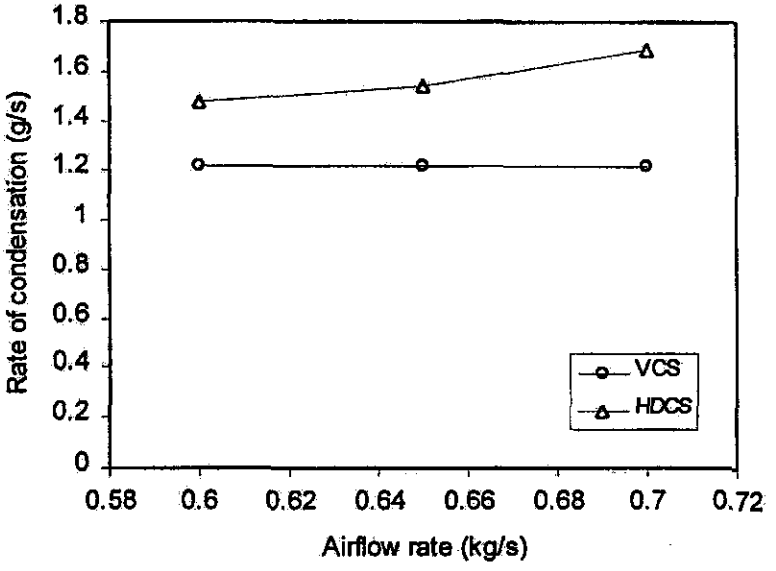

Figure D3. Influence of the airflow rate on the water rate of condensation.

Figure D4 shows the influence of airflow rate on the change of enthalpy in the system. This figure shows that the change of enthalpy is constant for both systems with the airflow rate. The change of enthalpy is higher in the hybrid-desiccant cooling system than vapor-compression. It means that the hybrid-desiccant can remove more heat from the air, which implies that the coefficient of performance for this system is higher than the vapor compression system alone.

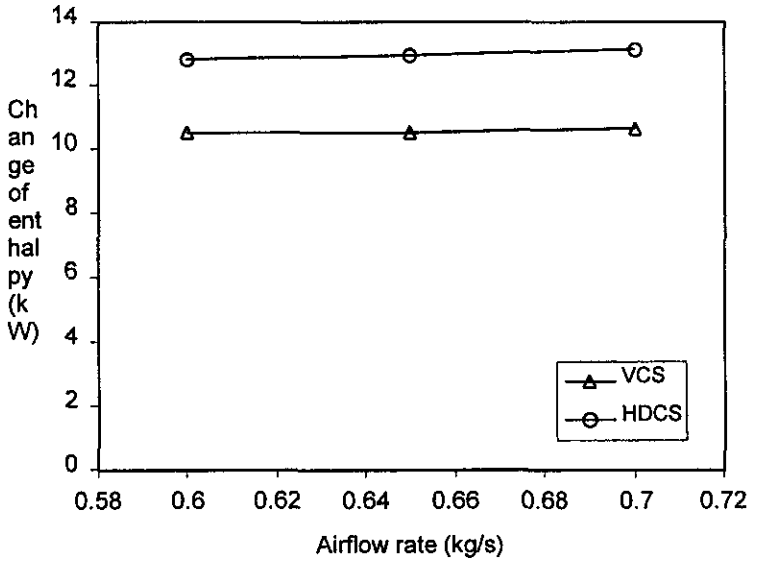

Figure D4. Influence of the airflow rate on the change of enthalpy in the system

Figure D5 shows the influence of airflow rate on the outlet air temperature in the system. This figure shows that the outlet temperature increases for both systems with the airflow rate. It is important to note that the outlet temperature of the air for the hybrid-desiccant system is always lower than that for the vapor compression system alone. For the same inlet conditions the hybrid-desiccant system is able to decrease the temperature by about 2°C less than the vapor-compression system alone.

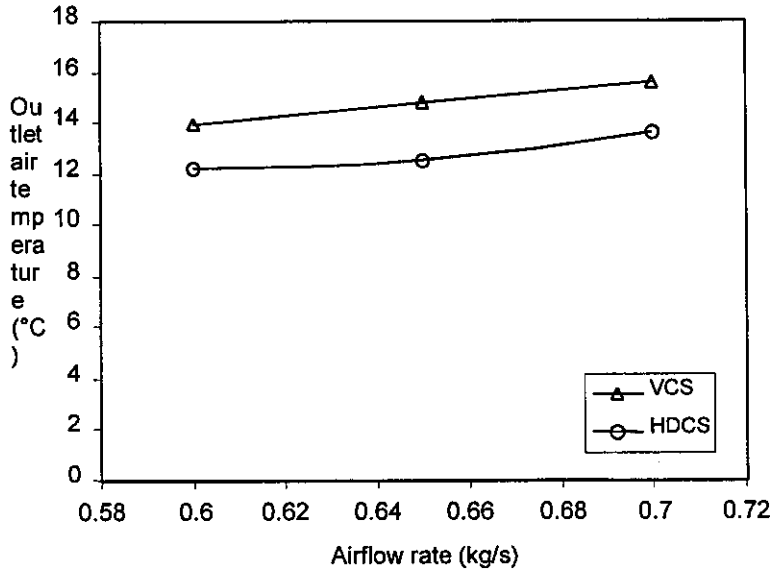

Figure D5: Influence of airflow rate on the outlet air temperature

Experiment 2. This experiment was conducted to study the influence of inlet desiccant temperature over different parameters in the system. The inlet desiccant temperatures used were 28, 29 and 30 (°C) and the others conditions were maintained constant.

Table D6. Data for the experiment 2

Vapor-Compression System			Hybrid Liquid-Desiccant Cooling System				
Inlet Air Conditions		Air Flow Rate	Inlet Air Conditions		Air flow Rate	Desiccant Conditions	
T_a (°C)	RH_a (%)	m_a (kg/s)	T_a (°C)	RH_a (%)	m_a (kg/s)	X (%)	V (m^3/s)
27	55	0.60	27	55	0.60	35	4.2664E-4

Table D7. Results for Liquid desiccant cooling System in Experiment 2.

Liquid temperature	Inlet Air Conditions Tower		Outlet Air Conditions Tower		Outlet Air Conditions system	
T °C	T °C	HR %	T °C	HR %	T °C	HR %
28	27	55	28.5	41	14.2	88
29	27	55	29.3	40	15.1	84
30	27	55	30.5	38.7	16.3	79

Table D7. Continuation.

Change of Humidity Ratio			Change of Enthalpy kW			Rate of Condensation g/s		
Tower	Evapor.	System	Tower	Evapor.	System	Tower	Evapor.	System
0.0023	0.0011	0.0034	2.57	10.46	13.02	1.38	0.67	2.05
0.0021	0.0012	0.0033	1.81	10.50	12.32	1.26	0.72	1.98
0.0017	0.0014	0.0032	0.50	10.87	11.37	1.04	0.86	1.90

Figure D6 shows the influence of inlet desiccant temperature on the water condensation rate. This figure shows that the water condensation rate decreases with the increase in inlet desiccant temperature. It can be explained because the vapor pressure of the liquid desiccant is proportional to the temperature, therefore with an increase in the temperature the driving force for dehumidification decreases.

Figure D7 shows that the outlet air temperature increases with the inlet desiccant temperature. It was seen in the previous figure (Fig. D6) that the rate of water condensation decreases with the increases in desiccant temperature. Since the air, entering the evaporator is now more humid the evaporator is unable to decrease the air temperature much. It is important

to note that if the water condensation rate in the desiccant tower decreases the evaporator has to take up more latent load, which defeats the purpose of a hybrid deisccant system.

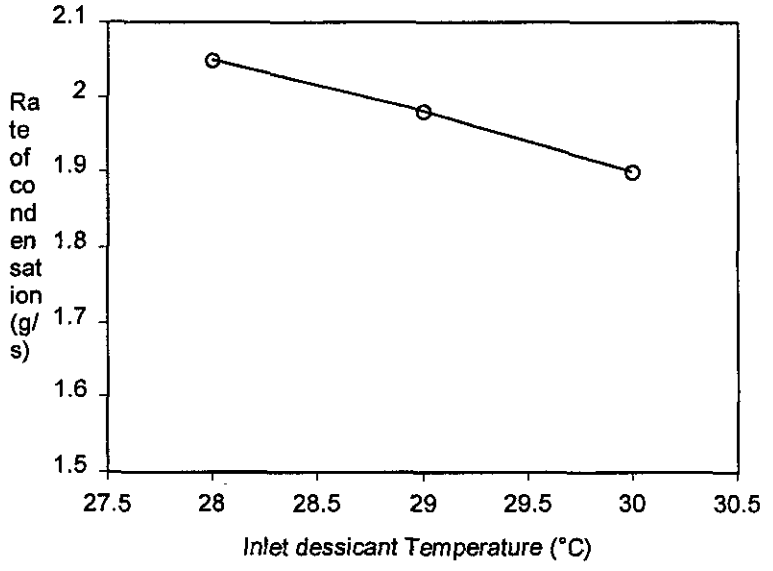

Figure D6. Influence of inlet desiccant temperature on water condensation rate

Figure D8 shows the influence of inlet desiccant temperature on the change of enthalpy in the system. This figure shows that the change of enthalpy decreases with the increase in the inlet desiccant temperature.

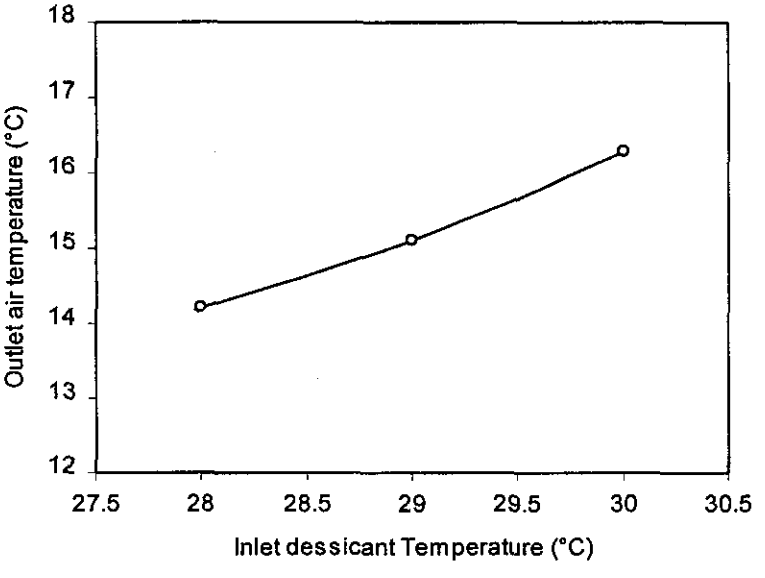

Figure D7. Influence of inlet desiccant temperature on the outlet temperature of the air

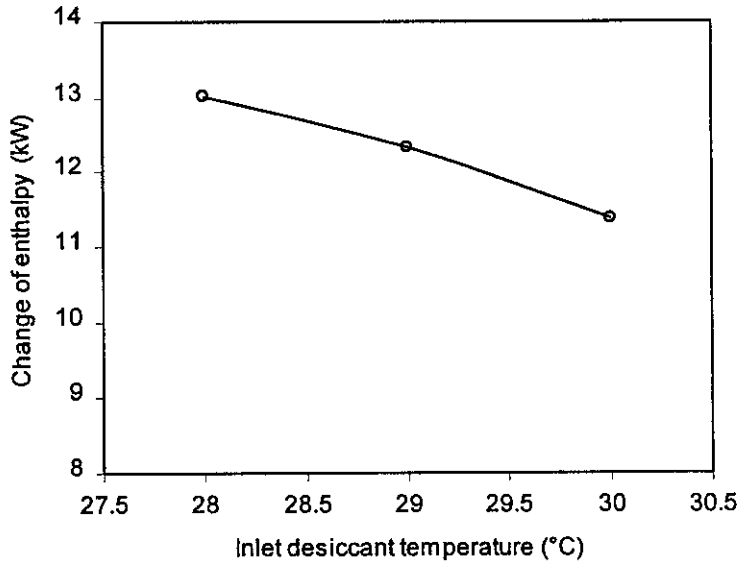

Figure D8. Influence of inlet desiccant temperature on change of enthalpy in the system

Experiment 3. This experiment was conducted to study the influence of the inlet air temperature over different parameters in the system. The inlet air temperatures used were 26, 28 and 29°C. The inlet temperature of the liquid desiccant was 27, 28, 30 °C respectively the experiments.

Table D8. Data for the experiment 3

Vapor-Compression System		Hybrid Liquid-Desiccant Cooling System			
Inlet Air Conditions	Air Flow Rate	Inlet Air Conditions	Air Flow Rate	Desiccant Conditions	
RH_a (%)	m_a (kg/s)	RH_a (%)	m_a (kg/s)	X (%)	V (m^3/s)
55	0.60	55	0.60	35	4.2664E-4

Table D9. Results for Vapor-Compression System in Experiment 3.

Inlet Air Conditions		Outlet Air Conditions		Change of Humidity ratio	Change of Enthalpy kW	Rate of Condensation g/s
T °C	HR %	T °C	HR %			
26	53	13.9	92.1	0.00203	10.48	1.22
28	53	17.2	81.9	0.00253	10.47	1.52
29	53	18.7	78.9	0.00269	10.43	1.62

Table D10. Results for Liquid desiccant Cooling System in Experiment 3.

Inlet Air Conditions Tower		Outlet Air Conditions Tower		Outlet Air Conditions System	
T °C	HR %	T °C	HR %	T °C	HR %
26	53	27.6	39.5	12.3	99.5
28	53	29.65	40.6	15.7	82.6
29	53	30.7	40.6	17.6	76.1

Table D10. Continuation.

Change of Humidity Ratio			Change of Enthalpy kW			Rate of Condensation g/s		
Tower	Evapor.	System	Tower	Evapor	System	Tower	Evapor.	System
0.0020	0.0002	0.0023	2.16	9.68	11.84	1.23	0.14	1.37
0.0020	0.0014	0.0034	2.06	10.61	12.68	1.20	0.82	2.03
0.0021	0.0017	0.0038	2.19	10.56	12.75	1.26	1.00	2.26

Figure D9 shows the influence of inlet air temperature on the outlet air temperature in the system. It is obvious that the outlet temperature would be higher with the increase in the inlet air temperature, but the purpose of this figure is to show that the hybrid-desiccant system is always able to give lower temperatures than the vapor compression system alone.

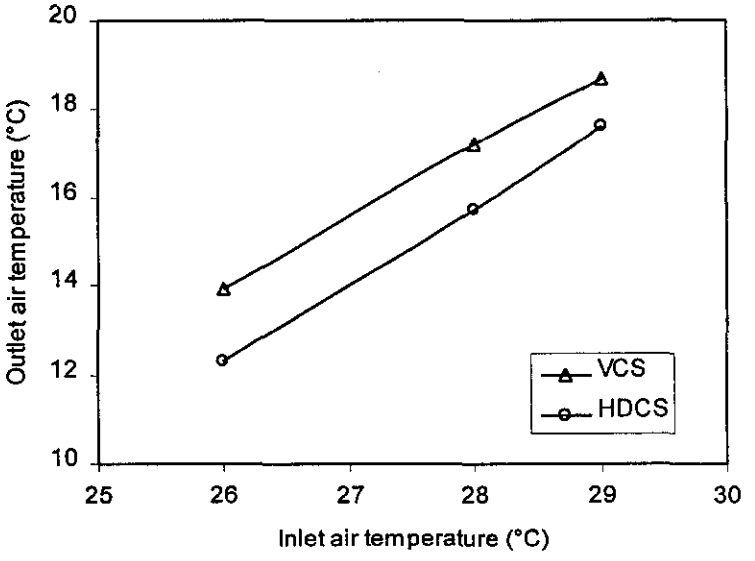

Figure D9. Influence of inlet air temperature on the outlet air temperature

Figure D10 shows the influence of inlet air temperature on the water condensation rate in the system. In the vapor-compression system the rate of water condensation increases when the

inlet air temperature is increased. It can be explained because with the increase in the inlet temperature the humidity ratio increases, therefore for the same rate of air flow the rate of condensation increases. Similarly, the water condensation rate increased with the inlet air temperature in the hybrid-desiccant system.

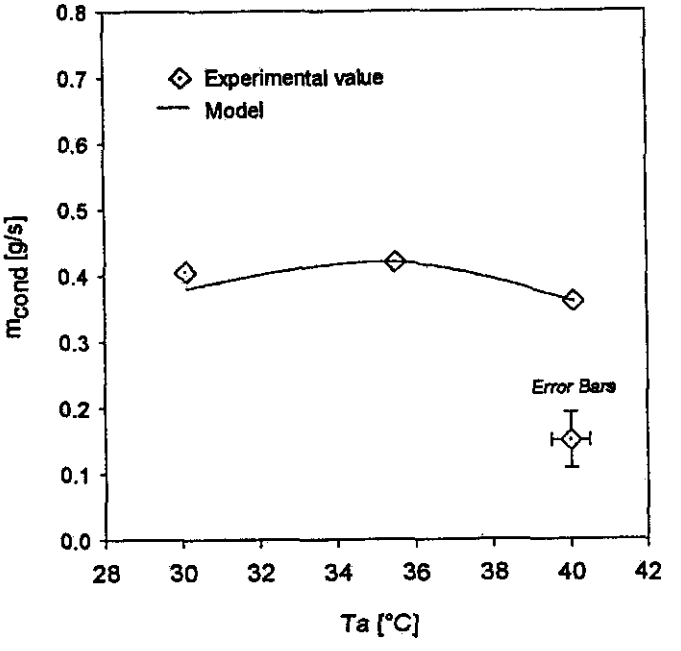

Figure D10. Influence of inlet air temperature on water condensation rate.

Figure D11 shows the influence of inlet air temperature on the change of enthalpy in the system. This figure shows that the change of enthalpy increases with the inlet air temperature in the hybrid desiccant system but remains constant in the vapor compression system.

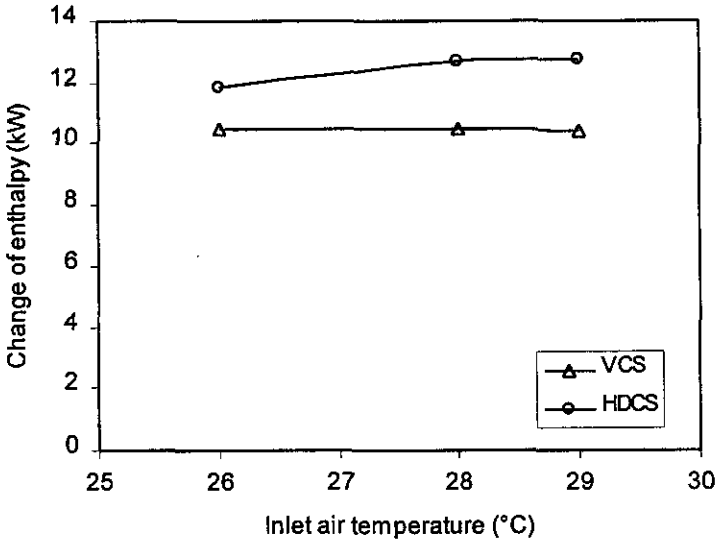

Figure D11. Influence of inlet air temperature on change of enthalpy of the system

Experiment 4. In this experiment was conducted for 100% fresh air in both the systems.

Table D11. Data for the experiment 4

Vapor-Compression System			Hybrid Liquid-Desiccant Cooling System				
Inlet Air Conditions		Air Flow Rate	Inlet Air Conditions		Air Flow Rate	Desiccant Conditions	
T_a (°C)	RH_a (%)	m_a (kg/s)	T_a (°C)	RH_a (%)	m_a (kg/s)	X (%)	T_L (°C)
24	84	0.6	24	84	0.60	36	26

Table D12. Results for Vapor-Compression System in Experiment 4.

Inlet Air Conditions		Outlet Air Conditions		Change of humidity ratio	Change of enthalpy kW	Rate of condensation G/s
T °C	HR %	T °C	HR %			
24	84	17	96	0.00415	10.63	2.49

Table D13. Results for Liquid desiccant cooling System in Experiment 4.

Inlet Air Conditions Tower		Outlet Air Conditions Tower		Outlet Air Conditions System	
T °C	HR %	T °C	HR %	T °C	HR %
24	84	27	49	15	87.2

Table D13. Continuation.

Change Humidity Ratio			Change of Enthalpy KW			Rate of Condensation g/s		
Tower	Evapor.	System	Tower	Evapor	System	Tower	Evapor.	System
0.0049	0.00165	0.0065	5.59	9.86	15.45	2.92	0.99	3.91

This experiment shows a bigger advantage for the hybrid desiccant system over the vapor compression system, then the previous case of recirculation air. The results shows that the liquid desiccant system is able to extract more heat from the air.. Also the hybrid liquid desiccant system is able to drop the outlet temperature by 2°C more than the vapor compression system alone. As there is more condensation in the liquid desiccant system, the final humidity of the air is much lower than the final conditions in the vapor compression system alone.

ANALYSIS OF ELECTRICITY USE

The measured data for the two systems is given in the chart and the tables below. The air mass flow rate is 0.6kg/s.

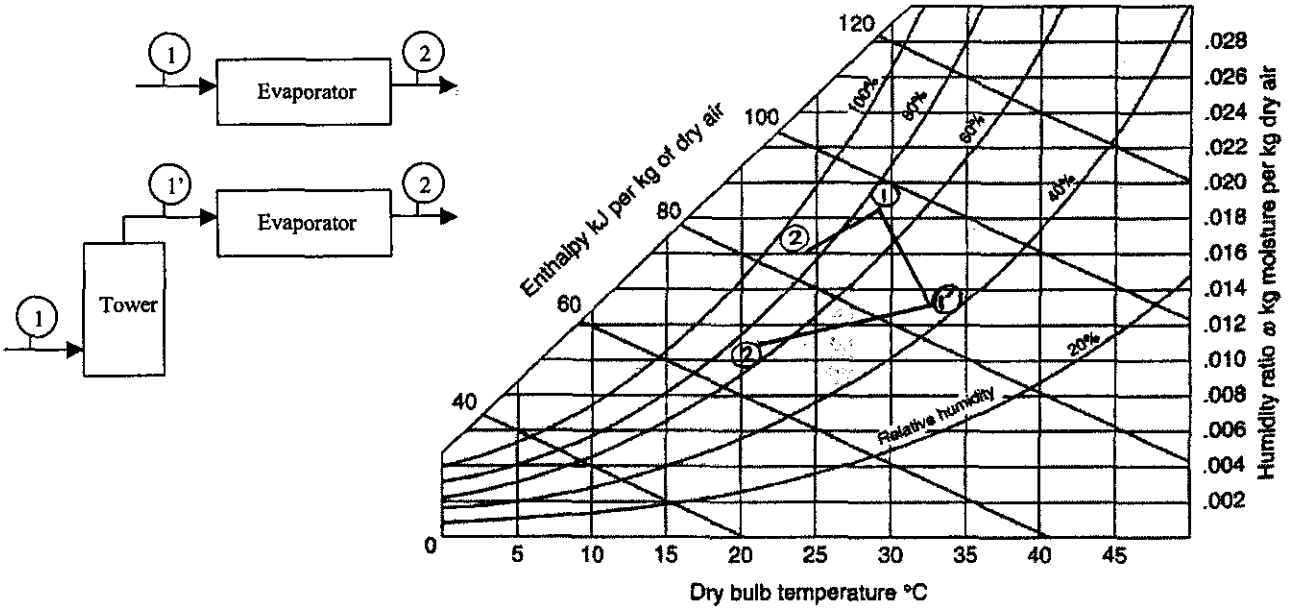

Figure D14. Representation of the air conditioning processes on the psychometric chart.

Table D14. Vapor Compression System. Process 1-2

Inlet		Outlet		Change of Enthalpy	Rate of condensation
T (°C)	RH (%)	T (°C)	RH (%)	evaporator (kW)	evaporator (g/s)
29	75	24.7	83.7	6.65	1.56

Table D15. Liquid Desiccant System, Process 1-1'-2. (Tower height 0.6 m).

Inlet Tower		Outlet Tower		Outlet Evap.		Change of Enthalpy (kW)			Rate of condensation (g/s)		
T (°C)	RH (%)	T (°C)	RH (%)	T (°C)	RH (%)	Tower	Evap	Syst.	Tower	Evap.	Syst.
29	75	32.5	45.1	21.6	68.1	5.77	11.0	16.8	3.10	1.72	4.82

The following chart and the tables show the data for a redesigned desiccant system and an equivalent vapor compression system. The inlet air-conditions are 29°C and 75% relative humidity and the outlet conditions are 20.4°C and 65% relative humidity. The air mass flow rate is 0.6kg/s.

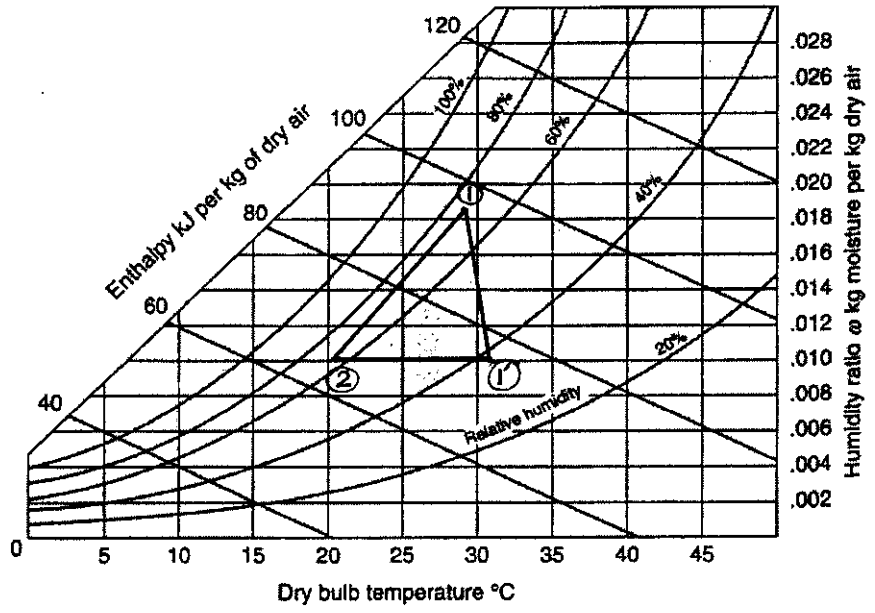

Figure D15. Representation of the air conditioning processes on the psychrometric chart.

Table D16. Vapor Compression System. Process 1-2.

Inlet		Outlet		Change of Enthalpy evaporator (kW)	Rate of condensation evaporator (g/s)
T (°C)	RH (%)	T (°C)	RH (%)		
29	75	20.4	65	19.52	5.58

Table D17. Liquid Desiccant System. Process1-1'-2. (Tower height 2.5 m).

Inlet Tower		Outlet Tower		Outlet Evap.		Change of Enthalpy (kW)			Rate of condensation (g/s)		
T (°C)	RH (%)	T (°C)	RH (%)	T (°C)	RH (%)	Tower	Evap	Syst.	Tower	Evap.	Syst.
29	75	31.03	37.64	20.4	65	11.69	7.83	19.52	5.06	0.52	5.58

To calculate the electricity consumption for these processes it is assumed that the vapor compression system has a SEER (seasonal energy efficiency ration) equal to 9 Btuh/W and the electricity cost of $0.03548/kWh and $6.25/kW-month for demand.

Process 1-2.

The cooling capacity of the evaporator is 19.52 kW = 66602.24 Btuh cooling)

$$Electricity\,consumption = 66{,}602.24 Btuh \times \frac{1W}{9 Btuh} \times \frac{1kW}{1000W} \times 2000\frac{h}{yr} = 14{,}800.5\frac{kWh}{yr}$$

$$Consumption\ costs = 14{,}800.5\frac{kWh}{yr} \times \frac{\$0.03458}{kwh} = \frac{\$525}{yr}$$

$$Demand\ cost = 7.4kW \times \frac{\$6.25}{kW - month} \times \frac{12 months}{yr} = \frac{\$555}{yr}$$

$$TotalCost = \frac{\$1{,}080}{yr}$$

Process 1-1'-2:

The cooling capacity of the evaporator is 7.8 kW = 26,613.6 Btuh cooling)

$$Electricity\ consumption = 26{,}613.6 Btuh \times \frac{1W}{9 Btuh} \times \frac{1kW}{1{,}000W} \times 2000\frac{h}{yr} = 5{,}914.13\frac{kWh}{yr}$$

$$Consumption\ cost = 5{,}914.13\frac{kWh}{yr} \times \frac{\$0.03458}{kwh} = \frac{\$210}{yr}$$

$$Demand\ cost = 2.95kW \times \frac{\$6.25}{kW - month} \times \frac{12 months}{yr} = \frac{\$221}{yr}$$

$$Total\ Cost = \frac{\$431}{yr}$$

The savings in electricity use using hybrid liquid-desiccant system instead of the vapor compression system alone are $649/yr or 60%.

Solar System for the Regeneration Process.

The solar closed loop choosen for the desiccant regeneration process has the following specification:

Active system: C1-120-128

Gallons HE Tank: 120

Dimensions of the tank: 58 5/8 of high and 24 7/16 of diameter

The tank has insulation with R value of 16.7

Collector area: 4 (4*8) = 128 ft^2

System Cost: $5336

Installation Cost: $1200

Total cost for the system: $6536

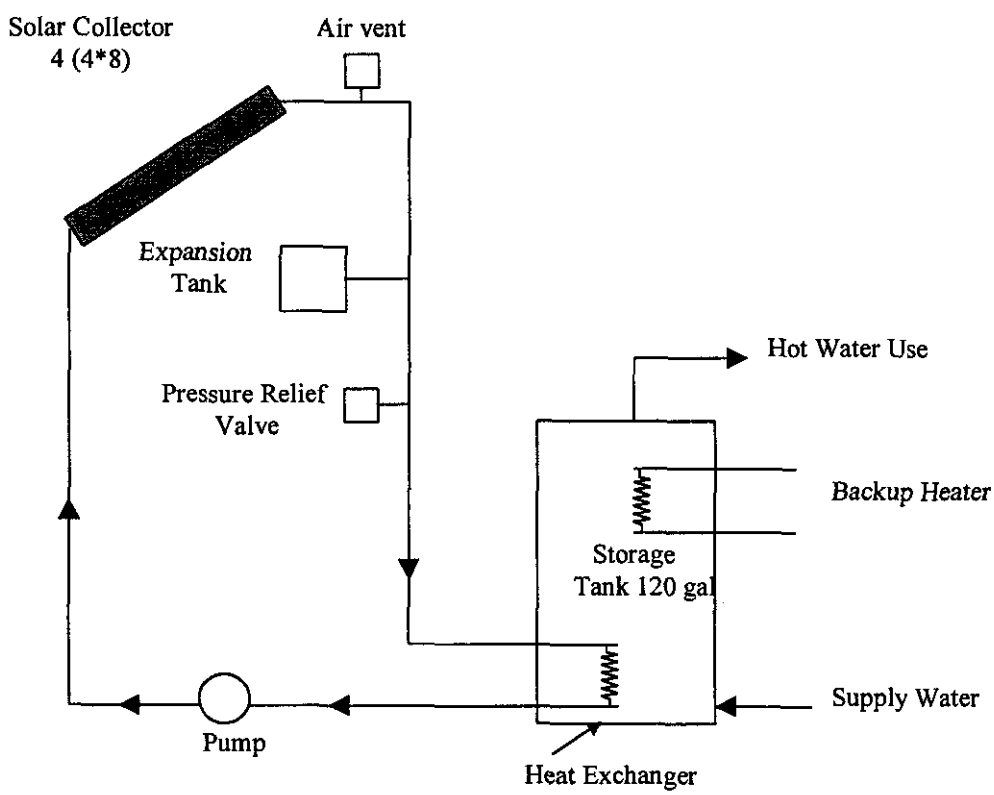

Figure D16. Closed loop system for the regeneration process.

To verify that this collector is able to give the total heat needed for the regeneration process it is necessary to calculate the total heat that is going to give this collector for Gainesville, FL.

Flat plate collector give a thermal efficiency of:

$$\eta = 0.7512 - 0.138 * (T_{fi} - T_{fo}) / Ic$$

$$K_{\tau\alpha} = 1 - 0.15\left(\frac{1}{Cos(i)} - 1\right)$$

Where: $(T_{fi}-T_a)/Ic$ is in $C - m^2/W$

Collector tilt = 30° (South facing)

Storage Volume = 120 gal = 454.3 L.

Nomenclature used:

T_a: temperature of the ambient.

T_{fi}: Initial temperature of the storage.

T_{fo}: Final Temperature of the storage.

m: mass flow of the water.

Q_u: useful energy collected

Taking the Initial storage temperature of 50°C, we get:

- The mass of water is: $m = m*t = V*\rho_m = 0.4543*1000 = 454.3$ Kg
- Specific heat of the water = 4.18 kJ/kg K (T=320 K)
- The useful heat = Qu = m Cp (Tfo – Tfi) = η Ic Ac.
- The total volume of liquid desiccant is 0.25 m^3.
- The density for Lithium Chlorite at 45 C and 33% of concentration is 1206.54 kg/m^3.
- The total mass of solution is 600 kg.

<u>Heat to evaporate the water:</u>

For 33% of concentration we have:

$m_{LiCl} / m_{total} = 0.33$ then mLiCl = 198 kg.

$m_w / m_{total} = 0.67$ then $m_w = 402$ kg.

For 35 % of concentration we have to evaporate certain amount of water, therefore:

$m_{LiCl} / m_{total} = 0.35$ then $m_{total} = 198 / 0.35 = 565.71$ kg.

$m_w / m_{total} = 0.65$ then $m_w = 0.65*284.74$ kg $= 367.71$ kg.

The amount of water that we need to evaporate is 402 –367.71= 34.29 kg.

The heat of evaporation is:

$Q = m_{evaporation} * h_{fg} = 34.29*2358.5 = 80863$ kJ / 3.6 kJ/Wh =

$= 22462$ Wh = 22.5 kW.

Heat for heat the dessciant:

$Q = m*cp*\Delta T = 600 * 2.6 * 25 = 39000$ kJ / 3.6 kJ/Wh = 10833 Wh = 10.8 kWh.

Heat loss in the tank:

Total area of the tank is:

$A = (\Pi*D*L) + 2*(\Pi*D^2/4)$

$A = (\Pi*58.63*24.44) + 2*(\Pi*24.44^2/4) = 5439$ in^2

$A = 37.76$ ft^2

For this cases we have two tanks, so the total are is 75.52 ft^2

The heat is:

$$Q = \left(\sum \frac{1}{R_t} \right) * A * \Delta T$$

$$\sum \frac{1}{R_t} = \frac{1}{R_{insulation}} + \frac{1}{h_{convective}} = \frac{1}{16.7} + \frac{1}{4} = 0.3098 \ \frac{Btu}{h - ft^2 F}$$

$$Q = 0.3098 \ * 75.52 * (140 - 77) = 1474 \frac{Btu}{h} = 432 W$$

For 24 h/day the total heat loss is:

Q = 10368 Wh = 10.4 kWh

The total heat that has to be supply by the solar system is:

$Q_{total} = 10.8 + 22.5 + 10.4 = 43.7$ kWh

Table D18. Results for the Solar Collector

Time	T_a °C	Ic-Total W/m^2	T_{fi} °C	T_{fi}-T_a °C	K	Efficiency	Q_u (Wh)	Q_u (kJ)	T_{fo}-T_{fi} °C	T_{fo} °C
7-8	24	198.9	50	26.00	0.34	0.1920	458.19	1649.47	0.9	50.9
8-9	25	476.4	50.7	25.65	0.78	0.4429	2531.81	9114.50	4.8	55.7
9-10	26	724.2	54.3	28.25	0.90	0.5098	4429.40	15945.85	8.4	64.1
10-11	27	915.8	60.6	33.55	0.95	0.5376	5906.63	21263.85	11.2	75.3
11-12	28	1037.4	69.0	40.95	0.97	0.5501	6844.85	24641.48	13.0	88.2
12-1	29	1078.7	78.7	49.69	0.98	0.5535	7160.28	25777.00	13.6	101.8
1-2	30	1037.4	88.9	59.38	0.97	0.5495	6834.79	24605.23	13.0	114.8
2-3	28	915.8	98.6	70.61	0.95	0.5363	5887.03	21193.31	11.2	125.9
3-4	27	724.2	107.0	79.99	0.90	0.5075	4403.30	15851.88	8.3	134.3
4-5	26	476.4	113.3	87.26	0.78	0.4393	2504.26	9015.34	4.7	139.0
5-6	25	198.9	116.8	91.83	0.34	0.1877	444.27	1599.36	0.8	139.9
						Total/day	47404.80	170657.28		

The solar system is going to supply 47.4 kWh/day and the total heat that in needed for the process is 43.7 kWh/day, it means that this solar system is able to handle the heat needed for the process.

Cost Analysis

The condensing unit for the vapor compression system is a 6-ton unit and the price of the equipment including installation is $2800

For the desiccant system can be used a condensing unit of 2.5-ton for which the price is $1250.
The price of the desiccant system is:
Pump: $250
Solution of lithium chlorite: $180
Piping and fittings: $120
Tower and packing: $100
Ducts: $350
Total: $1000

The price of the solar system is $6536
The total price for the desiccant system is $8756

The additional cost for using the desiccant system is $5986

The simple pay back for this equipment is:
SPB = $5986 / $649/yr = 9.2 years.

APPENDIX E

Liquid Desiccant Cooling of a Residential House

E. LIQUID DESICCANT COOLING OF A RESIDENTIAL HOUSE

The use of solar hybrid liquid desiccant air conditioning in a residential house has been examined. The floor plan of a residential house prototype is shown in figure E.1, and further details pertaining to the calculation of the cooling load of the residence are listed in tables E.1 and E.2. Figure E.2. shows a schematic of the solar desiccant system.

A transient simulation was carried out for a typical summer day (August 14) in Miami, Florida. For the simulation the transient simulation program TRNSYS was utilized (Solar Energy Laboratory, University of Wisconsin - Madison, 1990). This program consist of a number of subroutines that describe each system component. These subroutines are connected through an input file (a "deck" file) which also describes the system (for example the floor plan of the house, the size of the solar collector storage subsystem, etc.).

In the first step the hourly cooling load was calculated, and in the second step the solar desiccant regeneration was simulated. The output from the first step was used to calculate the input needed for the second step, i.e., the amount of regeneration heat needed. To simplify the analyses a number of assumptions were made. A summary of these assumption is given in table E.3. As shown in figure E.2, a fraction of the return air is brought through the dehumidifier to handle the latent cooling load. A conventional vapor compression system (DX-system) handles the sensible cooling. Part of the dilute desiccant is brought to the regenerator so that the same amount of water absorbed in the dehumidifier is evaporated in the desiccant regenerator. Before the regenerator, the desiccant is heated indirectly by water from a solar collector / storage subsystem. Auxiliary heat is provided to ensure that the desiccant reaches 65 °C before the regenerator. Ambient air is used as the moisture scavenging air stream in the regenerator. The

An example of the TRNSYS "deck" files used for the calculation of the cooling load and the solar desiccant regeneration are given in sections E.1 and E.2, respectively. For additional description of the TRNSYS program it is referred to the TRNSYS manual.

The results from the simulation are summarized in figures E.3, E.4, and E.5. Figure E.3 shows the "weather data" for August 14 in Miami, Florida. Figure E.4 shows the residential cooling load obtained. During the night hours, the cooling requirement is mainly latent cooling, whereas the latent cooling is about 30 % during the peak cooling hours. The electrical energy consumption of the vapor compression system is compared for a hybrid and a conventional air conditioning system. Then, the electrical energy savings for the vapor compression system, $W_{VC,diff}$, are compared to the regeneration auxiliary energy requirement of the hybrid system, Q_{AUX} (figure E.5). The results show that using the hybrid desiccant system between 11 am and 11 pm will save about 2.6 kWh electrical energy for the day simulated. However, using the hybrid system throughout the simulated 24 hour period is not feasible for the residential application simulated.

TABLE E.1. DESCRIPTION OF RESIDENTIAL PROTOTYPE

Parameters	Description
Physical Characteristics	
General:	
Residence Type	Single story slab on grade; "L" shaped ranch style with garage.
Aspect Ratio	1/1.6 (excluding garage)
Major Axis	east-west
Floor Area	139.4 m^2 (1500 ft^2)
Roof:	
Type / Construction	Pitched roof with 7.62 cm (3″) ceiling insulation.
Slope	22.62 °
Absorptance	0.8
Emittance	0.9
Overhangs	0.61 m (2 ft) on all sides
Walls:	
Construction	Frame wall with 10.2 cm (4″) insulation.
Outer Wall Absorptance	0.8
Inner Surface Reflectance	0.7
Internal Partition (to garage)	Frame partition with 1.9 cm (0.75″) gypsum board.
Windows:	
Transmittance for Diffuse Solar Radiation	0.8
Overall Transmittance for Solar Radiation	0.8
Window Loss Coefficient (not including convection at inside and outside surface)	5.97 W/m^2-°C (1.05 Btu/hr-ft^2-°F)

TABLE E.1. DESCRIPTION OF RESIDENTIAL PROTOTYPE, CONTINUED

Parameters	Description
Internal Loads	
Occupancy	4 people
Sensible Heat Gain per Person	65 W
Latent Heat Gain per Person	55 W
Peak Lighting	0.6 kW
Light Energy to Space	100 %
Miscellaneous Equipment	0.56 kW
Sensible Heat Gain from Equipment	67 %
Latent Heat Gain from Equipment	16 %
Infiltration Rate	0.75 ACH

TABLE E.2. LIGHTING SCHEDULE FOR RESIDENTIAL PROTOTYPE

Hour	Lighting (kW)
1	0
2	0
3	0
4	0
5	0
6	0.21
7	0.21
8	0
9	0
10	0
11	0
12	0
13	0
14	0
15	0
16	0
17	0.07
18	0.23
19	0.30
20	0.38
21	0.59
22	0.6
23	0
24	0

TABLE E.3. SUMMARY OF ASSUMPTIONS FOR RESIDENTIAL HOUSE SIMULATION

Auxiliary Cooling DX-System COP	3.0 (constant)
Desiccant Temperature to Dehumidifier	30 °C
Desiccant Concentration to Dehumidifier	0.95 kg TEG / kg solution
Residential Zone Temperature	24 °C
Residential Zone Humidity	Y=0.0095 kg / kg
Supply Temperature	13 °C
Dehumidifier and Regenerator Effectivenesses	0.8
Inlet Desiccant Temperature to Regenerator	65 °C
Solar Collector Area	80 m^2
Collector Fluid	Water
Solar Hot Water Storage Volume	2 m^3
Heat Exchanger Effectiveness	0.8 (ϵ_{HE2}=0.7)

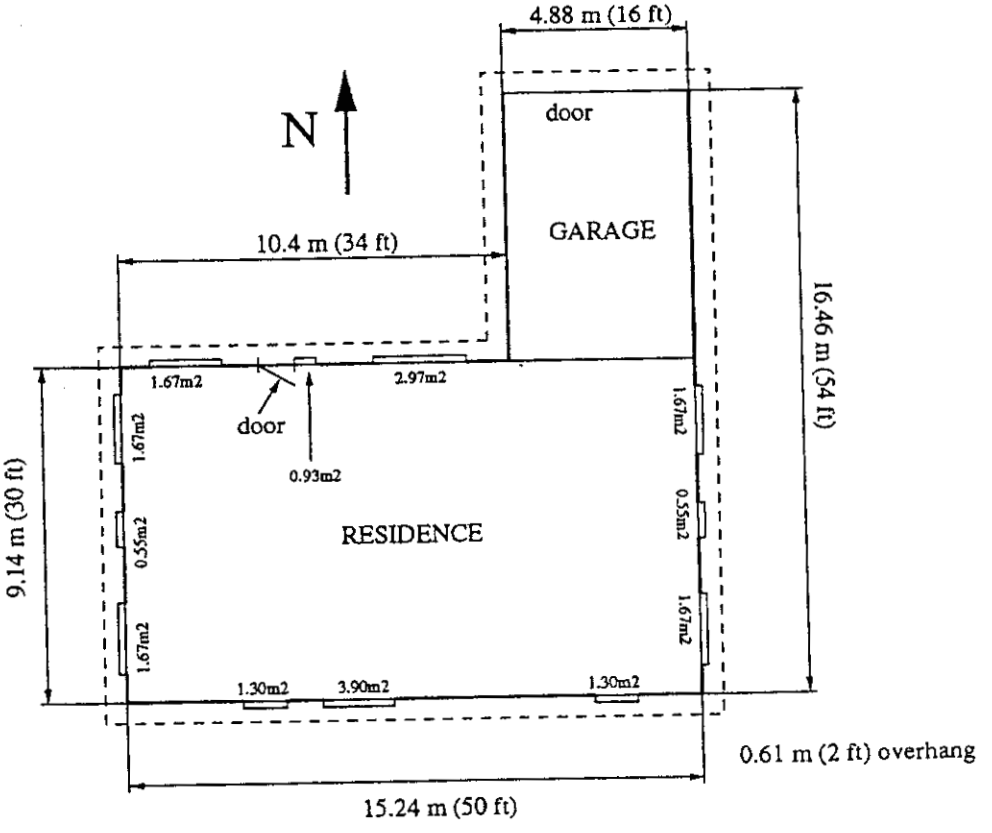

Figure E.1: Floor plan of the residential house prototype.

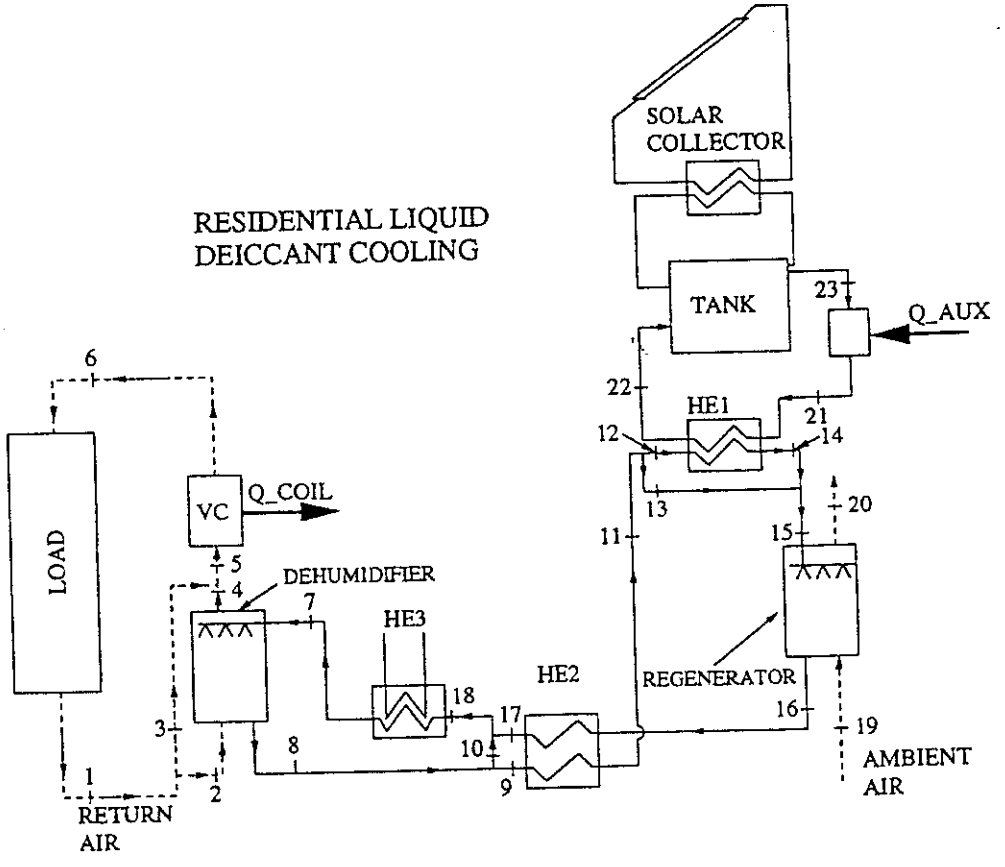

Figure E.2: Schematic of solar hybrid liquid desiccant air conditioning system for a residential house.

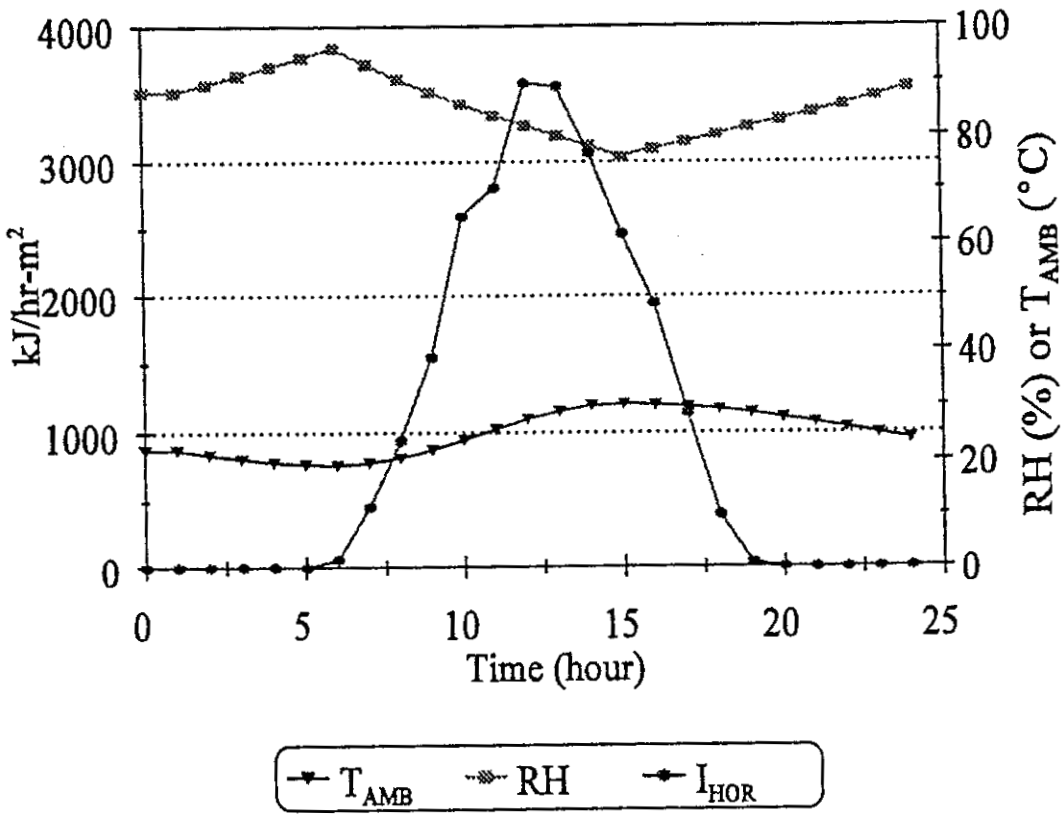

Figure E.3: Simulated weather data for August 14, Miami, Florida.

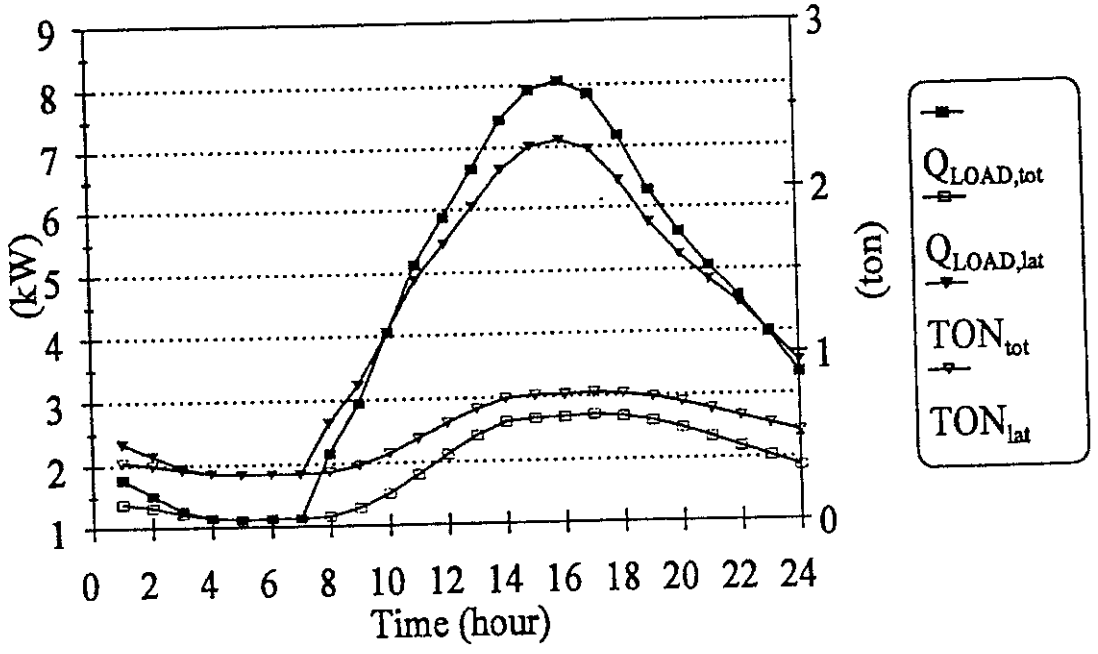

Figure E.4: Simulated cooling load for August 14, Miami, Florida.

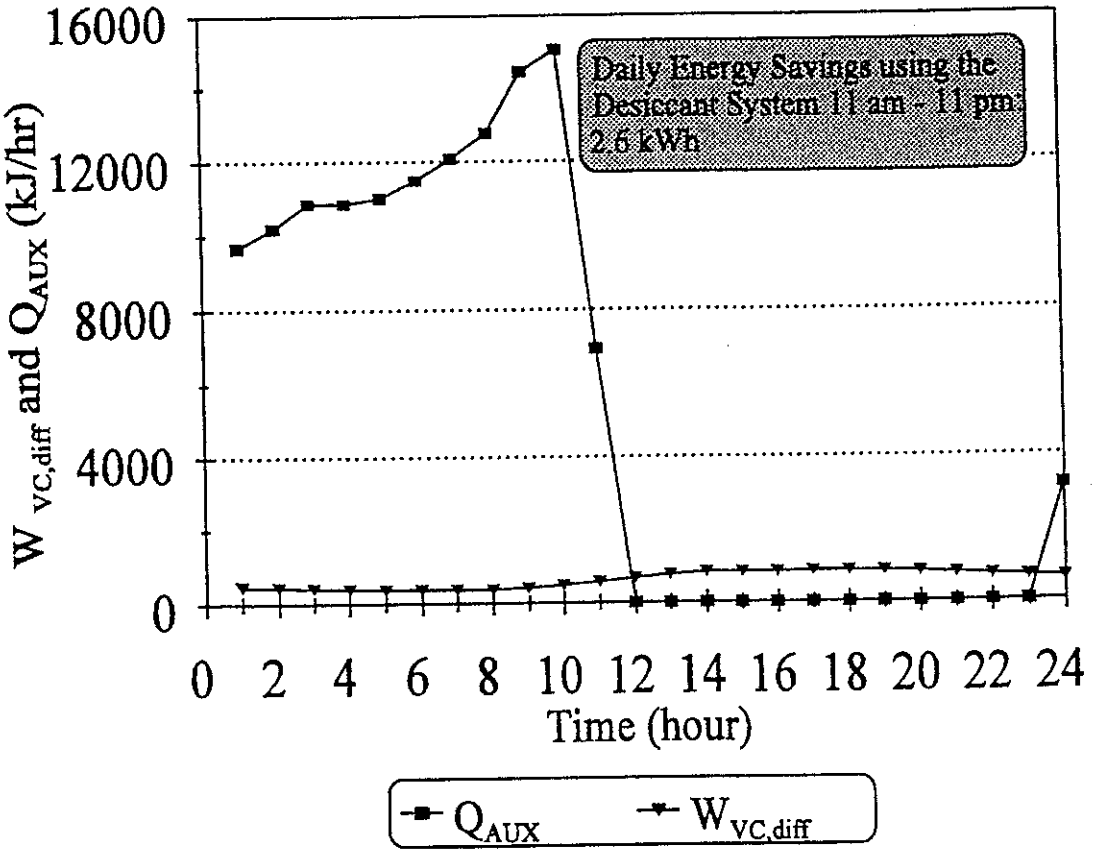

Figure E.5: Simulated auxiliary energy consumption and electrical energy savings, August 14, Miami, Florida.

E.1. Example TRNSYS deck-file for the calculation of the hourly residential cooling load.

```
**********************************************
*                                            *
*              RESIDENTIAL HOUSE LOAD        *
*              AUGUST 14                     *
*              MIAMI, FLORIDA                *
*                                            *
**********************************************

ASSIGN LOAD.OUT 6
ASSIGN WEATH14.DAT 20
ASSIGN ASHRAE.COF 8
ASSIGN LIGHT.DAT 10

SIMULATION 0 24 1

WIDTH 72

UNIT 1 TYPE 9  WEATHER READER
PARAMETERS 34
10 1 1 1 0 2 1 0 3 1 0 4 1 0 5 1 0 6 1 0 7 1 0
-8 1 0 -9 1 0 10 1 0 20 -1

UNIT 2 TYPE 9  LIGHT LOAD READER
PARAMETERS 10
2 1 1 1 0 2 1 0 10 -1

UNIT 3 TYPE 16 SOLAR RADIATION PROCESSOR 1
PARAMETERS 9
5 1 2 226 25.8 4871 -5.2 1 -1
INPUTS 14
1,8 1,5 1,6 1,19 1,20 0,0 0,0 0,0 0,0 0,0 0,0 0,0 0,0 0,0
0.0 22.0 88.2 0.0 0.0 0.2 90 0.0 90 90 90 180 90 -90

UNIT 4 TYPE 16 SOLAR RADIATION PROCESSOR 2
PARAMETERS 9
5 1 2 226 25.8 4871 -5.2 1 -1
INPUTS 10
1,8 1,5 1,6 1,19 1,20 0,0 0,0 0,0 0,0 0,0
0.10 22.0 88.2 0.0 0.0 0.2 22.62 0.0 22.62 180

UNIT 5 TYPE 34 SOUTH WALL OH
PARAMETERS 15
2.44 15.24 0.61 0.0 0.61 0.61 0 0 0 0 0 0 0 0 0
INPUTS 6
3,2 3,3 3,4 3,5 3,7 0,0
0.0 0.0 0.0 0.0 0.0 0.2

UNIT 6 TYPE 34 EAST WALL OH
PARAMETERS 15
2.44 9.14 0.61 0.0 0.61 0.1 0 0 0 0 0 0 0 0 90
INPUTS 6
```

```
3,2 3,3 3,4 3,5 3,12 0,0
0 0 0 0 0 0.2

UNIT 7 TYPE 34 NORTH WALL OH
PARAMETERS 15
2.44 10.36 0.61 0.0 0.61 0.61 1 0 0 0 0 0 0 0 180
INPUTS 6
3,2 3,3 3,4 3,5 3,15 0,0
0 0 0 0 0 0.2

UNIT 8 TYPE 34 WEST WALL OH
PARAMETERS 15
2.44 9.14 0.61 0.0 0.61 0.61 0 0 0 0 0 0 0 0 -90
INPUTS 6
3,2 3,3 3,4 3,5 3,18 0,0
0 0 0 0 0 0.2

UNIT 9 TYPE 18 PITCHED ROOF AND ATTIC
PARAMETERS 13
-1 1 0.8 0.9 92.3 11.2 92.3 11.2 139.3 553 0 22.62 22.62
INPUTS 8
1,5 4,6 6,1 4,11 8,1 1,10 0,0 11,1
22.0 0.0 0.0 0.0 0.0 5.0 30.0 24.0

UNIT 10 TYPE 19 GARAGE
*ZONE
PARAMETERS 10
2 1 87.2 0.75 0 0 100 6 24 0.0147
INPUT 11
1,5 1,7 1,5 0,0 1,7 0,0 0,0 0,0 0,0 0,0 1,10
22 0.0147 22 0 0.0147 0 0 2 0 0 6.5
*EXTERIOR WALLS
PARAMETERS 13
1 1 17.9 0.7 0.8 2 97 2 -1 11.9 3 -1 17.9
INPUT 3
6,1 7,1 8,1
0 0 0
*WALL SEPARATING GARAGE AND RESIDENCE
PARAMETERS 7
4 3 11.9 0.7 0.8 3 23
INPUT 3
11,11 11,1 0,0
24 24 0
*FLOOR
PARAMETERS 7
5 2 35.7 0.7 0.8 3 33
*ROOF
PARAMETERS 7
6 1 35.7 0.7 0.8 1 22
INPUT 1
3,4
0
*GEOMETRY MODE
```

```
PARAMETERS 1
0
*OUTPUT PARAMETERS
PARAMETERS 3
1 2 4

UNIT 11 TYPE 19 RESIDENCE
*ZONE INPUT AND PARAMETERS
PARAMETERS 14
1 1 337.6 0.75 0 0 3.000 11 24 0.0095 18 24 0.006 0.0095
INPUTS 11
1,5 1,7 1,5 0,0 1,7 0,0 0,0 0,0 2,2 0,0 1,10
22.0 0.0147 22.0 0.0 0.0147 0.13 4 2 0 1351 6.5
* EXTERIOR WALLS PARAMETERS AND INPUT
PARAMETERS 16
1 1 30.7 0.7 0.8 2 97 2 -1 18.4 3 -1 25.3 4 -1 18.4
INPUTS 4
5,1 6,1 7,1 8,1
0.0 0.0 0.0 0.0
* FLOOR PARAMETERS
PARAMETERS 7
5 2 139.3 0.7 0.8 3 33
*CEILING PARAMETERS AND INPUT (NON-ASHRAE WALL)
PARAMETERS 5
6 4 139.3 0.7 33
INPUTS 1
9,1
0.0
* SOUTH WINDOWS PARAMETERS AND INPUT
PARAMETERS 8
7 5 6.52 1 0.8 30 1 5
INPUTS 5
5,1 5,2 0,0 0,0 0,0
0.0 0.0 0.8 21.5 1
* EAST WINDOWS PARAMETERS AND INPUT
PARAMETERS 8
8 5 3.88 1 0.8 30 1 5
INPUTS 5
6,1 6,2 0,0 0,0 0,0
0.0 0.0 0.8 21.5 1
* NORTH WINDOWS PARAMETERS AND INPUT
PARAMETERS 8
9 5 5.56 1 0.8 30 1 5
INPUTS 5
7,1 7,2 0,0 0,0 0,0
0.0 0.0 0.8 21.5 1
* WEST WINDOWS PARAMETERS AND INPUT
PARAMETERS 8
10 5 3.88 1 0.8 30 1 5
INPUTS 5
8,1 8,2 0,0 0,0 0,0
0.0 0.0 0.8 21.5 1
*WALL SEPARATING RESIDENCE AND GARAGE
```

```
PARAMETERS 7
11 3 11.9 0.7 0.8 3 23
INPUTS 3
10,11 10,1 0,0
24 24 0
* VIEW FACTORS
PARAMETERS 41
1 2.44 9.14 15.24 2 1 4 3 5 6 5 8 2 3.57 0.2 1.94
2.0 7 1 5.62 0.51 1.63 4.0 10 4 3.57 0.2 1.94 2.0
9 3 8.06 0.75 1.39 4.0 11 3 4.88 0 2.44 4.88
*OUTPUT PARAMETERS
PARAMETERS 3
1 2 11
*
EQUATIONS 4
QSENS = [11,7]
QLAT = [11,8]
QCOOLS = MAX(QSENS,0)
QCOOLL = MAX(QLAT,0)
*

UNIT 25 TYPE 25 PRINTER 1
PARAMETERS 4
1 1 24 6
INPUTS 9
1,5 1,7 10,1 10,2 11,1 11,2 4,6 QCOOLS QCOOLL
TAMB YAMB TG YG TZN YZN I SORO QCOOLS QCOOLL

END
```

E.2. Example TRNSYS deck-file for the calculation of the solar desiccant regeneration.

```
**********************************************
*                                            *
*       SOLAR DESICCANT REGENERATION         *
*       AUGUST 14                            *
*       MIAMI, FLORIDA                       *
*                                            *
**********************************************

ASSIGN REGEN.OUT 6
ASSIGN WEATH14.DAT 20
ASSIGN TYPE21.DAT 10

SIMULATION 1 24 1

WIDTH 72
```

```
UNIT 1 TYPE 9  WEATHER READER
PARAMETERS 34
10 1 1 1 0 2 1 0 3 1 0 4 1 0 5 1 0 6 1 0 7 1 0
-8 1 0 -9 1 0 10 1 0 20 -1

UNIT 2 TYPE 9  LOAD READER
PARAMETERS 19
5 1 1 1 0 2 1 0 3 1 0 4 1 0 5 1 0 10 -1

UNIT 3 TYPE 16 SOLAR RADIATION PROCESSOR
PARAMETERS 9
5 1 2 226 25.8 4871 -5.2 1 -1
INPUTS 8
1,8 1,5 1,6 1,19 1,20 0,0 0,0 0,0
0.0 22.0 88.2 1.0 1.0 0.2 22.62 0.0

EQUATIONS 10
TWMIN=[2,5]
TL11=[2,4]
ML11=[2,3]
TTANK=[21,1]
TCHECK=MAX(TTANK,TWMIN)
TL14=MAX(65,(TL11+0.8*(TCHECK-TL11)))
ML14=MAX(133,(ML11*(65-TL11)/(TL14-TL11)))
MW=1.196*ML14
QHE1=ML14*2.5*(TL14-TL11)
TW22=TCHECK-QHE1/(MW*4.18)

UNIT 21 TYPE 21 LIQ. COLLECTOR - STORAGE
PARAMETERS 17
80 2 4957 4.19 4957 4.19 124 0.765 14.9 0.17 100 0.8
3 1000 1.0 2 65
INPUTS 10
TW22 MW 1,5 2,2 3,6 3,4 3,5 0,0 3,9 0,0
61.6 568 22.0 23.83 0.0 0.0 0.0 0.2 0.0 22.62

EQUATIONS 1
QAUX=MW*4.18*(TCHECK-TTANK)

UNIT 25 TYPE 25  PRINTER 1
PARAMETERS 4
1 1 24 6
INPUTS 8
TTANK TCHECK MW TW22 QAUX ML11 ML14 TL14
TTANK TCHECK MW TW22 QAUX ML11 ML14 TL14

END
```

APPENDIX F

Liquid Desiccant Cooling of Ventilation Air for a Small Commercial Building

F. LIQUID DESICCANT COOLING OF VENTILATION AIR FOR A SMALL COMMERCIAL BUILDING

Conditioning of ventilation air is a major source of energy consumption in commercial buildings. In humid climates, a large part of the cooling load associated with ventilation air pre-conditioning is latent. Therefore, using liquid desiccant cooling for this application should both result in better humidity control, and reduce the electrical energy consumption.

The use of hybrid liquid desiccant cooling for ventilation air pre-conditioning for a small office building was modeled using the simulation program TRNSYS (Solar Energy Laboratory, University of Wisconsin - Madison, 1991) which is briefly described in attachment E. The simulation was carried out for the day of August 14 for Miami, Florida. The details on the "weather" for this day has been previously shown in figure E.3. The desiccant system used is described in figure F.1, and further details relevant for the simulation are given in table F.1. Figure F.2 summarizes the result of the simulation. In this figure the load on the vapor compression coil is shown for the hybrid desiccant system, $Q_{coil,des}$, and for a conventional vapor compression DX-system, $Q_{coil,conv}$. In addition, the difference in electrical energy requirement between the vapor compression system in the desiccant system, and in the conventional system, $W_{VC,diff}$ is shown along with the auxiliary energy requirement for desiccant regeneration, Q_{AUX}. The TRNSYS deck for the simulation of the desiccant regeneration is listed below in section F.1.

For the 24 hour period simulated, the electrical energy saving is 41 kWh by using the hybrid desiccant system as compared to using a conventional air conditioning system. This saving is equal to 63 % of the electrical energy consumed by a conventional system. In addition to the energy savings, the desiccant system is also likely to provide a better humidity control.

However, the solar fraction of regeneration heat necessary to obtain energy savings with the desiccant system is large (0.92). Thus, large collector areas are required.

TABLE F.1. DESCRIPTION OF SMALL COMMERCIAL BUILDING VENTILATION AIR PRE-CONDITIONER

Parameter	**Description**
Ventilation Requirement	9.4 L/s-person (20 cfm/person)
Occupancy Schedule	8 am - 19 pm: 50 people 19 pm - 8 am: 2 people
Auxiliary Cooling DX-System COP	2.5 (constant)
Air Temperature Leaving the Ventilation Air Pre-Conditioner	24 °C
Air Humidity Ratio Leaving the Ventilation Air Pre-Conditioner	0.0095 kg/kg
Dehumidifier and Regenerator Effectivenesses	0.8
Inlet Desiccant Temperature to Regenerator	65 °C
Solar Collector Area	240 m^2
Collector Fluid	Water
Solar Hot Water Storage Volume	10 m^3
Heat Exchanger Effectiveness	0.8 (ϵ_{HE2}=0.7)

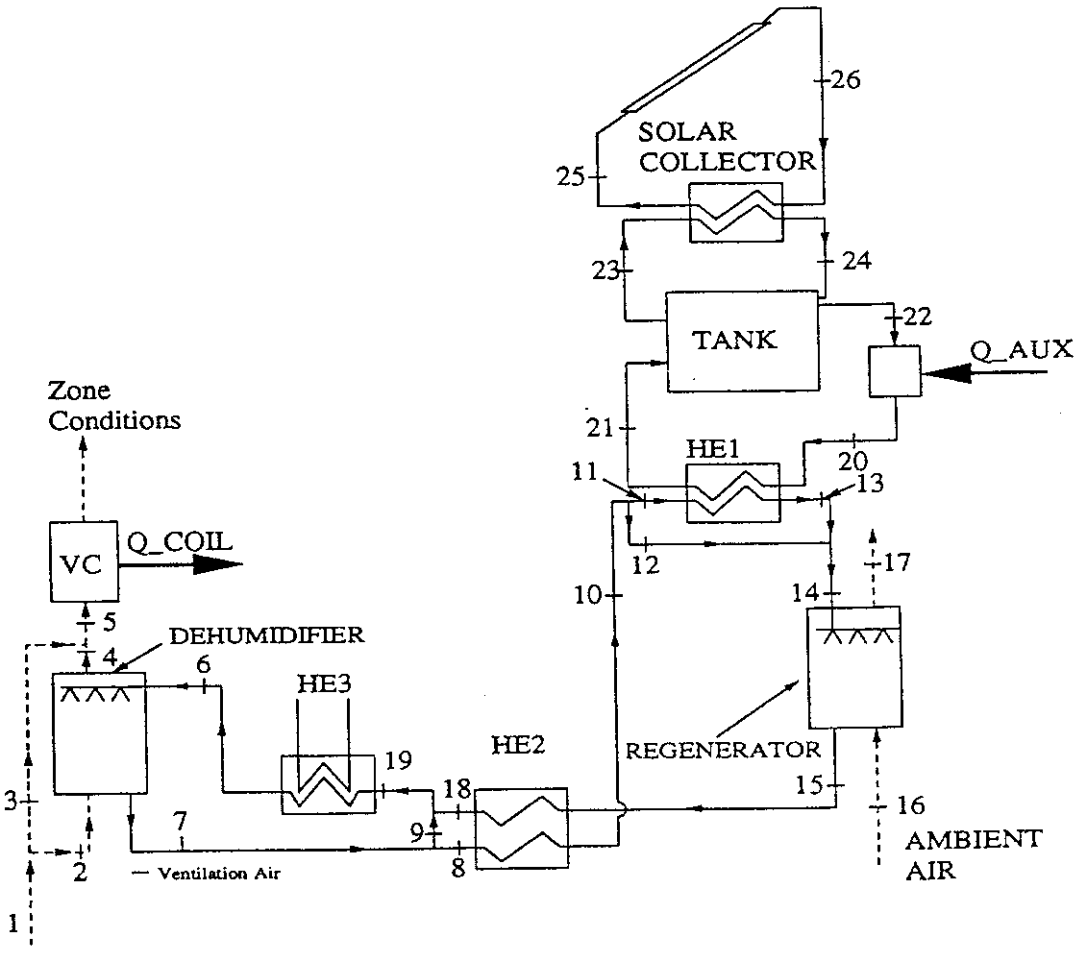

Figure F.1: Schematic of solar hybrid liquid desiccant air conditioning system for ventilation air pre-conditioning.

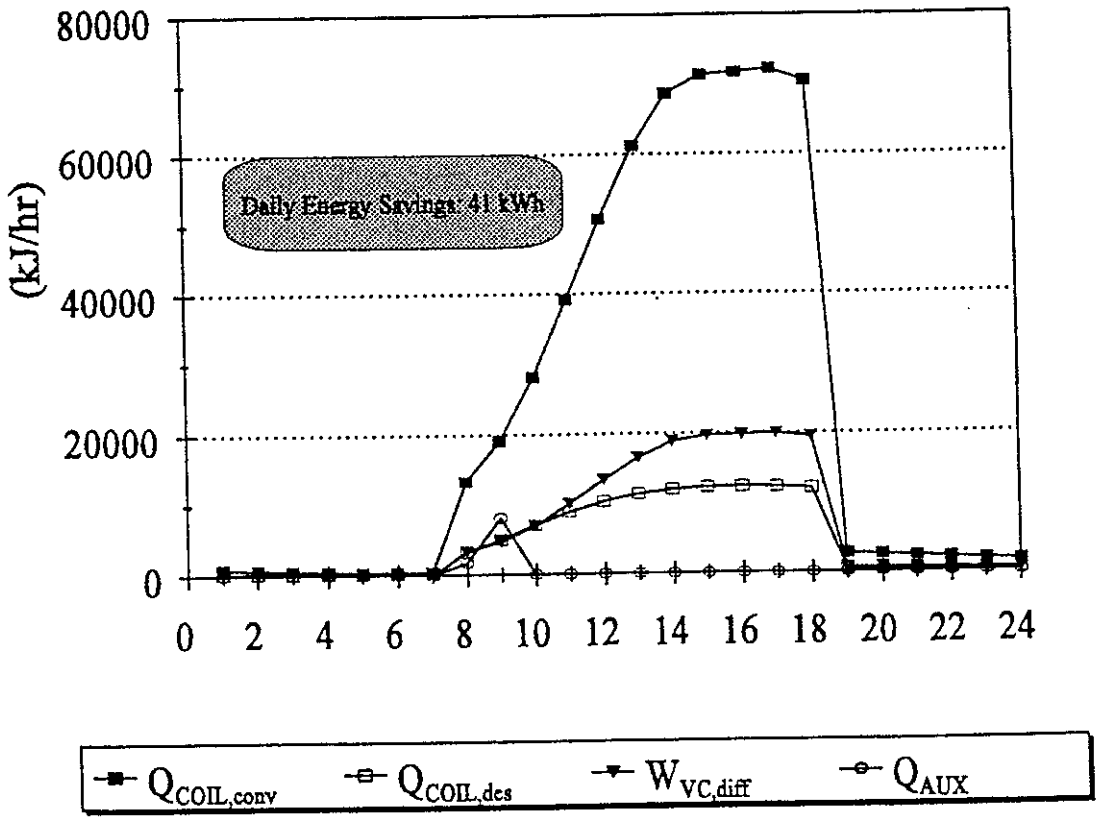

Figure F.2: Simulation summary of pre-conditioning of ventilation air for a small commercial building, August 14, Miami, Florida.

F.1. Example TRNSYS deck-file for the calculation of the solar desiccant regeneration.

```
**********************************************
*                                            *
*              SOLAR DESICCANT REGENERATION  *
*              AUGUST 14                     *
*              MIAMI, FLORIDA                *
*                                            *
**********************************************

ASSIGN REGEN.OUT 6
ASSIGN WEATH14.DAT 20
ASSIGN TYPE21.DAT 10

SIMULATION 1 24 1

WIDTH 72

UNIT 1 TYPE 9 WEATHER READER
PARAMETERS 34
10 1 1 1 0 2 1 0 3 1 0 4 1 0 5 1 0 6 1 0 7 1 0
-8 1 0 -9 1 0 10 1 0 20 -1

UNIT 2 TYPE 9 LOAD READER
PARAMETERS 16
4 1 1 1 0 2 1 0 3 1 0 4 1 0 10 -1

UNIT 3 TYPE 16 SOLAR RADIATION PROCESSOR
PARAMETERS 9
5 1 2 226 25.8 4871 -5.2 1 -1
INPUTS 8
1,8 1,5 1,6 1,19 1,20 0,0 0,0 0,0
0.0 22.0 88.2 1.0 1.0 0.2 20.0 0.0

EQUATIONS 11
TWMIN=[2,4]
TL10=[2,3]
ML10=[2,2]
TTANK=[21,1]
TCHECK=MAX(TTANK,TWMIN)
TL13=MAX(65,(TL10+0.8*(TCHECK-TL10)))
ML13=MAX(29.2,(ML10*(65-TL10)/(TL13-TL10)))
MW=1.196*ML13
QHE1=ML13*2.5*(TL13-TL10)
QHE1a=ML10*2.5*(65-TL10)
TWHE1=TCHECK-QHE1/(MW*4.18)

UNIT 21 TYPE 21 LIQ. COLLECTOR - STORAGE
PARAMETERS 17
240 2 14300 4.19 14300 4.19 130 0.765 14.9 0.17 100 0.8
10.0 1000 1.75 1.0 70
INPUTS 10
TWHE1 MW 1,5 0,0 3,6 3,4 3,5 0,0 3,9 0,0
```

```
61.8 109 22.0 24 0.0 0.0 0.0 0.2 0.0 20.0

EQUATIONS 1
QAUX=MW*4.18*(TCHECK-TTANK)

UNIT 25 TYPE 25 PRINTER 1
PARAMETERS 4
1 1 24 6
INPUTS 9
3,6 TTANK TCHECK TL13 21,3 QAUX QHE1 QHE1a 21,4
I T TTANK TCHECK TL13 QU  QAUX QHE1 QHE1a QLOSS

END
```